34400

National Library of Canada
Bibliothèque nationale du Canada

CANADIAN THESES ON MICROFICHE

THÈSES CANADIENNES SUR MICROFICHE

NAME OF AUTHOR/*NOM DE L'AUTEUR* ANITA KREBS

TITLE OF THESIS/*TITRE DE LA THÈSE* FUNCTION AND STRUCTURE OF TWO BACTERIAL PHOSPHOTRANSFERASES

UNIVERSITY/*UNIVERSITÉ* UNIVERSITY OF ALBERTA

DEGREE FOR WHICH THESIS WAS PRESENTED/ *GRADE POUR LEQUEL CETTE THÈSE FUT PRÉSENTÉE* PhD

YEAR THIS DEGREE CONFERRED/*ANNÉE D'OBTENTION DE CE GRADE* 1977

NAME OF SUPERVISOR/*NOM DU DIRECTEUR DE THÈSE* DR. W. A. BRIDGER

Permission is hereby granted to the NATIONAL LIBRARY OF CANADA to microfilm this thesis and to lend or sell copies of the film.

The author reserves other publication rights, and neither the thesis nor extensive extracts from it may be printed or otherwise reproduced without the author's written permission.

L'autorisation est, par la présente, accordée à la BIBLIOTHÈQUE NATIONALE DU CANADA de microfilmer cette thèse et de prêter ou de vendre des exemplaires du film.

L'auteur se réserve les autres droits de publication; ni la thèse ni de longs extraits de celle-ci ne doivent être imprimés ou autrement reproduits sans l'autorisation écrite de l'auteur.

DATED/*DATÉ* Sept 26, 1977 SIGNED/*SIGNÉ* Anita Krebs

PERMANENT ADDRESS/*RÉSIDENCE FIXE*
INSTITUT FÜR GENETIK
DER UNIVERSITÄT ZU KÖLN
WEYERTAL 121, D-5 KÖLN 41, GERMANY

NL-91 (3-74)

National Library of Canada

Cataloguing Branch
Canadian Theses Division

Ottawa, Canada
K1A 0N4

NOTICE

The quality of this microfiche is heavily dependent upon the quality of the original thesis submitted for microfilming. Every effort has been made to ensure the highest quality of reproduction possible.

If pages are missing, contact the university which granted the degree.

Some pages may have indistinct print especially if the original pages were typed with a poor typewriter ribbon or if the university sent us a poor photocopy.

Previously copyrighted materials (journal articles, published tests, etc.) are not filmed.

Reproduction in full or in part of this film is governed by the Canadian Copyright Act, R.S.C. 1970, c. C-30. Please read the authorization forms which accompany this thesis.

THIS DISSERTATION
HAS BEEN MICROFILMED
EXACTLY AS RECEIVED

NL-339 (3/77)

Bibliothèque nationale du Canada

Direction du catalogage
Division des thèses canadiennes

AVIS

La qualité de cette microfiche dépend grandement de la qualité de la thèse soumise au microfilmage. Nous avons tout fait pour assurer une qualité supérieure de reproduction.

S'il manque des pages, veuillez communiquer avec l'université qui a conféré le grade.

La qualité d'impression de certaines pages peut laisser à désirer, surtout si les pages originales ont été dactylographiées à l'aide d'un ruban usé ou si l'université nous a fait parvenir une photocopie de mauvaise qualité.

Les documents qui font déjà l'objet d'un droit d'auteur (articles de revue, examens publiés, etc.) ne sont pas microfilmés.

La reproduction, même partielle, de ce microfilm est soumise à la Loi canadienne sur le droit d'auteur, SRC 1970, c. C-30. Veuillez prendre connaissance des formules d'autorisation qui accompagnent cette thèse.

LA THÈSE A ÉTÉ
MICROFILMÉE TELLE QUE
NOUS L'AVONS REÇUE

THE UNIVERSITY OF ALBERTA

STRUCTURAL AND KINETIC STUDIES OF TWO BACTERIAL PHOSPHOTRANSFERASES

by

© ANITA KREBS

A THESIS
SUBMITTED TO THE FACULTY OF GRADUATE STUDIES AND RESEARCH
IN PARTIAL FULFILMENT OF THE REQUIREMENTS FOR THE DEGREE
OF DOCTOR OF PHILOSOPHY

DEPARTMENT OF BIOCHEMISTRY

EDMONTON, ALBERTA
FALL, 1977

THE UNIVERSITY OF ALBERTA

FACULTY OF GRADUATE STUDIES AND RESEARCH

The undersigned certify that they have read, and recommend to the Faculty of Graduate Studies and Research for acceptance, a thesis entitled STRUCTURAL AND KINETIC STUDIES OF TWO BACTERIAL PHOSPHOTRANSFERASES submitted by ANITA KREBS in partial fulfilment of the requirements for the degree of Doctor of Philosophy.

Supervisor

H W Duckworth

External Examiner

Wm Paranchych

Neil Madsen

Tigerstrom

Date July 27, 1977

Two paths diverged in a wood, and I -
I took the one less traveled by,
And that has made all the difference.

Robert Frost.

ABSTRACT

Certain considerations, including nucleotide specificity and preliminary reports of molecular weight and subunit structure, suggested that structural or mechanistic homology might exist between the enzymes succinyl-CoA synthetase and phosphoenolpyruvate carboxykinase. Aspects of the structure and catalytic properties of these two enzymes isolated from *Escherichia coli* were therefore examined.

Succinyl-CoA synthetase was shown to have a molecular weight of 140,000 by sedimentation equilibrium techniques. At low protein concentrations, the $\alpha_2\beta_2$ tetramer dissociate to lower molecular weight species, i.e., dimers and monomers. The phosphorylated enzyme is known to be more stable and resistant to tryptic digestion than is the apoenzyme, suggesting a structural rearrangement accompanying phosphorylation. However, circular dichroism spectra failed to demonstrate any difference between the apo- and phosphoenzyme, indicating the phosphorylation does not involve a gross conformational change with alteration in the contributions of α-helix or β-structure. The ultraviolet extinction coefficient, $E^{1\%}_{1\,cm}$, was determined to be 5.0 by two independent measurements of protein concentrations, namely colorimetric measurements using biuret and microbiuret methods and by interference fringe displacement in the ultracentrifuge.

Similar molecular weight studies and ultraviolet extinction coefficient determinations were done for the second phosphotransferase, phosphoenolpyruvate carboxykinase (PEPCK). This enzyme was found to be a monomer under denaturing and nondenaturing conditions and has a molecular weight of 65,000 as determined by sedimentation equilibrium and gel

electrophoresis in the presence of denaturants. The extinction coefficient, $E^{1\%}_{1\,cm}$, was measured to be 12.5. The amino acid composition reveals that the bacterial enzyme is quite different from the pig liver enzyme although their molecular weights are very similar (65,000 for the bacterial enzyme and 73,000 for the pig liver enzyme).

A previous report (Wright and Sanwal, (1969) J. Biol. Chem., 244, 1838) described allosteric inhibition of PEPCK by NADH and the appearance of sigmoidal substrate-saturation plots in the presence of this inhibitor. Since our molecular weight studies established the enzyme to be a monomer, a structure not normally associated with sigmoid kinetics, we reinvestigated the kinetics of NADH inhibition. In our hands, inhibition by NADH did not change the normal hyperbolic substrate saturation curves. The inhibition was later shown by others to be an artifact of the colorimetric assay employed. No such inhibition was apparent when the enzyme was coupled to malate dehydrogenase in the presence of NADH.

Some interesting features of PEPCK were determined by a variety of kinetic studies. The ATP-dependence of the $HCO_3^- \leftrightarrow$ oxaloacetate exchange, the relative rapidity of the exchange, together with the lack of demonstrable covalent intermediates, suggest a role of 'substrate synergism' for ATP in promoting the decarboxylation of oxaloacetate. Initial rate studies, product inhibition, and detailed measurements of the kinetics of isotope exchange at chemical equilibrium are most easily reconciled with a random order of substrate attachment and product release. However, the data suggest a preference for a sequence in which phosphoenolypyruvate is the last substrate to add to the enzyme. Central complex interconversion appears to be slow relative to Michaelis complex equilibration.

ACKNOWLEDGMENTS

I would like to express my appreciation for the guidance, patience and advice provided by my supervisor, Professor William A. Bridger, throughout the course of my graduate studies. Mr Ed Brownie's generous assistance with the preparation of enzymes is greatly appreciated. I should also like to thank my coworkers and collegues in the laboratory for creating an inspiring and harmoneous working atmosphere.

I am also grateful to Drs. C.M. Kay, N.B. Madsen, B. Paranchych and R. von Tigerstrom for serving on my special committee. Special thanks goes to V. Ledsham, R. Iwanika, M. Nattriss and K. Oikawa for their technical assistance and to Dr W. McCubbin for his assistance with running the computer analyses for molecular weight studies. I also want to thank Dr J. Sygush for the many hours of discussion on kinetics. My sincere appreciation goes toward Elke Lohmeier for her superb drawing talents and to Kathy Hicks for her photographic work.

Lastly, I am indebted to my typist, Jaclyn Dorsey for her excellent work typing this manuscript and her patience during this trying period.

TABLE OF CONTENTS

Page

LIST OF TABLES xi

LIST OF ILLUSTRATIONS xii

LIST OF ABBREVIATIONS xiv

CHAPTER I INTRODUCTION 1

CHAPTER II GENERAL MATERIALS AND EXPERIMENTAL METHODS 16

- A. General Materials 16
  - (1) Chemicals 16
  - (2) Enzymes 16
- B. General Experimental Methods 16
  - (1) Polyacrylamide Gel Electrophoresis 16
  - (2) Sedimentation Equilibrium Runs 17
  - (3) Refractometric Protein Determination 19
  - (4) Estimation of Protein Concentration by Buiret and Microbuiret 19
  - (5) Preparation of Succinyl-CoA-Synthetase from *E. coli*. 20
    - a. Succinly-CoA Synthetase Assay 20
  - (6) Preparation of Phosphoenolpyruvate Carboxykinase from *E. coli* 21
    - a. Phosphoenolpyruvate Carboxykinase Assays
      - (i) Carboxylation Assay Type A 21
      - (ii) Carboxylation Assay Type B 22
      - (iii) Carboxylation Assay Type C 22
      - (iv) ATP-Dependent OAA — $H^{14}CO_3^-$ Isotope Exchange Reaction 22
      - (v) OAA $\leftrightharpoons$ $H^{14}CO_3^-$ and ^{14}C-ATD $\leftrightharpoons$ ADP Exchange at Chemical Equilibrium . 23
      - (vi) Decarboxylation Assay. 24

(Continued)

Page

CHAPTER III PHYSICO-CHEMICAL STUDIES OF SUCCINYL-CoA SYNTHETASE 25

A. Introduction 25

B. Methods 25

C. Results and Discussion 26

(1) Molecular Weight Studies 26

(2) Circular Dichroism Experiments 31

(3) Determination of Extinction Coefficient . . 34

CHAPTER IV PHYSICO-CHEMICAL STUDIES OF PHOSPHOENOLPYRUVATE CARBOXYKINASE 37

A. Introduction 37

B. Method 39

C. Results and Discussion 40

(1) Molecular Weight and Subunit Structure . . 40

(2) Amino Acid Analysis and Determination of Extinction Coefficient 51

CHAPTER V KINETIC STUDIES OF PHOSPHOENOLPYRUVATE CARBOXYKINASE 56

A. Introduction 56

(1) Inhibition by NADH 56

(2) Comparison of Relative Rates 56

(3) Initial Rate Kinetics and Product Inhibition 57

(4) Isotope Exchange Rates at Chemical Equilibrium 59

(5) Nucleotide Specificity 60

(continued)

Page

B. Methods 61

(1) Inhibition by NADH 61

(2) Comparison of Relative Rates 61

(3) Initial Rate Kinetics and Product Inhibition 62

(4) Isotope Exchange Rates at Chemical Equilibrium 62

(5) Nucleotide Specificity 62

C. Results and Discussion 62

(1) Inhibition by NADH 62

(2) Comparison of Relative Rates 68

(3) Initial Rate Kinetics and Product Inhibition 78

(4) Isotope Exchange Rates at Chemical Equilibrium 100

(5) Nucleotide Specificity 114

CHAPTER VI CONCLUSION 119

BIBLIOGRAPHY 125

APPENDIX I PUBLISHED PAPERS ARISING FROM THIS WORK 131

LIST OF TABLES

Table		Page
I	Determination of ultraviolet extinction coefficient of succinyl-CoA synthetase.	35
II	Molecular weight of *E. coli* PEPCK in presence and absence of denaturants.	44
III	Amino acid composition of phosphoenolpyruvate carboxykinase.	52
IV	Determination of the ultraviolet extinction coefficient of phosphoenolpyruvate carboxykinase.	54
V	Comparison of relative rates of phosphoenolpyruvate carboxykinase.	69
VI	Type of line patterns of double reciprocal plots predicted by inspection for several sequential and ping-pong mechanisms.	79
VII	K_m and K_i values for substrates of PEPCK.	98
VIII	Effects of PEP concentration on the rates of exchange of $HCO_3^- \rightleftharpoons$ OAA and ATP $\rightleftharpoons$ ADP.	112
IX	Nucleotide specificity for PEPCK.	115

LIST OF ILLUSTRATIONS

Figure		Page
1	Dependence of weight-average molecular weight (Mw) on the concentration of succinyl-CoA synthetase.	29
2	For ultraviolet circular dichroism spectrum of succinyl-CoA synthetase.	33
3	Determination of molecular weight of PEPCK by sedimentation equilibrium.	42
4.	Polyacrylamide gel electrophoresis of a preparation of PEPCK.	46
5.	Determination of molecular weight of basic structural unit of PEPCK by SDS gel electrophoresis.	48
6.	Electrophoresis on 5% polyacrylamide gels in the presence of SDS.	50
7.	Double reciprocal plots of velocity *vs* [PEP] showing inhibitory effect of NADH in the presence of $MgCl_2$.	65
8.	Effect of replacement of $MgCl_2$ by $MnCl_2$ on kinetic and NADH inhibition by NADH.	67
9.	Double reciprocal plots of velocity *vs* [ATP] for the ATP-dependent isotope exchange reaction showing inhibitory effect of PEP.	72
10.	Double reciprocal plots of velocity *vs* [OAA] showing substrate inhibition at concentrations of OAA at concentrations >1mM.	77
11.	Double reciprocal initial velocity plots showing effects of varying [ADP] and [PEP] at a fixed saturating concentration of HCO_3^-.	82
12.	Double reciprocal initial velocity plots showing effects of varying [HCO_3^-] and [PEP] at saturating ADP concentration.	84
13.	Double reciprocal initial velocity plots showing effects of varying [ADP] and [HCO_3^-] at a fixed saturating concentrations of PEP.	86
14.	Double reciprocal plots of velocity versus [ADP] at increasing concentrations of ATP and near saturating concentrations of HCO_3^- and PEP.	89

(Continued)

Figure Page

15. Double reciprocal plots of velocity versus [PEP] at increasing concentrations of ATP and near-saturating concentrations of HCO_3^- and ADP. 91

16. Double reciprocal plots of velocity versus [ADP] at increasing concentrations of ATP and fixed concentrations of PEP and HCO_3^- at their approximate K_m values. 94

17. Double reciprocal plots of velocity versus [PEP] at increasing concentrations of ATP and fixed levels of ADP and HCO_3^- at their approximate K_m values. 96

18. Effects of varying [ADP] in constant ratio with [ATP] on the rate of $HCO_3^- \rightleftharpoons$ OAA exchange and on the rate of ATP $\rightleftharpoons$ ADP exchange. 102

19. Effects of varying [OAA] in constant ratio with [HCO_3^-] on the rate of $HCO_3^- \rightleftharpoons$ OAA exchange and on the rate of ATP $\rightleftharpoons$ ADP exchange. 105

20. Effects of varying [ATP] in constant ratio with [PEP] on the rate of exchange of $HCO_3^- \rightleftharpoons$ OAA and ATP $\rightleftharpoons$ ADP. 107

21. Effects of varying [PEP] in constant ratio with [OAA] on the exchange rates of $HCO_3^- \rightleftharpoons$ OAA and ATP $\rightleftharpoons$ ADP. 110

22. Structures of tubercidin 5'-triphosphate, arabinose-ATP, N-6-CH_3ATP, formycin 5'-triphosphate and εATP. 117

LIST OF ABBREVIATIONS

cAMP	3', 5' cyclic adenosine monophosphate
araATP	9-β-D-arabinofuranosyl adenosine-5'-triphosphate
ε-ATP	$1,N^6$-ethenoadenosine 5' triphosphate
DMS	dimethylsuberimidate
DTNB	5,5-dithio-(bis)-nitrobenzoic acid
$E^{1\%}_{1\,cm}$	absorbance of a 1% solution in a 1 cm pathlength
E. coli	*Escherichia coli*
FTP	formycin-5'-triphosphate
PEPCK	Phosphoenolpyruvate Carboxykinase
PEP	Phosphoenolpyruvate
r	radial distance from axis of rotation
SCS	Succinyl-CoA Synthetase
SDS	sodium docecyl sulfate
tris	tris-(hydroxylmethyl) aminomethane
TuTP	tubercidin -5'-triphosphate
$\bar{v}$	partial specific volume
w/v	concentration expressed as fraction by weight of the final volume.

CHAPTER I

INTRODUCTION

Enzymes which catalyze phosphate cleavage and phosphate transfer reactions are a general feature among biological pathways and serve many functions: 'maintain structures, provide functional interactions, promote and regulate metabolic processes, mediate neural and hormonal mechanisms, transport across membranes, and have a determining influence on genetic events' (1). Among these enzymes many have been shown to involve covalently-bound phosphoryl groups as reaction intermediates, while others may undergo a transient phosphorylation that is not detected by current methodology. Taborsky (1) in his review on phosphoproteins shows that all major types of phosphoryl transfer enzymes are represented among the documented phosphoenzymes. Among the phosphatases-transferases, glucose-6-phosphatase binds the phosphate that is cleaved from glucose-6-phosphate at a histidine residue and then transfers it to water. The mutases, such as phosphogluco- and phosphoglyceromutase, also cleave the phosphate group from its substrates but then transfer it to a different site on the same substrate molecule, thereby catalyzing an intramolecular transfer via a phosphoryl-protein intermediate. The kinases or synthetases follow a pattern with nucleotides acting as separate substrates that serve either to donate or accept phosphate groups intermolecularly. Pyruvate kinase, for example, is responsible for the substrate-level phosphorylation of ADP to ATP and for the biosynthesis of pyruvate from phosphoenolpyruvate.

The identification of a possible phosphoryl residue is marked with difficulty. The steady state concentration of a covalent phosphoryl protein may be too low for detection or the bond may be hydrolyzed or may have migrated to a different residue during its isolation. For the occurrence of a phosphoryl intermediate one might expect a multistep mechanism with a partial reaction such as an ATP ⟷ ADP exchange to phosphorylate the protein. Such an exchange, however, can be misleading. Hexokinase, for example, catalyzes a slow ATP ⟷ ADP exchange in the absence of other substrates and a glucose⟷glucose-6-phosphate exchange in the absence of nucleotides (2). These exchanges are too slow to be in keeping with the overall kinetics. It was later determined (3) that hexokinase indeed exhibits ATPase activity, but that it is independent of its kinase activity and it seems not to be a phosphoprotein during its normal role (1). ATP citrate lyase (4) provides another example of the difficulty of identifying a phosphorylated residue. When its phosphoenzyme form was digested with pronase and the phosphopeptides were subjected to Lossen rearrangement the results intimated the site of phosphorylation to be the γ-carboxyl group of a glutamic acid residue (4). However, 3-^{32}P-phosphohistidine was identified when the phosphorylated protein was hydrolyzed with potassium hydroxide and chromatographed on an anion exchange column (5, 6). The apparent contradiction could be reconciled by the possible existence of two different protein-bound phosphoryl groups or a possible partial intramolecular migration as was suggested by Das *et al.* (7).

Succinyl-CoA synthetase (SCS) catalyzes a reaction that is contained within the Krebs cycle. Its chief role is substrate-level phosphorylation; it provides ATP as well as converting succinyl-CoA to succinate. Its phosphohistidine intermediate has been identified (8, 9) and the amino acid sequence has been determined for a dodecapeptide containing this residue (10).

The first subject of the present research was succinyl-CoA synthetase (SCS) from *Escherichia coli*. Earlier work in this laboratory and elsewhere had been concerned mainly with the kinetic mechanism and identification of reaction intermediates. Our work with SCS was focussed on establishing fundamental physical parameters in order to provide a firm basis for understanding aspects of its structure such as subunit composition, number of binding sites per molecule, etc.

The second enzyme we studied was phosphoenolpyruvate carboxykinase (PEPCK). It catalyzes the following reaction:

$$\mathrm{OAA} + \mathrm{ATP} \rightleftharpoons \mathrm{PEP} + \mathrm{ADP} + \mathrm{HCO_3^-} \qquad [1]$$

The reason we chose to work on PEPCK was that this enzyme showed promise of having some structural and mechanistic relationships to SCS. PEPCK shows parallel nucleotide specificity to SCS: bacterial PEPCK (11) and SCS (12) usually prefer adenine nucleotides whereas the corresponding enzymes from mammalian sources are specific for inosine or guanosine nucleotides. Chang and Lane (13) reported that liver mitochondria undergo rapid adaptation to PEP formation because of the presence of an active GTP (or ITP)-generating system which they suggested to be the major metabolic role for SCS. Therefore, the functions of these enzymes may be effectively coupled.

Another obvious similarity which stimulated our interest in PEPCK was that both it and SCS had the same molecular weight trend when isolated from different sources. SCS from pig heart (14) has a molecular weight of 70,000 while that of the *E. coli* enzyme is 140,000 (15, and this work). PEPCK is similar in that the pig heart enzyme also has a molecular weight of 70,000 (13) and that of *Bacillus stearothermophilus* is 140,000 (16). Since SCS from heart is a dimer ($\alpha\beta$) (14) and the *E. coli* enzyme a tetramer ($\alpha_2\beta_2$) (17), we suspected the same relationship to exist for the PEPCK enzyme, the mammalian enzyme perhaps consisting of a dimer and the bacterial enzyme a dimer of dimers.

We also suspected that catalysis by both enzymes might involve the same covalent intermediate such as the phosphohistidine residue of SCS. If so, that could indicate an evolutionary relationship. Carrying this argument to the extreme, the α subunit of SCS, the site of phosphorylation of that enzyme (18), might be a constituent of PEPCK, carrying out the same partial reaction. If only the active site on the enzyme is conserved, while the rest of the molecular structure diverged, we could expect to see similar mechanistic features. Such conservation of structural characteristics has been documented for the serine proteases (19, 20, 21), NAD-linked dehydrogenases (22) and the Ca-binding proteins (23), for example. In our work on PEPCK we therefore set out to establish possible similarities to SCS with respect to structure or mechanism.

Succinyl-CoA Synthetase Background

Kaufman (24) showed in 1951 that SCS from spinach catalyzed the following reaction:

$$\text{succ-CoA} + \text{NDP} + \text{P}_i \rightleftharpoons \text{succinate} + \text{NTP} + \text{CoA} \qquad [2]$$

This reaction is fully reversible and requires divalent cations for activity.

The first suggestion of a phosphorylated intermediate was made by Kaufman (24) who proposed an E-P form on the basis of an isotope exchange between ATP $\rightleftharpoons$ ADP in the presence of spinach SCS and Mg^{2+}, but in the absence of other substrates. In Boyer's laboratory the phosphoenzyme was isolated from both *E. coli* (8) and pig heart (9) and the phosphoryl group was found to be attached to the N_3 position of a histidine residue (25). Using a rapid mixing and quenching device to measure the kinetics of establishment of the steady state, Bridger *et al.* (26) determined that the kinetics of E-P formation during the pre-steady state were those expected of an obligatory intermediate of the reaction.

SCS was shown to exchange ^{18}O between inorganic phosphate and the succinate carboxyl oxygen in the absence of di- and trinucleotides in both bacterial (27) and mammalian enzymes (28), suggesting either a covalent succinyl-phosphate intermediate or a concerted reaction mechanism with direct attack of succinate oxygens upon the P-N bond of phosphohistidine. Kaufman (24) investigated in 1955 the possibility of a succinyl-phosphate intermediate by reacting synthetic succinyl-phosphate with SCS, but he could not detect product formation. This was reinvestigated by Nishimura and Meister in 1965 (29), who reported that succinyl-phosphate was used by the bacterial enzyme in the formation of both ATP and succinyl-CoA when SCS was incubated with doubly-labelled succinyl-phosphate (^{14}C and ^{32}P). They also showed that SCS in the presence of γ-^{32}P-ATP and succinate and in the absence of CoA formed succinyl-phosphate. The above reaction was shown to be reversible in that succinyl-phosphate could be isolated from the reaction mixture containing E-P and succinate (30). SCS from pig heart could be dephosphorylated by incubating E-P with succinate.

The involvement of a phosphate and a succinyl-phosphate intermediate is consistent with the following three-step reaction:

$$E + NTP \rightleftharpoons E\text{-}P + NDP \qquad [3]$$

$$E\text{-}P + \text{succinate} \rightleftharpoons E\cdot\text{succinyl-phosphate} \qquad [4]$$

$$E\cdot\text{succinyl-phosphate} + CoA \rightleftharpoons \text{succinyl-CoA} + P_i + E \qquad [5]$$

$$\text{Sum: } NTP + \text{succinate} + CoA \rightleftharpoons NDP + \text{succinyl-CoA} + P_i \qquad [6]$$

Wang (31, 32), in this laboratory, confirmed the phosphorylated intermediate to be a phosphohistidine by a comparative acid hydrolysis of a synthetic phosphohistidine model and E-P, and then finally by isolating and sequencing the dodecapeptide at the active site containing the phosphorylated histidine residue.

The first evidence for the presence of subunits was reported by Ramaley *et al.* (15) who observed dissociation into phosphorylated and non-phosphorylated components following treatment of SCS with p-mercuribenzoate. Grinnell and Nishimura (33, 34) also detected in immunodiffusion patterns apparent dissociation into subunits in the presence of mercurials. Leitzmann *et al.* (35) studied partially dissociated enzyme upon succinylation or upon treatment with denaturants such as guanidinium hydrochloride. They suggested that the enzyme dissociated into four apparently identical subunits as indicated by several methods: polyacrylamide gel electrophoresis, sucrose density gradient centrifugation, gel filtration, and ultracentrifugation analyses. This suggestion was not supported by plots shown from their sedimentation equilibrium runs of fringe displacement *vs.* r^2; these showed slight curvature which is indicative of size heterogeneity (a range of approximately 32,000 to 25,000 molecular weight). Bridger (17) provided unambiguous evidence by SDS polyacrylamide gel electrophoresis that SCS from E. coli is composed of two non-identical subunits, i.e. $(\alpha\beta)_n$. From amino acid composition of the α and β subunit it was also established that the smaller α subunit is not derived from β, but that α and β are separate gene products (18). Bridger's data were easily reconciled with preliminary molecular weight studies (15) to suggest an $\alpha_2\beta_2$ tetrameric structure, the smaller α subunit bearing the phosphohistidine and having a molecular weight of 29,500 and β having a molecular weight of 38,500.

As mentioned earlier, pig heart SCS appears to be half the size of the *E. coli* enzyme (14). It is composed of an (αβ) dimer of molecular weight of near 75,000, but each of its subunits is somewhat larger than that from the *E. coli* source (14). The molecular weights of α and β are 34,500 and 42,500 respectively with the α subunit also bearing the phosphohistidine residue. A further difference between the bacterial and mammalian enzymes is that of nucleotide specificity. Bacterial SCS prefers ADP and ATP as substrates while SCS from mammalian sources use only GDP and GTP or IDP and ITP indicating a requirement for the 6-keto substituent on the purine ring.

At first glance, it might be thought that the kinetic properties of this enzyme with its phosphorylated intermediate might show the typical ping-pong pattern (36) with ATP binding first to transfer its terminal phosphate to the enzyme followed by dissociation of ADP before attachment of the second substrate. A classical example of a phosphoryl enzyme showing such ping-pong kinetics is nucleoside diphosphokinase (37). Its phosphorylation reaction is 10-fold faster than the overall reaction (24,000 and 2,700 min^{-1} respectively). In the case of SCS, however, although the phosphoenzyme is known to be an obligatory intermediate, the rate of ADP ↔ ATP exchange reflecting E-P formation in the absence of other substrates is very low. The slow exchange is enhanced by the presence of the other substrates, a phenomenon known as 'substrate synergism' (26). In keeping with the slow ATP ↔ ADP exchange, the initial rate kinetics were found not to obey a simple ping-pong kinetic pattern, but rather a sequential one (12). Further, by measurements of the kinetics of isotope exchange at chemical equilibrium Moffet and Bridger (38) determined that the kinetic mechanism for SCS is fully random, while the preferred route is shown in the following scheme:

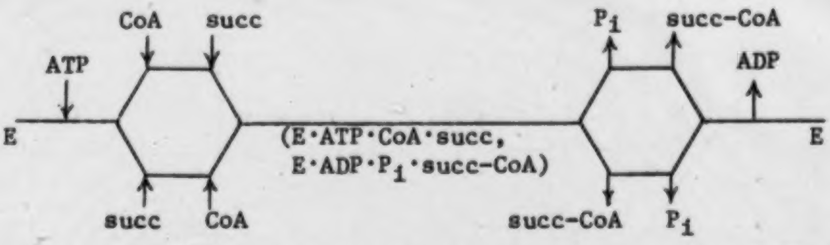

Scheme A. Proposed partially random sequential mechanism for the overall SCS reaction

Although these experiments seem to establish the kinetic mechanism, other fundamental questions remained. One, for example, is the extent of phosphorylation of SCS and its relationship to subunit association and dissociation. The $\alpha_2\beta_2$ structure of SCS, probably possessing two active sites, suggests that two phosphoryl groups should be incorporated per mole of enzyme, yet it has been found to incorporate only one phosphate with relative ease, showing 'half-of-the-sites reactivity' (10). Another question that may be correlated to the extent of phosphorylation is the disparity of specific activity between different enzyme preparations that have been purified to apparent homogeneity (35). Greater stability of SCS and resistance to proteolytic digestion has been attributed to a conformational change accompanying phosphorylation of the smaller subunit (18, 31).

An area that had not been thoroughly investigated, but that is fundamental to previous and future work, concerns the basic physical parameters of this enzyme. We set out to do molecular weight studies by various methods, ultraviolet extinction coefficient determination and circular dichroism measurements. These experiments are described in Chapter III.

Phosphoenolpyruvate Carboxykinase Background

PEPCK is at a branchpoint of two metabolic pathways: it leads from the Krebs cycle and is the first obligatory enzyme to catalyze reactions in the gluconeogenic pathway. From mammalian sources it is found mostly in gluconeogenic tissue (liver and kidney) indicating that its main role is PEP synthesis as part of the carbohydrate synthetic pathway. The importance of the reverse reaction, i.e. an anaplerotic role of OAA synthesis is restricted by the requirement for high concentrations of HCO_3^-. The K_m of which is about 15 mM, compared to the levels of HCO_3^- in man of only 5-8 mM (16). Shrago and Lardy (39) showed that PEPCK is the rate-limiting step in glucose synthesis in perfused rat liver. Even though PEPCK is believed to regulate the flux of gluconeogenesis and a wealth of reports relating to induction and repression by physiological factors have been published (see Ref. 40), there is little information concerning factors that directly affect the catalytic activity. PEPCK production responds to certain dietary and hormonal manipulation (16) and its activity is also controlled by compartmentation (41) within the mammalian cell. Krone *et al.* (42) induced PEPCK in the rat liver by injecting a cyclic AMP analogue ($N^6,O^{2'}$-dibutyryl cyclic adenosine 3',5' monophosphate) into adrenalectomized rats. The initial stimulation ceased after two hours despite repeated cAMP administration, but could be restored when hydrocortisone had been given at zero time. This suggests that the maintenance of cAMP-mediated induction of PEPCK is dependent on the simultaneous presence of glucocorticoids. A more drastic fluctuation in PEPCK levels is observed when carbohydrate intake is altered. Fasting produces a 2.5-fold increase in PEPCK in rat liver where the enzyme is in the cytosolic fraction (43). This increase is not observed in pigeon liver where PEPCK is found exclusively in mitochondria (44). Refeeding of a carbohydrate diet repressed enzyme synthesis. In *E. coli*, glucose was found to be the most effective carbohydrate repressor of PEPCK; others such as fructose, galactose and gluconate were less effective (45). PEPCK synthesis was induced when the bacterial culture was grown in medium containing C_3 and C_4 compounds as sole nutrients. Growth on succinate, pyruvate, fumarate, α-ketoglutarate or malate effected a 10-fold increase in PEPCK production (46).

Recently Lardy and his coworkers (47, 48, 49) reported interesting effects of anions and divalent metal cations on rat liver PEPCK. Ability of Fe^{2+} to stimulate PEPCK was lost during enzyme purification and restored by the addition of liver cytosol, suggesting that an agent lost during purification was responsible for activation. A large protein fractionated from the cytosol of molecular weight near 80,000 (49) was found to be responsible for the Fe^{2+} stimulatory effect. This 'ferroactivator' showed the same sub-cellular distribution as does PEPCK, consistent with a role in regulation of gluconeogenesis (48). Since its activity is the same in fasted or fed rats it is conceivable that the ferroactivator may play a role in controlling pyruvate kinase and pyruvate carboxylase to prevent futile substrate cycling (48).

Possible factors affecting the activity of PEPCK include the availability of substrates (16). The K_m for HCO_3^- (10 - 20 mM) is very high compared to the intracellular concentration of HCO_3^- of 5 - 8 mM in man (16), for example. Other enzymes involved in CO_2 fixation display a much lower requirement for HCO_3^-; for example, PEP-carboxylase (16) and pyruvate carboxylase (50) both have a K_m of 1 mM or less. This would suggest that PEPCK does not play an important anaplerotic role of OAA synthesis. Some controversy exists over the K_m value for OAA which is surprisingly high, 0.1 - 1.0 mM in mammalian cells (16) and even higher for bacterial cells, 2.5 mM (51). During fasting the intramitochondrial OAA concentration increases 8-fold, elevating the concentration to only 1.8 µM (52) which is still two to three orders of magnitude lower than the established K_m values. The low concentration of OAA suggests that PEPCK would favour OAA production rather than utilization. Attempts were made to account for the discrepancy between K_m and OAA concentration. Ballard (53) showed the K_m to be in the range of 9 - 30 µM for PEPCK isolated from rat, chicken or sheep liver. He reported the K_m for OAA to be dependent on the source of the enzyme, on the nature of the divalent cations and on the presence of malate. The problem requires further study which is made difficult because Michaelis-Menten kinetics are not observed when OAA concentration is varied (54). No such problem exists for the trinucleotides whose K_m values are well below physiological concentrations (approximately 3 mM for ATP in *E. coli* (55), and 1.0 mM for GTP in mammalian cells (56)).

ATP, the indicator of the energy state of the cell, plays a major role in controlling glycolysis, gluconeogenesis, lipogenesis and terminal oxidation in eucaryotic cells (55). Fluctuations in the ATP-AMP levels also control some glycolytic enzymes in the bacterial cell (55). For example, *E. coli* phosphofructokinase is activated by ADP (57), one of the two pyruvate kinases is activated by AMP (58), and pyruvate dehydrogenase is also activated by AMP (59). Wright and Sanwal (51) suggested that NADH may be the crucial control for gluconeogenesis. They reported that PEPCK from *E. coli* is allosterically inhibited by NADH.[1] This inhibition parallels that of NADPH-specific malic enzyme and malate dehydrogenase. All three enzymes are also induced during gluconeogenesis when grown on C_3 and C_4 compounds (55). NADH could be considered appropriate for controlling gluconeogenesis since its intracellular level is indicative of the state of glycolysis. The level of NADH in glucose-grown cells increases by a factor of 1.6 compared to that in succinate-grown cells (55).

Lane and coworkers (60, 61) investigated the kinetic mechanism of mitochondrial PEPCK isolated from pig liver. Chang *et al.* (60) studied the relative rates of the overall carboxylation, decarboxylation and an ITP-dependent $H^{14}CO_3^- \rightleftharpoons$ OAA[2] exchange reaction. The relative rates were found to be 1, 8.3 and 30 for OAA production, for PEP formation and for the ITP-dependent $H^{14}CO_3^- \rightleftharpoons$ OAA exchange reaction, respectively. Under the same conditions they failed to observe significant exchanges between GDP-8-^{14}C and GTP, ^{32}P-PEP and ITP or PEP-1-^{14}C and OAA. This was taken as evidence against the possibility that a phosphorylated intermediate exists in the ITP-dependent $HCO_3^- \rightleftharpoons$ OAA exchange reaction. Based on the faster rate of the ITP-dependent $H^{14}CO_3^- \rightleftharpoons$ OAA exchange reaction compared to the rates of PEP or OAA formation, Chang *et al.* (60) postulated a two-step reaction (60) as shown:

---

[1] After this writing the inhibition by NADH was shown to be an artifact.

[2] See Chapter V, Section A2, for detailed description of this assay.

$$E + PEP + IDP \underset{k_{-1}}{\overset{k_1}{\rightleftharpoons}} E\text{-}X \qquad [7]$$

$$E\text{-}X + HCO_3^- \underset{k_{-2}}{\overset{k_2}{\rightleftharpoons}} OAA + ITP \qquad [8]$$

Such a scheme could explain the disparity of relative rates. The more rapid ITP-dependent OAA $\rightleftharpoons$ $H^{14}CO_3^-$ exchange may be ascribed to k_2 and k_{-2} being greater than k_1 and k_{-1}. Miller and Lane (61), also working with pig liver PEPCK, proposed the following mechanism of the carboxylation reaction from initial rate kinetics and binding studies:

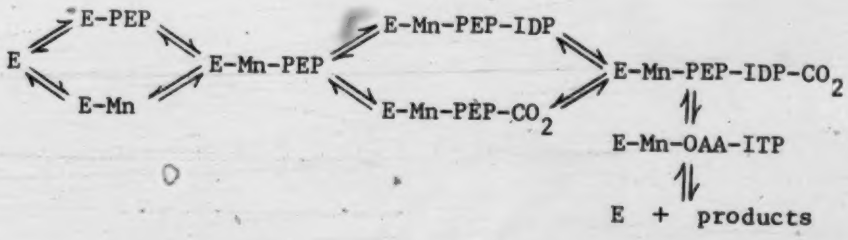

Scheme B

The above Scheme B shows that the reaction is a partially ordered sequential one. It shows that PEP and/or Mn^{2+} are the first substrates to bind the free enzyme and that IDP and CO_2 then bind randomly to the ternary E-Mn-PEP complex. (The authors believe that CO_2 rather than HCO_3^- is the active carboxylating species.) The concerted chemical mechanism proposed shows that ITP and IDP and also OAA and PEP share the same binding site. The CO_2-binding site overlaps the OAA-binding site which explains why CO_2 is a competitive inhibitor with OAA in the overall decarboxylation reaction (61).

Felicioli *et al.* (62) studied the kinetic mechanism of chicken liver

PEPCK by initial rate kinetics and product inhibition studies of the ITP-dependent OAA $\rightleftharpoons$ $H^{14}CO_3^-$ exchange reaction and the decarboxylation reaction. They reported an ordered bi-ter sequential mechanism with ITP binding to the free enzyme before OAA and with products being released in the following order: HCO_3^-, PEP and IDP. IDP showed competitive product inhibition with ITP only and showed uncompetitive inhibition with OAA, whereas PEP was a non-competitive product inhibitor with both OAA and ITP.

With the *E. coli* enzyme, Wright and Sanwal (51) suggested a partially ordered random mechanism. From their data obtained by initial rate kinetics and product inhibition studies they determined that the nucleotides (ATP, ADP) bind to the free enzyme form followed by random binding of the other substrates. This is in keeping with the foregoing proposal (62) that the nucleotides bind first to the free enzyme, but in opposition to Miller and Lane's scheme (61) which designates PEP to be the first substrate to bind the enzyme.

Chapters III and IV of this thesis deal with studies of some physical parameters and kinetic mechanism of PEPCK isolated from *E. coli*. The subunit structure is of particular interest since the mammalian PEPCK is known to have a molecular weight of 70,000 (13), the *Bacillus stearothermophilus* enzyme, 140,000 (16), and the yeast enzyme 252,000 (62). These figures suggested that the bacterial and yeast enzymes were multiples of the mammalian subunit structure. This trend was also reminiscent of SCS, where the bacterial enzyme is a dimer of the dimeric form of the pig heart enzyme. Interest in a comparative subunit study of PEPCK from different sources was bolstered by the report of allosteric homotropic cooperativity for the *E. coli* enzyme in the presence of the inhibitor, NADH

(51). The reported allosteric properties implied the enzyme to be an aggregate of subunits, which is the simplest model to account for more than one binding site per substrate. This prompted us to do a detailed structural study of *E. coli* PEPCK under dissociating and non-dissociating conditions.

CHAPTER II

GENERAL MATERIALS AND EXPERIMENTAL METHODS

A. GENERAL MATERIALS

1. Chemicals

Tris (enzyme grade) and ammonium sulfate (ultrapure) were purchased from Schwarz/Mann Research Laboratories. Sephadex G-50 (20-80 μ), Sephadex G-100 (40-120 μ), Sephadex G-200 (40-100 μ), DEAE-Sephadex A-25 (40-120 μ) and QAE-Sephadex A-50 (40-120 μ) were obtained from Pharmacia Fine Chemicals, Uppsala, Sweden. Calcium phosphate gel was prepared by Mr. E.R. Brownie according to the method described by Tsobai *et al.* (63). Dowex Chelex 100 (200-400 μ) (analytical grade) was purchased from Bio-Rad Laboratories. Disc electrophoresis supplies were obtained from Canalco. All other chemicals were reagent grade and were used without further purification.

All isotopically labelled compounds were purchased from New England Nuclear. Analogues of ATP were prepared by Douglas Johnson *et al.* (64). Scintiverse scintillation mixture is the product of Fisher Scientific Co.

2. Enzymes

Phosphorylase *a* was kindly donated by Dr. N.B. Madsen and all other proteins (except SCS and PEPCK) were purchased from Sigma Chemical Co. or from Pharmacia Fine Chemical Co.

B. GENERAL EXPERIMENTAL METHODS

1. Polyacrylamide Gel Electrophoresis

Analytical gel electrophoresis was conducted according to standard procedures (65). For electrophoresis in the presence of SDS the method of Weber and Osborn (66) was followed, using the normal 10% acrylamide solution or 7% acrylamide for larger proteins. Gels for cross-linked proteins were prepared according to Davies *et al.* (67).

Protein samples for analytical gels were centrifuged from 75% (saturated, w/v) $(NH_4)_2SO_4$ suspension and dialyzed against 0.05 M potassium phosphate buffer pH 7.2. For SDS gels, samples were dialyzed at room temperature for 3 hr against the above buffer supplemented with 1% SDS and 1% mercaptoethanol. Protein samples for cross-linking experiments were incubated for 3 hr at room temperature with dimethylsuberimidate (0.015 - 0.375 mg/ml) in 0.2 M triethanolamine hydrochloride, pH 8.5 (67). In all gels 3 μl per tube of 0.05% Bromphenol blue was used as the marker dye and electrophoresis was carried out at 4 - 8 mA per gel for 4 hr.

2. Sedimentation Equilibrium Runs

All molecular weight studies were done by the conventional low-speed sedimentation equilibrium method described by Chervenka (68). When loading concentrations were greater than 1 mg per ml, runs were done with the Beckman Spinco Model E ultracentrifuge equipped with Rayleigh interference optics. For lower loading concentrations a Beckman Model E ultracentrifuge was used which was equipped with a photoelectric scanner. Both analytical ultracentrifuges were controlled with electronic speed controls and refrigeration units.

The data were analyzed with the aid of an IBM 360 computer (with the guidance of Dr. W.D. McCubbin) with programmes made available to us by Dr. W.T. Wolodko (69). The apparent weight average molecular weight, Mw, of a homogeneous protein determined by sedimentation equilibrium, is given by the following equation:

$$Mw = \left(\frac{2RT}{(1-\bar{\nu}\rho)\omega^2}\right)\left(\frac{d \ln c}{dr^2}\right) \qquad [9]$$

where: R is the universal gas constant,

T is the experimental temperature in °K,

$\bar{\nu}$ is the partial specific volume of the protein,

ρ is the solvent density

ω is the angular velocity,

c is the protein concentration at r, and

r is the distance from the axis of rotation.

When Rayleigh interference optics were employed a c_m (protein concentration at the meniscus) had to be calculated according to the following equation:

$$c_m = c_o - \frac{r_b^2(c_b-c_m) - \int_{c_m}^{c_b} r^2\, dc}{r_b^2 - r_m^2} \qquad [10]$$

where: c_o is the initial protein concentration,

r_m is the distance from the meniscus to the axis of rotation,

r_b is the distance from the cell bottom

c is the protein concentration at r, and

r is the distance from the axis of rotation.

With the photoelectric scanner the absorbance value, A, was a direct measure of protein concentration at any point along the cell. A plot of natural logarithm of protein concentration (Y, expressed as fringes or absorbance units, A) *vs.* r^2 (distance from axis of rotation) yielded a straight line with a slope of d ln c/dr^2 for a homogeneous system. The weight average molecular weight at any position along the cell was then determined by the above equation for M_w.

The partial specific volume ($\bar{v}$) was calculated according to Cohn and Edsall (70) from the amino acid composition of the enzyme (see Chapter IV).

For ultracentrifugation experiments, protein samples were prepared by dialyzing extensively against buffer (50 mM potassium phosphate, 50 mM potassium chloride, pH 7.2), which had previously been passed through a column (2 x 20 cm) of Dowex Chelex 100 resin to remove heavy metal contaminants, some of which are known to dissociate SCS (15). This precaution was found not to be necessary for molecular weight studies of PEPCK.

3. Refractometric Protein Determination

Essentially following the method of Babul and Stellwagen (71), measurements of protein concentration based on refractive index increment were done in a Beckman Model E analytical ultracentrifuge equipped with Rayleigh interference optics. The number of fringes corresponding to each of several loading concentrations of protein were counted with the aid of a Nikon Model 6C microcomparater, and the protein concentration was calculated from the average refractive index increment of 4.10±0.13 fringes mg^{-1} ml^{-1} determined by Babul and Stellwagen (71). The ultraviolet extinction coefficient was then determined from a plot of previously measured absorbances at 280 nm *vs.* protein concentration (mg/ml).

4. Estimation of Protein Concentration by Biuret and Microbiuret

For the determination of protein concentrations both biuret (72) and microbiuret (73) methods were used. In both cases bovine serum albumin and ribonuclease A were used as standards. Their concentrations were calculated from their respective extinction coefficients (74).

5. Preparation of SCS from *E. coli*

Succinyl-CoA synthetase was prepared by Mr. E.R. Brownie from succinate-grown *E. coli* (Crooke's strain) according to the method of Leitzmann *et al.* (35) with the following changes: QAE-Sephadex was used in place of DEAE-Sephadex for ion exchange chromatography and a final gel filtration step on G-100 Sephadex was added. The enzyme used throughout the physico-chemical studies was chromatographically pure (showed a single protein peak) and electrophoretically homogeneous and had a specific activity of 30 units per mg. Isolated SCS was routinely stored as a precipitate in 75% (saturated, w/v) $(NH_4)_2SO_4$ at 4° and is very stable under these conditions.

The phosphorylated enzyme was prepared by incubating at 4° for 10 min, 15 mg SCS, 50 mM tris-HCl pH 7.2, 0.1 mM ATP and 5 mM $MgCl_2$. Separation of P-SCS from unreacted ATP was achieved by passage through a Sephadex G-50 (1 x 30 cm) column. In an attempt to dephosphorylate SCS, the isolated enzyme (5 mg) was enclosed in a dialysis bag and dialyzed for 8 hr against 100 mM tris-Cl pH 7.2, 5 mM EDTA, 10 mM $MgCl_2$, 0.1 mM ADP, 5 mM glucose and 1 mg yeast hexokinase.

a. SCS Assay

Routine assays of SCS were carried out as described by Ramaly *et al.* (15) using the increase in absorbance at 230 nm due to the formation of thioester (succinyl-CoA). The assay mixture (1 ml) contained 10 mM succinate, 0.1 mM CoA, 0.4 mM ATP, 10 mM $MgCl_2$, 50 mM tris-Cl pH 7.2 in a 1 cm pathlength cuvette. Rate of increase of absorbance at 230 nm was measured with a Cary Model 15 recording spectrophotometer. One unit of SCS is defined as the amount of enzyme required to catalyze the formation of one μmole of succinyl-CoA per minute at 25°.

6. Preparation of PEPCK from *E. coli*

Escherichia coli, Crooke's strain, was grown in a 300 litre fermentor on a minimal medium (15) containing 2.2% sodium succinate as the sole carbon source. After harvesting 2500 gm of wet cells they were stored frozen in 500 gm batches; these cell lots were usually the quantity used for a single enzyme preparation. Cells were disrupted by sonication (3 x 15 min bursts) at 4° and the enzyme was purified by a procedure based on that developed by Wright and Sanwal (51). We deviated from their isolation procedure by using an Amicon concentrator rather than lyophilization and an extra ion exchange chromatography step on QAE-Sephadex before DEAE-Sephadex chromatography. Wright and Sanwal (51) achieved only partial purification of PEPCK so the following steps were added to their procedure. The enzyme was subjected to gel filtration on G-150 Sephadex (2.5 x 100 cm column) and then to chromatography on a calcium phosphate-cellulose (1:10) column (5 x 60 cm) (75) which was eluted with a linear gradient of potassium phosphate (5 - 50 mM), pH 7.2. An additional four-fold purification was achieved by these steps giving an enzyme preparation found to be virtually homogeneous (see Chapter IV for documentation of purity).

a. PEPCK Assays

(i) Carboxylation Assay Type A

The rate of OAA formation was coupled to MDH and oxidation of NADH was followed spectrophotometrically at 340 nm (13). The assay medium contained 100 mM imidazole buffer, pH 6.8, 0.2 mM DTT, 50 mM HCO_3^-, 1 mM PEP, 2 mM ADP, 3 units MDH, 5 mM MnCl and 0.2 mM NADH. The progress of the reaction was followed as the reduction in absorbance at 340 nm with a Cary 15 recording spectrophotometer. This assay was very reproducible and was used extensively during initial rate studies. The rate was linear up to 2 μg of PEPCK. Total volume of assay was 1.3 ml.

(ii) Carboxylation Assay Type B

The overall carboxylation coupled to MDH as described above was monitored by the rate of isotope incorporation into malate (acid stable ^{14}C) from $H^{14}CO_3^-$ (13). The assay medium was incubated at 30° for 15 min and the reaction was terminated by the addition of 1 ml 2 N HCl. 0.5 ml aliquots were taken to dryness under an infra-red lamp in a well-ventilated fume hood to remove unreacted $H^{14}CO_3^-$. The residue containing the ^{14}C-malate was then taken up in 1 ml H_2O and counted in 10 ml Scintiverse with a Beckman LS250 Liquid Scintillation Counter. The plot of rate *vs*. concentration of PEPCK was linear up to 0.7 μg of protein.

(iii) Carboxylation Assay Type C

Production of OAA in this third carboxylation assay was monitored colorimetrically by complexing OAA to an azo dye, Azoene fast violet B. The color complex absorbs in the visible range at 520 nm (51). A minor change was made to the published procedure by adding the dye concurrently with the ethanol to stop the enzymatic reaction in order to minimize OAA decarboxylation in solution. This assay is limited in that the OAA produced decarboxylates during the 10 minutes of reaction time and also that the color complex formed between OAA and the azo dye fades quite rapidly. The rate is proportional to enzyme concentration up to 1.4 μg of PEPCK.

(iv) ATP-Dependent OAA $\rightleftharpoons$ $H^{14}CO_3^-$ Isotope Exchange Reaction

The radioactive exchange assay (13, 51, 76) measures the exchange between $H^{14}CO_3^-$ and OAA in the presence of ATP and $MnCl_2$. The reaction mixture contained 100 mM imidazole-HCL at pH 6.7, 3 mM $MnCl_2$, 2 mM DTT, 3 mM ATP, 40 mM HCO_3^- (1.5×10^6 cpm), 2 mM OAA and PEPCK (0.1 - 0.3 μg). To stop the 4-minute PEPCK reaction and to convert ^{14}C-OAA to the acid-stable ^{14}C-malate, 40 mM EDTA, 10 mM NADH and 5 units MDH were added. After 5 minutes, 0.5 ml 4 N HCl was added to stop all reactions. This was the most sensitive assay, the rate being proportional to PEPCK concentration up to 0.3 µg per ml.

(v) OAA $\rightleftharpoons$ $H^{14}CO_3^-$ and ^{14}C-ATP $\rightleftharpoons$ ADP Exchange at Chemical Equilibrium

Radioactive isotope exchange at chemical equilibrium is extensively used in the determination of kinetic mechanisms (38, 77, 78, 79). The rates of the two isotope exchanges were measured: ^{14}C-ATP $\rightleftharpoons$ ADP and $^{14}C\text{-}HCO_3^-$ $\rightleftharpoons$ OAA. The equilibrium constant for PEPCK in the direction of PEP formation was determined to be 3.1 M by Jomain-Baum (80). The relative exchange rates of ATP $\rightleftharpoons$ ADP and HCO_3^- $\rightleftharpoons$ OAA were measured while raising the concentration of a substrate-product pair at a constant ratio. Preliminary experiments were done to establish enzyme and isotope concentrations as well as sampling time for each of the two exchange reactions.

After the addition of enzyme to the reactants the mixture was incubated in a small, well-stoppered tube for 10 min at room temperature to allow for minor adjustments to chemical equilibrium. Approximately 250,000 cpm of the specific isotope, either ^{14}C-ATP or $^{14}C\text{-}HCO_3^-$, was added after the 10 min-preincubation in a very small volume (5 µl) in order not to disturb the equilibrium. 50 µl samples were removed from the reaction mixture for the ATP $\rightleftharpoons$ ADP exchange and pipetted into 25 µl of 100 mM EDTA at times before and after isotopic equilibrium had been reached. ATP was separated from ADP on Wattman #4 paper by descending chromatography using a solvent containing 66% isobutyric acid 33% H_2O and 1%

NH_4OH. ATP and ADP spots were located under u.v. light, cut out and counted in 10 ml Scintiverse in a Beckman LS 250 liquid scintillation counter. For the $^{14}C\text{-}HCO_3^- \longrightarrow$ OAA exchange reaction, timed aliquots were pipetted into test tubes containing 0.1 ml of 40 mM EDTA, 10 mM NADH and 5 units MDH to convert ^{14}C-OAA to acid-stable ^{14}C-malate. The MDH reaction was quenched after 5 min by the addition of 50 λ 4 N HCl. Aliquots of this were brought to dryness in scintillation vials. One ml H_2O was added to solubilize ^{14}C-malate and the sample was counted as before.

Rates of the isotope exchange reactions at chemical equilibrium were calculated from the following equations (81, 82). F represents the fraction of isotopic equilibrium attained at time t. R is expressed as mM per min per mg of PEPCK in 0.5 ml at room temperature.

$$R = \frac{[ATP] \times [ADP]}{[ATP] + [ADP]} \times \frac{1}{t} \times \frac{\ln(1-F)}{\text{mg PEPCK}} \qquad [11]$$

$$R = \frac{[KHCO_3] \times [OAA]}{[KHCO_3] + [OAA]} \times \frac{1}{t} \times \frac{\ln(1-F)}{\text{mg PEPCK}} \qquad [12]$$

(vi) Decarboxylation Assay

The overall decarboxylation (the forward reaction) of PEP formation as described by Chang and Lane (13) could not be successfully repeated in our laboratory. OAA was found to be very unstable and non-enzymatic decarboxylation occurred at a rate equal to or greater than the rate of enzymatic decarboxylation.

CHAPTER III

PHYSICO-CHEMICAL STUDIES OF SUCCINYL-CoA SYNTHETASE

A. INTRODUCTION

An area that was somewhat neglected for succinyl CoA synthetase was a thorough study of the fundamental physical parameters of the enzyme. Aside from high resolution n.m.r. and X-ray crystallographic study, the body of our knowledge about the function and regulation of enzymes has come through careful physical and chemical studies. Among the most basic physical parameters that must be precisely determined are such things as molecular weight, states of aggregation, measure of degree of secondary structure and conformational changes in quaternary or tertiary structure by ligand interaction. Estimation of protein concentration in such studies is facilitated by knowledge of the ultraviolet extinction coefficient.

In this chapter we deal with these physical parameters. The ultraviolet extinction coefficient for calculating protein concentration was based on two independent measurements of protein concentration. Molecular weight studies were done by sedimentation equilibrium ultracentrifugation in nondissociating buffers under various protein concentrations to assess the state of subunit aggregation. Circular dichroism was used as a convenient method for quantitating secondary structural content contributed by α-helix, β-structure and random coil.

B. METHODS

Methods for determining molecular weights and extinction coefficient are described in Chapter II, General Methods, under Sections 2 to 4.

Ultraviolet circular dichroism measurements, using methods described by Oikawa *et al.* (1966) (83), were made with a Cary Model 6001 circular dichroism attachment to a Cary 60 recording spectropolarimeter. The temperature was maintained at 27°. Nitrogen was flushed through the cell compartment during measurements over the wavelength of 200-250 nm. Spectra were measured at protein concentrations of 0.76 mg per ml in a cell of 1.0 cm path length. The results are reported in terms of mean residue molecular ellipticity $[\theta]$, given by the relation, $[\theta] = \theta M/100\ l\ c$, where M is the mean residue weight (105 for SCS), θ is the observed ellipticity, l is the path length in decimeters, c is the concentration of SCS in gm per ml. The units of $[\theta]$ are deg cm^2 dmole^{-1}.

C. RESULTS AND DISCUSSION

1. Molecular Weight Studies

Results from polyacrylamide gel electrophoresis under denaturing conditions in the presence of sodium dodecyl sulfate (17) gave estimates for the molecular weights of the α and β subunit components of 29,600 ±500 and 38,700±300, respectively. Since quantitative molecular weight data were clearly consistent with the presence of equimolar amounts of the two subunit species, it was suggested that the native enzyme is a tetramer of the $\alpha_2\beta_2$ type. This structure would predict a molecular weight for the oligomeric enzyme to be around 136,000, which corresponds nicely to 141,000 as determined in a preliminary sedimentation equilibrium experiment (15).

Detailed molecular weight studies by sedimentation equilibrium were done at varying loading concentrations. A range of protein concentration was chosen in order to determine whether SCS exists as a heterogeneous population in non-dissociating medium. Great care was taken to assure that the enzyme was not subjected to heavy metal ion contamination which is known to dissociate the subunits (15). Ultracentrifuge cells were loaded with Teflon needles and all buffers were first treated with Dowex Chelex 100 to remove heavy metal contaminants for all our molecular weight studies. The results are given in Fig. 1. At loading concentrations of 1 mg per ml or greater the enzyme tended toward the oligomeric weight of approximately 140,000 but at concentrations lower than 0.5 mg per ml the tendency toward the αβ dimer could be detected. With even lower loading concentrations (≤0.2 mg per ml) dissociation toward monomers is suggested by our results. Teherani and Nishimura (84) found predominant αβ dimer formation in their study of SCS which had been cross-linked with dimethyl suberimidate. They did not observe an increase in αβ dimer formation when protein concentration was reduced to the range where dissociation occurred during sedimentation equilibrium runs. It is interesting to note at this point that physiological concentrations are roughly 1 mg per ml. We can expect the enzyme to be mostly in the active tetrameric structure *in vivo*.

The dissociation of oligomeric proteins at intermediate concentrations is not uncommon. For example, SCS seems to resemble the yeast aldolase system (85) which coexists as a monomer-dimer mixture. In the range of concentrations of 0.42 to 1.24 mg per ml the native dimeric aldolase gives a biphasic profile of molecular weights of 40,000 and 80,000 as shown by sedimentation equilibrium. In the presence of dissociating medium, a single inactive species of molecular weight of 40,000 is observed.

If the state of phosphorylation is related to the tendency to dissociate, we can attribute the heterogeneity observed in sedimentation

FIGURE 1. Dependence of weight-average molecular weight on the concentration of succinyl-CoA synthetase. Panel A: replicate runs with data collected by means of photoelectric scanner at a wavelength of 235 nm. The different symbols indicate three different enzyme preparations, all of which showed no detectable impurity when analyzed by gel electrophoresis in either the presence or absence of detergent. In all cases, the initial loading concentration was 0.2 mg/ml.
Panel B: data collected by means of interference optics; initial loading concentration was 1.5 mg/ml. All experiments were performed at a rotor speed of 9000 rpm and at a temperature of 20°.

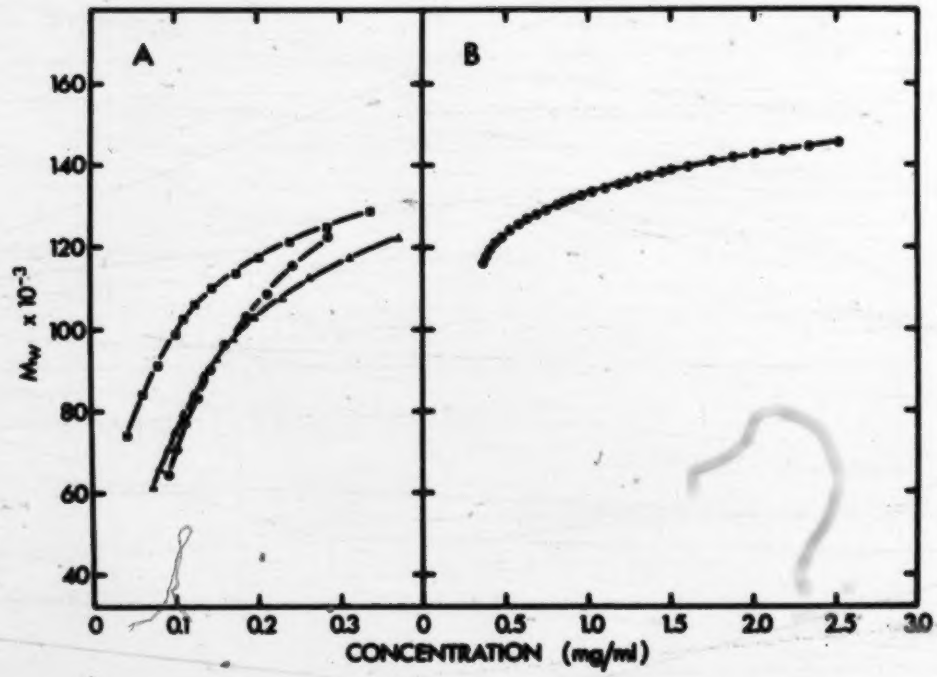
A
B
160
140
120
100
80
60
40
$M_w \times 10^{-3}$
0
0.1
0.2
0.3
0
0.5
1.0
1.5
2.0
2.5
3.0
CONCENTRATION (mg/ml)

equilibrium runs to the fraction of dephosphorylated enzyme. Protein samples that were not incubated with ATP prior to sedimentation equilibrium studies consisted of a heterogeneous mixture of stable phosphorylated and unstable dephosphorylated enzyme. At this point we should also be reminded of the disparity of specific activity among different enzyme preparations, although purification to homogeneity was carefully monitored by polyacrylamide gel electrophoresis. In the absence of a phosphoryl group, the apoenzyme is relatively unstable or 'loose' (31) and perhaps under particular conditions it will dissociate from its tetrameric form to produce trimers, dimers and monomers.

Pearson and Bridger (86, 87) studied the assembly of the enzyme following isolation of the α and β subunits. They showed that the tetramerization requires that the α subunit be phosphorylated. Phosphorylation of the α subunit must change its conformation in such a manner that it is able to refold correctly and interact productively with the β subunit. In that study (86, 87), only 40-60% of the original specific activity was recovered after recombination. Perhaps the partial recovery of the activity is due to aberrant recombination.

The pig heart enzyme, on the other hand, is an αβ dimer of molecular weight near 75,000 (14, 88, 89). The molecular weights of the α and β subunits are 34,500 and 42,500 respectively, as determined by polyacrylamide gel electrophoresis (18). Their molecular weights are slightly larger than those of the α and β subunits, respectively, of bacterial enzyme. Phosphorylation of this enzyme showed incorporation of one phosphoryl group per dimer. The α monomer carries the active site phosphohistidine residue (14). The pig heart also shows stability upon phosphorylation as does the *E. coli* enzyme (89). Cross-linking experiments with the mammalian enzyme showed only formation of dimeric species (84) which is in keeping with the dimeric structure.

2. Circular Dichroism Experiments

The effect of phosphorylation on enzyme conformation can be monitored by circular dichroism measurements. This method quantitatively probes the contribution of α helix, β-sheet and random coil. Changes in the distribution of secondary structure might be expected to accompany phosphorylation of the α subunit since this process is known (10, 31) to effect changes in stability and subunit interaction. A spectrum of the circular dichroism in the far-ultraviolet region (200-250 nm) for the phosphorylated form of SCS is given in Fig. 2. The observed minimum molar ellipticity of -6900° at 219 nm is indicative of a structure possessing mainly random coil structure. Chen *et al.* (90) have derived an equation that relates parameters from the dichroism spectrum to the amounts of the three structural components (α helix, β-sheet and random coil) using reference proteins whose structures have been elucidated by X-ray crystallography. Fractional contributions of the α-helix (f_H), β-sheet (f_β) and random coil (f_R) have been thus calculated to be 0.14, 0.08 and 0.78 respectively. Attempts to compare the dephosphorylated enzyme were hindered by technical difficulties. When SCS was incubated with hexokinase, glucose and ADP, the proteases inherent in the commercial hexokinase preparation (31) inactivated SCS. When SCS was dialyzed with hexokinase in the buffer outside the dialysis bag, complete dephosphorylation was not achieved. Partial dephosphorylation of up to 50% was achieved, but the circular dichroism data were superimposable with the data obtained with maximally phosphorylated SCS. SCS was subsequently dephosphorylated by incubation with succinate and $MgCl_2$ (91). Circular dichroism measure-

FIGURE 2. Far ultraviolet circular dichroism spectrum of succinyl-CoA synthetase. See Section B, Methods, in this chapter for experimental details.

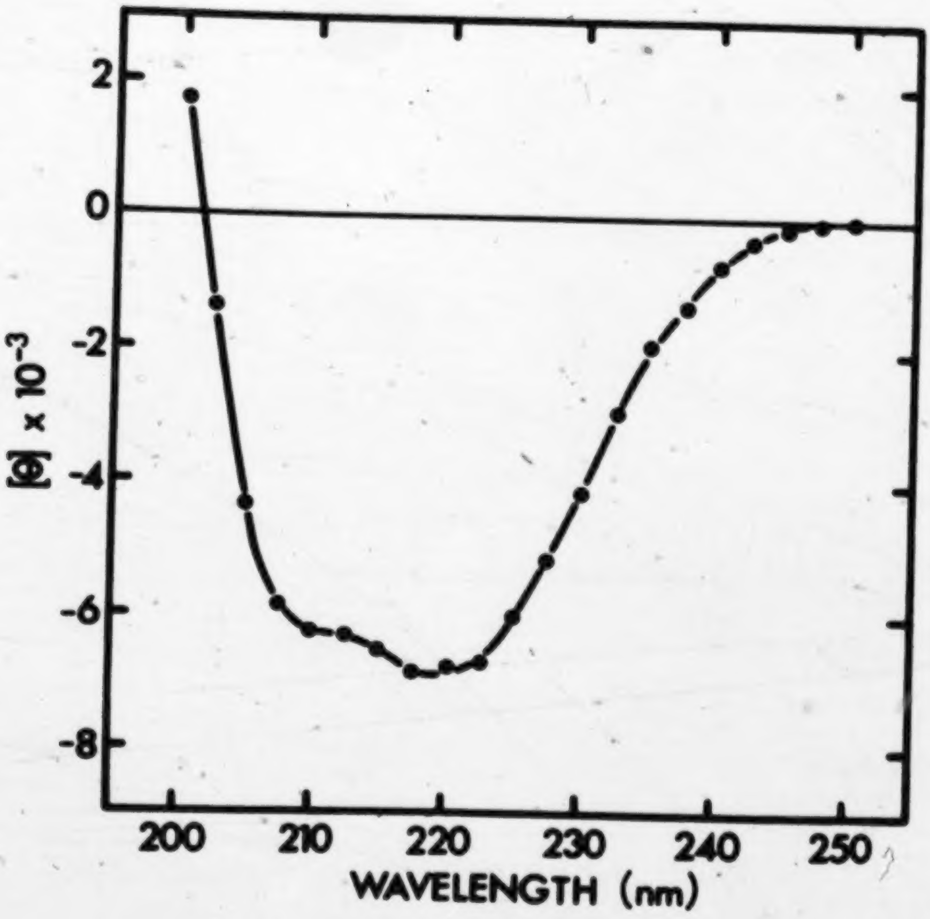

2
0
-2
-4
-6
-8
$[\Theta] \times 10^{-3}$
200
210
220
230
240
250
WAVELENGTH (nm)

ments with completely dephosphorylated SCS showed no significant difference in the contribution of the three structural components and the spectrum was again superimposable with that of the phosphorylated protein. Thus we conclude that phosphorylation of the enzyme does not cause it to undergo a conformational change of sufficient magnitude to involve significant change in distribution of structural components. This finding is somewhat surprising in view of the fact that phosphorylation is accompanied by a very large decrease in susceptibility to proteolytic attack (31).

3. Determination of Extinction Coefficient

To establish another useful characteristic of SCS and to deduce possible errors in calculations of concentration (e.g., in determining specific activity or stoichiometry of phosphorylation) it is important to have an accurate evaluation of the absorbance of SCS at 280 nm. Previous determinations were done by Ramaley *et al.* (15) by dry weight and by Grinnell and Nishimura (34) by a method devised by Lowry *et al.* (92). In our estimation of protein concentration, two colorimetric methods were used: biuret (72) and microbiuret (73). Both of these spectrophotometric methods are dependent on the formation of a color complex with peptide bonds. It was therefore significant to determine this parameter by a method independent of a colorimetric procedure (8, 34). Concentrations of protein samples of known absorbance were measured by refractometry in the analytical ultracentrifuge with Rayleigh interference optics. Refractive index increments of proteins vary less than ±2%, whereas the molar refraction of amino acid residues show a greater variation (71). Absorbances at 280 nm were plotted against SCS concentration and the absorption of 0.49 at 280 nm was determined for 1 mg per ml of protein [$E_{1cm}^{1\%}$ at

TABLE I

Determination of Ultraviolet Extinction Coefficient of Succinyl-CoA Synthetase

Method for Protein Determination	Calculated $E_{1cm}^{1\%}$ at 280 nm ± SD
Interference fringe displacement	5.1±0.04
	4.5±0.09
Microbiuret	4.9±0.03
	5.0±0.24
	5.0±0.03
Biuret	4.8±0.06
	4.9±0.04
	5.3±0.08
	4.8±0.04
	4.9±0.07
Mean	4.9±0.07

280 nm is 4.9±0.2]. The concentration of SCS was based on standard nonheme globular proteins which possessed an average fringe displacement of 4.10±0.13 interference fringes per mg per ml. Table I gives a summary of results from the three methods used, which are in general agreement with the value of 5.11 determined earlier by Ramaley *et al.* (15) using dry weight determination, and Grinnell and Nishimura (34) using protein determination pioneered by Lowry *et al.* (92). The low extinction correlates well to the low content of tyrosines and tryptophans in SCS. These amino acids contribute maximally to the major absorbance peak at 280 nm. They constitute only 2% of the entire protein (18).

CHAPTER IV

PHYSICO-CHEMICAL STUDIES OF PHOSPHOENOLPYRUVATE CARBOXYKINASE

A. INTRODUCTION

PEPCK from *Bacillus stearothermophilus* has been reported to have a molecular weight of 130,000 (Cannata, cited in Utter and Kolenbrander (16)). Following comparison to the mammalian and yeast PEPCK of molecular weights 73,000 and 252,000 respectively (16), the authors postulate the mammalian enzyme to be a monomer, the bacterial enzyme to be a dimer, and the yeast enzyme to be a tetramer. However, there is no further evidence to substantiate the proposed oligomeric structures.

Wright and Sanwal (51), working with *E. coli* enzyme, estimated the molecular weight to be approximately 65,000, in distinct contrast to that noted above for the *Bacillus* enzyme. Their determination was obtained by gel filtration and by zone centrifugation in sucrose gradients. No experiments were undertaken in dissociating medium to investigate the possible subunit structure of PEPCK. During the study of the kinetic mechanism of PEPCK, Wright and Sanwal (51) suggested aggregation to explain the sigmoidal kinetics in the presence of NADH, since this type of homotropic cooperativity is generally considered a property of oligomeric enzymes. This prompted us to study molecular weights under non-denaturing and denaturing conditions in order to establish the subunit structure of bacterial PEPCK.

To study possible ligand-induced aggregation, polyacrylamide gel electrophoresis in the presence of SDS was used in conjunction with a cross-linking reagent. Protein samples were previously incubated with SDS or with the bifunctional reagent, dimethylsuberimidate (DMS) (67).

Much information can be gleaned from such cross-linking studies about arrangement of subunits and the alteration of such arrangement incurred by binding of effectors. For example, as mentioned earlier, Teherani and Nishimura (84) applied this approach to SCS and separated five bands on SDS polyacrylamide gel electrophoresis. The conspicuous absence in their patterns of dimers of like subunits (i.e. α_2 and β_2) and the predominance of $\alpha\beta$ dimers intimate that only unlike subunits are adjacent. Kohlhaw and Boatman (93), in another relevant study, applied the cross-linking method to study ligand effects on the quaternary structure of *Salmonella* isopropylmalate synthase. Incubating with DMS and subsequent SDS gel electrophoresis gave rise to four bands (molecular weights 50,000, 100,000, 150,000 and 200,000); upon this basis a tetrametric structure was proposed. In the absence of ligands, the pattern consisted mainly of tetramers and dimers. This pattern changed to one of dimers and monomers in the presence of the feedback inhibitor leucine. Similar studies were done on PEPCK in the presence of some or all substrates or possible effectors to detect possible changes in the quaternary structure.

Amino acid analysis was done by the standard method described by Moore and Stein (94). Composition of bacterial PEPCK is decidedly different from that of the yeast and mammalian enzyme. From the analysis we were also able to calculate the partial specific volume (70) ($\bar{\nu}$ = 0.730) which was used in the calculation of molecular weights from sedimentation equilibrium data. The N-terminal residue of PEPCK seems to be blocked; attempts to identify it by the "Dansyl-Edman" technique (described by Gray (95, 96)) ended in failure. The ultraviolet extinction coefficient for calculating protein concentration was based on two independent measurements of protein concentration: microbiuret (73) and measurements of the refractive index increment in the analytical ultracentrifuge (71).

B. METHODS

Molecular weight studies were done by sedimentation equilibrium and by SDS gel electrophoresis on dissociated and cross-linked protein samples. The techniques are described in Chapter II under General Methods. The procedures for determination of extinction coefficient are also given in Chapter II.

Protein samples for amino acid analysis were prepared by dialyzing the enzyme against 0.05 M N-ethylmorpholine buffer (pH 8.0) and lyophilizing before hydrolysis. Analyses were performed after protein hydrolysis in 2 ml of 6 N constant-boiling HCl for 24, 48, 72 and 96 hours at 110°C in Pyrex tubes (25 mm x 65 mm) sealed under vacuum. The hydrolysates were then evaporated to dryness in a rotary evaporator and dissolved in a suitable amount of deionized water. The amino acid composition of protein was determined on a Beckman Spinco Model 121 or Durham D500 under standard conditions in sodium citrate buffer, essentially as described by Moore and Stein (94). The values of the amino acid residue composition were calculated on the basis of number of moles per molecular weight of protein. The yields of serine, threonine, methionine and tyrosine were extrapolated to zero time to correct for hydrolytic destruction.

Tryptophan was determined by an independent method described by Liu and Chang (97). Protein samples were hydrolyzed in 3 N p-toluenesulfonic acid containing 0.2% 3-(2-aminoethyl)-indole in evacuated sealed tubes for 22, 48 and 72 hours at 110°C, followed by the standard automated amino acid analysis described above. The number of sulfhydryl groups were estimated from a DTNB modification of these residues under dissociating conditions, as described by Habeeb (98). The total cysteine and cystine content was measured as cysteic acid by performic acid oxidation (99).

C. RESULTS AND DISCUSSION

1. Molecular Weight and Subunit Structure

The molecular weight for *E. coli* PEPCK was estimated by Wright and Sanwal (51) to be approximately 64,000 based on Sephadex G-200 gel filtration and zone centrifugation in sucrose gradients. These investigators did not explore the subunit structure of PEPCK by studying molecular weights in dissociating buffers, but assumed the enzyme to be an aggregate of more than one subunit to account for the allosteric kinetics produced by NADH. They observed that NADH induced homotropic cooperativity and sigmoidal kinetics on substrate saturation curves when HCO_3^- and PEP were varied. This phenomenon is generally regarded as a property of oligomeric proteins where multiple binding sites per substrate are made available by the aggregation of subunits[3].

Fig. 3 shows a representative sedimentation equilibrium run in non-dissociating medium. The molecular weight (M_w) of 65,000 was calculated from a plot of ln c *vs.* r^2 which behaves as an ideal single-component system. In this and several other experiments negligible aggregation

---

[3] Examples of allosteric monomeric proteins have been cited in the literature (100, 101). Ribonucleotide reductase (100) is activated whereas homoserine transacetylase from *Bacillus polymyxa* (101) is subjected to feedback inhibition by methionine and its derivatives. Both of these monomeric enzymes show allosteric control, but neither shows homotropic cooperativity in kinetic patterns.

FIGURE 3. Determination of molecular weight of PEPCK by sedimentation equilibrium. Data were taken from the photoelectric scanner (λ = 280 nm). The conditions of the run were as follows: solvent, 0.1 M tris-HCl, pH 7.5 with 0.1 mM dithiothreitol and 80 mM $MgCl_2$; temperature, 22°C; speed, 11,000 rpm.

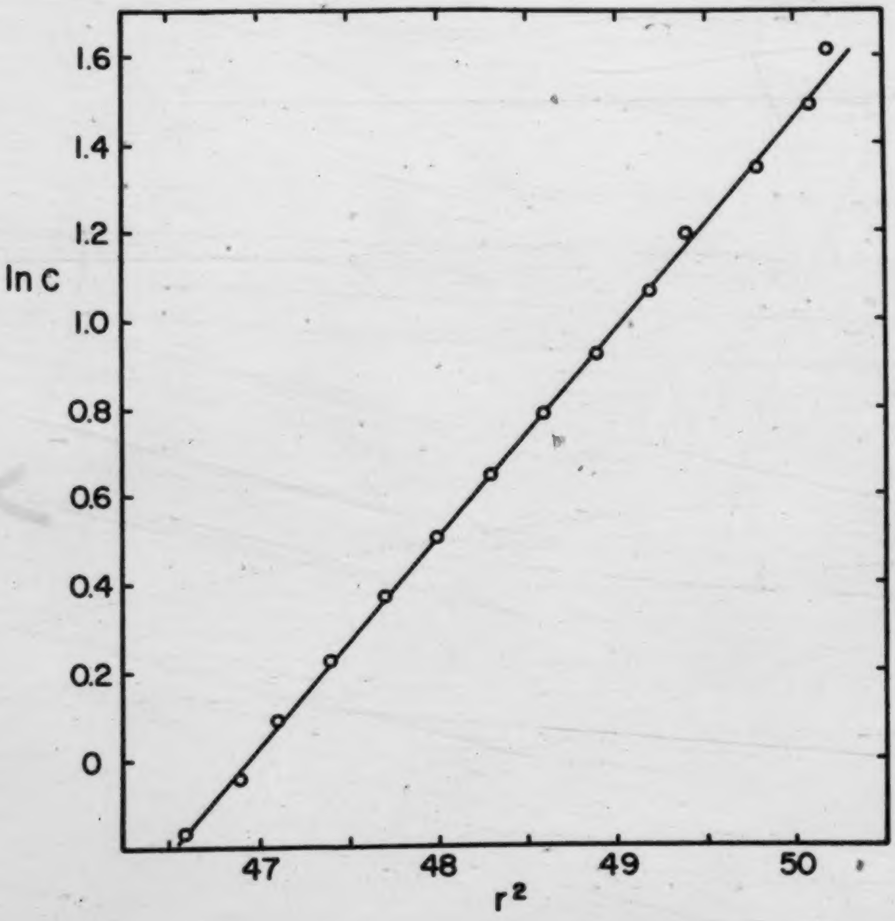
ln c
1.6
1.4
1.2
1.0
0.8
0.6
0.4
0.2
0
47
48
49
50
r²

is observed at relatively high concentration (1 mg per ml) near the cell bottom regardless of the presence or the absence of divalent metal ions in the medium. Table II lists the results of several molecular weight estimations in the presence and absence of denaturants. The average molecular weight of 65,000 under non-dissociating conditions by sedimentation equilibrium confirms Wright and Sanwal's (51) earlier estimate.

Polyacrylamide gel electrophoresis enables the reliable determination of the molecular weights of monomeric proteins or of the monomeric polypeptide chains of proteins containing several subunits (102, 66). Gel B in Fig. 4 shows that a single band is produced by electrophoresis in non-dissociating conditions, attesting to the purity of the enzyme preparation. PEPCK also shows a single band following electrophoresis in the presence of SDS, as shown by gel A of Fig. 4. This rules out the possibility that the enzyme is constituted of subunits of substantially differing sizes.

Weber and Osborn (66) have shown that a linear relationship exists between the logarithm of molecular weight and the electrophoretic mobility of polypeptides in the presence of SDS. This method can be used with confidence to determine the size of polypeptide chains for a wide variety of proteins. The molecular weight of PEPCK was calculated from such a plot of logarithm of molecular weight of standard proteins. Fig. 5 shows that the molecular weight of the basic structural unit of PEPCK is 64,000±2,000. From the results of our molecular weight study in dissociating and non-dissociating medium we are left with the clear conclusion that PEPCK is a monomer exhibiting the same molecular weight (*ca.* 65,000) under all conditions.

The conclusion that PEPCK is a monomer is further supported by

TABLE II

Molecular Weight of *E. coli* PEPCK in presence and absence of denaturants

Conditions	Observed Molecular Weight
Sed. eqm., 0.1 M Tris-HCl, 0.1 mM dithiothreitol, pH 7.5, 80 mM $MgCl_2$, 20°C	65,000
Sed. eqm., 0.1 M Tris-HCl, 0.1 mM dithiothreitol, pH 7.5, 1.6 mM $MnCl_2$, 20°C	62,500
Sed. eqm., 0.1 M Tris-HCl, 0.1 mM dithiothreitol, pH 7.5, 1 mM EDTA, 20°C	69,500
Sed. eqm., 0.1 M Tris-HCl, 0.1 mM dithiothreitol, pH 7.5, 1 mM EDTA, 4°C	59,000
Calibrated gel filtration column	64,000*
Centrifugation in sucrose density gradient	65,000*
SDS-gels (mean ± SD for seven determinations)	64,000±2,000

* Ref. 51

FIGURE 4. Polyacrylamide gel electrophoresis of a preparation of PEPCK. Gel A: Electrophoresis conducted in the presence of SDS using 7% gels. Gel B: Analytical run in 7% in absence of denaturants.

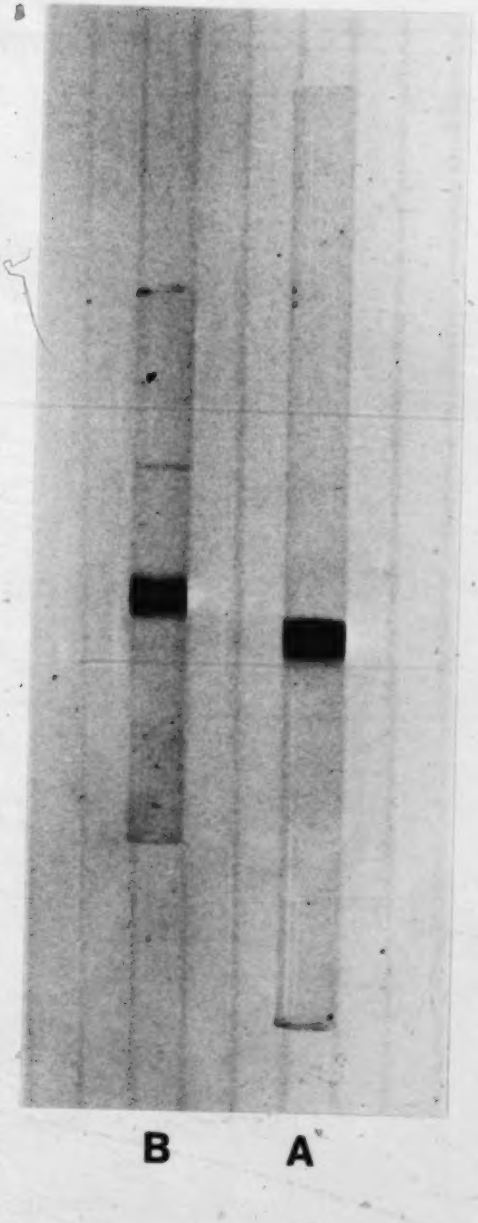

B
A

FIGURE 5. Determination of molecular weight of basic structural unit of PEPCK by SDS-gel electrophoresis. 7% Gels were used. The standards are: 1, bovine serum albumin dimer; 2, glycogen phosphorylase; 3, bovine serum albumin monomer; 4, glutamate dehydrogenase; 5, ovalbumin. The molecular weight calculated for PEPCK is based upon the migration (mean ± SD) measured in seven replicate experiments.

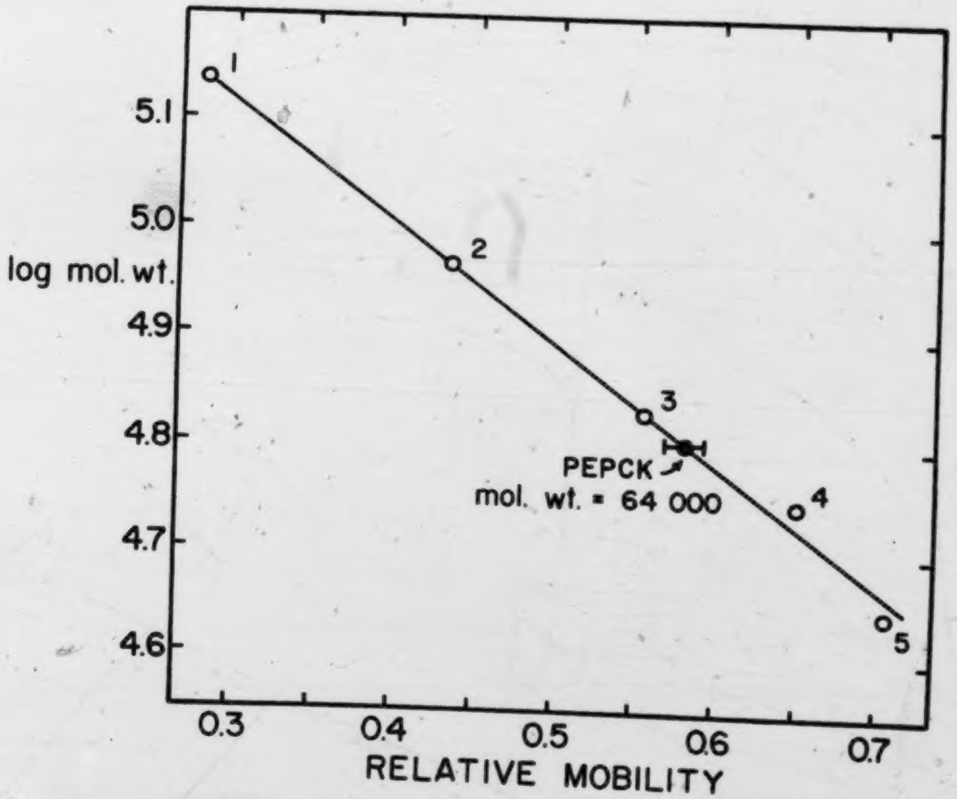
log mol. wt.
5.1
5.0
4.9
4.8
4.7
4.6
0.3
0.4
0.5
0.6
0.7
RELATIVE MOBILITY
1
2
3
4
5
PEPCK
mol. wt. = 64 000

FIGURE 6. Electrophoresis on 5% polyacrylamide gels in the presence of SDS. A. Cross-linking of PEPCK with DMS. Gel 1: 17 µg PEPCK cross-linked with 7.5 µg DMS. Gel 2: 15 µg PEPCK cross-linked with 163 µg DMS. Gel 3: 15 µg PEPCK in the absence of DMS. B. Cross-linking of SCS with DMS (control). Gel 1: 24 µg SCS cross-linked with 7.5 µg DMS. Gel 2: 21 µg SCS cross-linked with 163 µg DMS. Gel 3: 21 µg SCS in the absence of DMS.

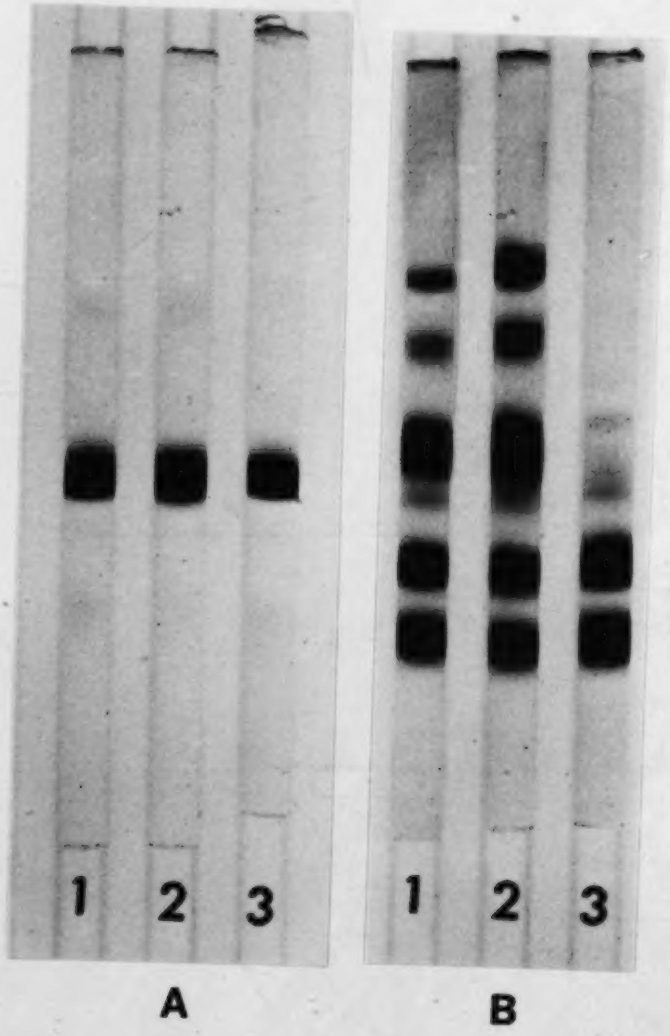
1
2
3
1
2
3
A
B

the failure of the cross-linking reagent DMS to produce cross-linked oligomers when incubated with PEPCK either alone or together with substrates or NADH. Protein samples were incubated with minimum and maximum concentrations (0.015 mg and 0.38 mg) of DMS and in the absence and presence of substrates or effectors to encourage possible association of subunits. In all cases (see Fig. 6) SCS, which was used as a control, showed the typical five-band pattern whereas PEPCK remained a single band. In keeping with a monomeric structure for PEPCK, we cannot induce ligand effects on the quaternary structure in the presence of substrates or inhibitor as was observed in isopropylmalate synthase (93), which was discussed in the introduction to this chapter. Our results give clear evidence that PEPCK is a monomer with all ligand binding sites contained on a single polypeptide chain. Such a monomeric structure is difficult to reconcile with the sigmoidal kinetics shown by Wright and Sanwal (51). This difficulty prompted us to reinvestigate the inhibition studies with NADH to determine whether this monomeric enzyme is capable of showing true homotropic cooperativity (see Chapter V).

2. Amino Acid Analysis and Determination of Extinction Coefficient

A comparison of the amino acid composition of the pig liver enzyme (13), yeast enzyme (103) and *E. coli* enzyme (from this work) is given on Table III. On preliminary inspection they show similarities in that all three enzymes contain approximately equal percentages of basic, acidic and aromatic residues. Closer inspection of individual amino acid contributions show that lysine, aspartate, threonine and tyrosine are all >2% lower and that arginine, glutamate and proline, are all >2% higher in the pig liver PEPCK (13) than in the *E. coli* PEPCK. A comparison between yeast (103) and

TABLE III

Amino Acid Composition of Phosphoenolpyruvate Carboxykinase

	PEPCK					
Amino Acid	Pig Liver (Ref. 13)		Yeast (Ref. 103)		*E. coli* (This work)	
	*	%	*	%	*	%
Lysine	26	3.9	155	6.9	37	6.3
Histidine	12	1.8	69	3.1	17	2.9
Arginine	48	7.2	95	4.2	24	4.1
Tryptophan	13	2.0	30	1.3	7	1.2
Aspartic Acid	53	8.0	224	9.9	64	10.9
Threonine	31	4.7	147	6.5	38	6.5
Serine	31	4.7	142	6.3	26	4.4
Glutamic Acid	70	10.6	231	10.2	52	8.9
Proline	56	8.4	116	5.1	36	6.1
Glycine	64	9.7	155	6.9	49	8.4
Alanine	55	8.3	180	8.0	53	9.0
Half-Cystine	15	2.3	41	1.8	6	1.0
Valine	44	6.6	145	6.4	38	6.5
Methionine	20	3.0	16	0.7	14	2.4
Isoleucine	28	4.2	150	6.6	30	5.1
Leucine	58	8.7	181	8.0	53	9.0
Tyrosine	12	1.8	90	4.0	20	3.4
Phenylalanine	27	4.1	95	4.2	22	3.8

*Number of residues per molecule of enzyme. Pig liver, yeast and *E. coli* PEPCK have molecular weights of 73,000, 252,000 and 65,000 respectively.

bacterial PEPCK shows other differences: glycine and methionine are approximately 2% lower, glutamate is somewhat higher in the yeast (103) than in the bacterial enzyme.

Free sulfhydryl groups were determined by DTNB modification in the presence of SDS. (In non-denaturing medium the sulfhydryl groups were not available for reacting with DTNB, but were buried in the interior of the molecule and became exposed only when the protein was unfolded.) This determination showed PEPCK to have four sulfhydryl groups per mole. Total half-cystine content determined by performic acid oxidation to cysteic acid was six per mole of enzyme. It is possible that unfolding of the polypeptide chain in the presence of SDS was incomplete leaving two of the sulfhydryl groups buried in the secondary structure and inaccessible to DTNB.

The protein concentration for the determination of the ultraviolet extinction coefficient was determined by microbiuret (73) and interference fringe displacement in the ultracentrifuge (71). Data from several experiments are listed in Table IV from which the average value of $E_{1cm}^{1\%}$ is calculated at 280 nm to be 12.5±1.5. This value correlates well with that previously determined for SCS when we compare the content of amino acid residues which contribute to the absorption near 280 nm. In PEPCK the tyrosine and tryptophan content is 4.6% whereas in SCS their content is roughly 2%. For these proteins the extinction coefficients at 280 nm are 12.5 and 5 respectively. This argument cannot be extended to the ultraviolet absorption of the pig liver PEPCK (13). The value for its $E_{1cm}^{1\%}$ is 6.13, determined by estimating the protein concentration from amino acid analysis and from refractometric measurements and using the

TABLE IV

Determination of the Ultraviolet Extinction Coefficient of Phosphoenolpyruvate Carboxykinase

Method for Protein Determination	Calculated $E_{1cm}^{1\%}$ at 280 nm ± SD
Interference fringe displacement	12.0±0.15
	9.1±0.2
Microbiuret	11.6±0.9
	15.9±3.3
	14.1±3.1
Mean	12.5±1.5

value of 1.862 x 10^{-4} as the specific refractive index increment per mg per ml. The total tyrosine and tryptophan content is 3.7%, almost the same as the bacterial PEPCK which has an absorbance of twice the value. The lower extinction coefficient in the pig liver PEPCK could perhaps be due to stacking of aromatic amino acids and resultant π-electron delocalization.

CHAPTER V

KINETIC STUDIES OF PHOSPHOENOLPYRUVATE CARBOXYKINASE

A. INTRODUCTION

1. Inhibition by NADH

During the course of the structural investigation we determined *E. coli* PEPCK to be a monomer in the presence and absence of denaturants. Since Wright and Sanwal (51) had shown that this enzyme gave rise to sigmoidal substrate saturation plots when assayed in the presence of NADH, we were eager to reinvestigate and confirm this possible case of a monomeric enzyme exhibiting homotropic cooperativity.

Our results presented in this section differ from those of Wright and Sanwal (51) in that we do not detect sigmoidal substrate saturation plots in the presence of NADH. Such lack of homotropic cooperativity is, however, easily reconciled with our conclusion that *E. coli* PEPCK has a monomeric structure.

2. Comparison of Relative Rates

Chang *et al.* (60) studied the kinetics of various possible exchange reactions together with the overall decarboxylation and carboxylation reactions catalyzed by PEPCK from pig liver. They found that the rate of the Mn-ITP-dependent $H^{14}CO_3^- \leftrightarrow$ OAA exchange was faster than the rates of either net PEP or OAA formation. The relative rates at pH 6.8 were 30 for the exchange reaction, 8.3 and 1 for the PEP and OAA formation, respectively. The authors were unable to detect significant exchanges of GDP-8-^{14}C with GTP, ^{32}PEP with ITP or PEP-1-^{14}C with OAA and concluded that a covalent intermediate, either a bound phosphoryl group or a nucleotide was not involved in the reaction mechanism. Based on the faster $HCO_3^- \leftrightarrow$ OAA exchange reaction and the ITP requirement indicates that cleavage of the β-carboxylate C-C bond of OAA occurs concomitantly with or following a prior reaction of ITP, the authors proposed that the overall catalysis must occur in two steps:

$$E + PEP + IDP \underset{k_{-1}}{\overset{k_1}{\rightleftharpoons}} E\text{-}X \qquad [13]$$

$$E\text{-}X + HCO_3^- \underset{k_{-2}}{\overset{k_2}{\rightleftharpoons}} E + OAA + ITP \qquad [14]$$

The first step, k_1 and k_{-1}, would be the rate-limiting step and k_2 and k_{-2} the fast step that exchanges ^{14}C between HCO_3^- and OAA.

With the *E. coli* enzyme, a similar study indicated the rate of ATP-dependent $H^{14}CO_3^- \leftrightarrow$ OAA exchange to be four times faster than the overall carboxylation. The relative rate of the decarboxylation of OAA could not be measured due to the faster non-enzymatic decarboxylation of OAA in solution at pH 6.8 relative to the enzymatic decarboxylation. In order to investigate the disparity of relative rates under more equal and controlled conditions, we measured isotope exchanges between $H^{14}CO_3^- \leftrightarrow$ OAA and ^{14}C-ATP $\leftrightarrow$ ADP at chemical equilibrium. The specific reactant concentrations in the two parallel experiments were identical and calculated from the equilibrium constant of 3.1 M (80). When measured under identical conditions the exchange rate of $H^{14}CO_3^-$ $\leftrightarrow$ OAA was confirmed to be four times faster than the ^{14}C-ATP $\leftrightarrow$ ADP exchange.

3. Initial Rate Kinetics and Product Inhibition of PEPCK

From initial rate studies and studies of exchange of ^{14}C between OAA and HCO_3^- in the presence of ITP, Chang *et al.* (60) proposed a two-step sequence for the pig liver enzyme as shown in the previous section (equations 13 and 14). Since the exchange reaction was found to be 30- and 4- times faster than the overall carboxylation and decarboxylation rate, respectively, the first step was suggested to be rate-limiting. The observation that PEP inhibits the ITP-dependent $HCO_3^- \leftrightarrow$ OAA exchange reaction and does not inhibit the overall decarboxylation is consistent with the above two-step sequence. In a later paper, Miller and Lane (61) abandoned the two-step mechanism for a concerted one on the grounds of a more thorough investigation of initial rate kinetics. The formation of a central complex consisting of enzyme, Mn^{2+}, PEP, IDP and HCO_3^- proceeds by a mixed ordered-random addition of components. PEP and/or Mn^{2+} add first to the free enzyme to yield an active enzyme complex (if HCO_3^- binds first a dead-end complex was formed) then IDP and HCO_3^- may bind (61) in a random fashion. From the primary double reciprocal plots it was shown that only OAA was a competitive product inhibitor with HCO_3^-, and that ITP showed a 'mixed' type inhibition.

Wright and Sanwal (51) suggested a sequential mechanism for bacterial PEPCK, based on initial rate studies in the absence of products. All the primary plots of $1/\nu$ *vs.* $1/S$ showed a pattern of intersecting lines to the left of the ordinate. A sequential mechanism could be either ordered with substratesbinding to the enzyme in a compulsory binding sequence, or rapid equilibrium random, with substrates binding to the enzyme in a completely random and rapid manner and only the interconversion of the quaternary complex being rate limiting, or a partially ordered-random mechanism. Product inhibition studies (51) indicated that only ATP and ADP bind to the free enzyme but technical difficulty prevented determination of the order of binding of PEP and HCO_3^-. If ATP had been shown to be competitive with all substrates, a rapid equilibrium random mechanism could have been proposed. Since ATP gave non-competitive inhibition with PEP and HCO_3^-, a rapid equilibrium random mechanism was ruled out. Another consequence of random binding of substrates (for non-rapid equilibrium) (36) is that the replots of slopes and intercepts of the double reciprocal plots against product inhibitor are nonlinear. In their work Wright and Sanwal (51) found only linear replots. From all of this they proposed an ordered binding sequence for bacterial PEPCK.

In the present study, initial velocity data suggest that the major kinetic mechanism for bacterial PEPCK is fully random sequential.

4. Isotope Exchange Rates at Chemical Equilibrium

The initial rate kinetic experiment described in the previous section defines a rapid random equilibrium kinetic mechanism for PEPCK and this must be a major pathway of the catalytic process. However, these studies are not sufficiently sensitive to rule out the possible operation of minor pathways under various conditions. A more sensitive probe of reaction mechanism is the study of the kinetics at equilibrium in the absence of net chemical change made possible by the use of isotopically-labelled substrates.

A discrepancy remains between the rates of the overall carboxylation measured by a sensitive coupled enzymatic reaction and the ATP-dependent $HCO_3^- \longleftrightarrow$ OAA exchange reaction discussed previously under 'Comparison of Relative Rates'. To investigate the disparity of exchange rates we measured the two exchanges, $HCO_3^- \longleftrightarrow$ OAA and ATP ⟷ ADP in the presence of a substrate-product pair at an increasing concentration ratio. This would differentiate between an ordered or random sequential mechanism, as was elucidated by the pioneering work of Boyer and Silverstein (82) to support our initial rate kinetic study. It will also indicate whether the mechanism is fully random or possesses minor pathways of ordered substrate binding or of dead-end binding complexes as would be indicated by the disparity of relative rates. In a compulsory binding sequence, the most rapid exchange must occur between the last reactant to bind and the first product to dissociate; all other exchanges must be slower or equal in rate.

5. Nucleotide Specificity

SCS and PEPCK both exhibit a nearly identical nucleotide specificity. Their functions could be perhaps coupled by the capacity of SCS to generate the nucleotide triphosphates. SCS from mammalian sources prefer guanosine or inosine nucleotides. The pig heart enzyme is also capable of utilizing GTP derivatives: 8-aza GTP (104) or 6-thio GTP (88). The *E. coli* PEPCK was thought to adhere to strict specificity for adenine nucleotides, but it has been established recently that ATP can be replaced by GTP and ITP showing decreasing effectiveness in that order (18).

PEPCK is similar in that the mammalian enzyme prefers GTP and GDP or ITP and IDP as substrates. Barzu *et al.* (105) reported that guinea pig liver PEPCK shows a stringent requirement for nucleotides with intact keto and NH groups at C_6 and N_1 of the purine ring. This selection would include GTP, GDP, ITP, IDP, XTP and XDP. Analogues of GDP in which the N_1 is masked and the keto group at C_6 is converted to the enol form shows no substrate properties. The *E. coli* PEPCK has been noted to be quite selective for ATP in the catalysis of the ATP-dependent $HCO_3^- \longleftrightarrow$ OAA exchange. This was investigated by Wright and Sanwal (51) who found GTP and ITP to be inert as substrates for the bacterial enzyme.

Since SCS proved to be not as stringent in its requirement for specific nucleotides, we were interested to reinvestigate the nucleotide specificity of the bacterial PEPCK with inosine and guanine nucleotides together with several analogues of ATP.

B. METHODS

1. Inhibition by NADH

The colorimetric assay used for NADH inhibition study is described in Chapter II under General Experimental Methods. The study was carried out in 80 mM $MgCl_2$ and several experiments were repeated in which the $MgCl_2$ was replaced by 5.0 mM $MnCl_2$ in order to compare the kinetic properties.

2. Comparison of Relative Rates

For this study all assay systems used are given in Chapter II under General Experimental Methods. To determine the rate of the overall carboxylation, all three assays for OAA formation were used: isotope incorporation from $^{14}C\text{-}HCO_3^-$ into ^{14}C-OAA, spectrophotometric measurements of NADH oxidation at 340 nm when the reaction was coupled to malate dehydrogenase and the colorimetric assay in which OAA forms a colored complex with an azo dye and absorbs at 520 nm. The concentration of substrates for the first two assays were as follows:

5.0 mM $MnCl_2$, 2.0 mM DTT, 40 mM $KHCO_3$, 1.45 mM PEP and 2.0 mM ADP. For the colorimetric measurements the substrate concentrations were 5.0 mM $MnCl_2$, 0.2 mM DTT, 50 mM $KHCO_3$, 9.47 mM PEP and 4 mM ADP. Substrate concentrations for the isotope exchange reactions were: for the $H^{14}CO_3^- \leftrightarrows$ OAA exchange 5.0 mM $MnCl_2$, 2.0 mM DTT, 40 mM $KHCO_3$, 3mM ATP and 2 mM OAA. For the exchanges at chemical equilibrium, concentrations were adjusted according to the K_{eq} of 3.1 M (for PEP formation) (80): 1.7 mM $MnCl_2$, 13.3 mM $KHCO_3$, 0.2 mM PEP, 0.2 mM ADP, 0.01 mM ATP 16.7 mM OAA and 2.0 mM DTT.

3. Initial Rate Kinetics and Product Inhibition of PEPCK

The coupled enzymatic assay used in the study of initial rates and product inhibition is described in detail in Chapter II.

4. Isotope Exchange Reactions at Chemical Equilibrium

Isotope exchanges between $HCO_3^- \leftrightarrows$ OAA and ADP $\leftrightarrows$ ATP were done with $^{14}C\text{-}HCO_3^-$ and ^{14}C-ATP. Methods of isolating the radioactive products are described in Chapter II.

5. Nucleotide Specificity

Nucleotide triphosphate dependent $H^{14}CO_3^- \leftrightarrows$ OAA isotope exchange assay was used in determining the nucleotide specificity. The assay system is described in Chapter II.

C. RESULTS AND DISCUSSION

1. Inhibition by NADH

Wright and Sanwal (51) found that plots of velocity versus the concentration of PEP and HCO_3^- become sigmodial in the presence of NADH. Our own conclusion that the enzyme consists of a single subunit is irreconcilable with current models for homotropic cooperativity. However, in contrast to the previous results we observed normal substrate saturation curves in our study of inhibition by NADH. Fig. 7 shows a duplicate of Wright and Sanwal's experiment (Fig. 8 of Ref. 51). In this and several other identical experiments with several preparations of pure PEPCK, inhibition was observed but there is no evidence that NADH induces homotropic cooperativity.

Ballard (53), in his study on mammalian cytosol PEPCK, showed that malate was a competitive inhibitor with respect to OAA when Mn^{2+} was the added divalent cation but non-competitive when Mg^{2+} was the cation. Such an altered inhibition characteristic was not observed for the *E. coli* enzyme when Mn^{2+} was exchanged for Mg^{2+} in the inhibition study with NADH. This is shown in Fig. 8. It has previously been observed that in the presence of Mn^{2+} (rather than Mg^{2+}) the K_m values are lowered (53). Fig. 7 illustrates that the K_m for PEP in the presence of Mg^{2+} is 8 mM while in the presence of Mn^{2+} (Fig. 8) the K_m for the PEP is reduced to 0.5 mM. The maximum velocity in the presence of Mn^{2+} as the activating cation was slightly increased (1.5-fold) compared to that in the presence of Mg^{2+}.

Subsequent to our study, it was reported (106) that the inhibition of PEPCK by NADH was an artifact of the colorimetric assay. This conclusion agrees well with our observation that NADH is not inhibiting when the coupled enzymatic assay was used in which activity was followed by the oxidation of NADH to NAD^+ at 340 nm. In all coupled enzymatic assays 0.15 to 0.3 mM NADH was added. At this concentration maximum velocity was achieved while at higher concentration of NADH the velocity decreased. However the decreased rate at NADH concentration over 0.3 mM could perhaps

Figure 7 Double reciprocal plots of velocity *vs* [PEP] showing inhibitory effect of NADH. Other components of the assay solution were 80 mM $MgCl_2$, 0.2 mM DTT 40 mM $NaHCO_3$, 3.8 mM ADP and 0.1 M tris-HCl, pH 7.5. The rate of oxaloacetate formation was measured colorimetrically.

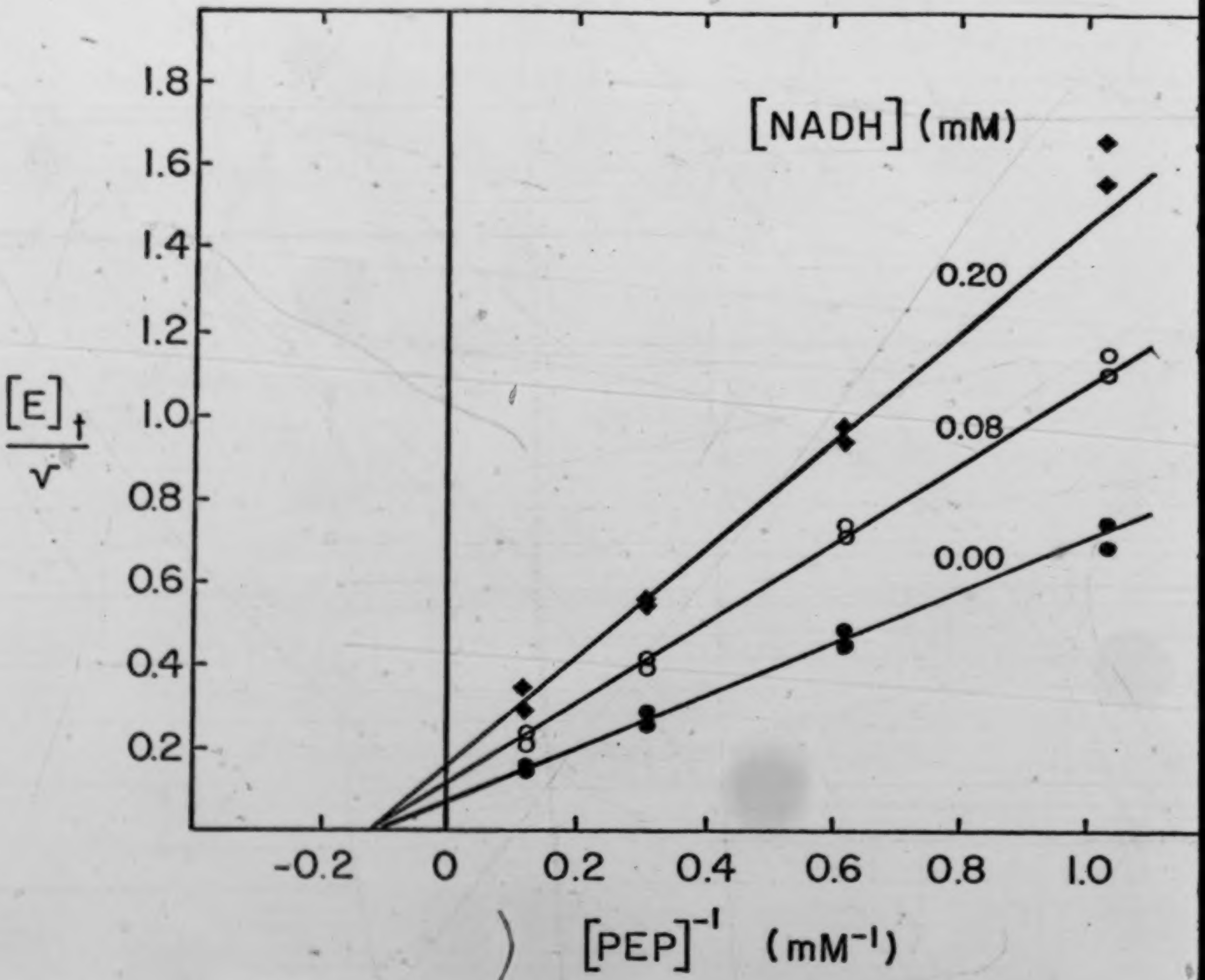
[NADH] (mM)
0.20
0.08
0.00
$\frac{[E]_t}{v}$
1.8
1.6
1.4
1.2
1.0
0.8
0.6
0.4
0.2
-0.2
0
0.2
0.4
0.6
0.8
1.0
$[PEP]^{-1}$ (mM^{-1})

Figure 8 Effect of replacement of $MgCl_2$ by $MnCl_2$ on kinetics and NADH inhibition of PEPCK. Conditions are as given under Figure 7, expect that 5.0 mM $MnCl_2$ was substituted for $MgCl_2$.

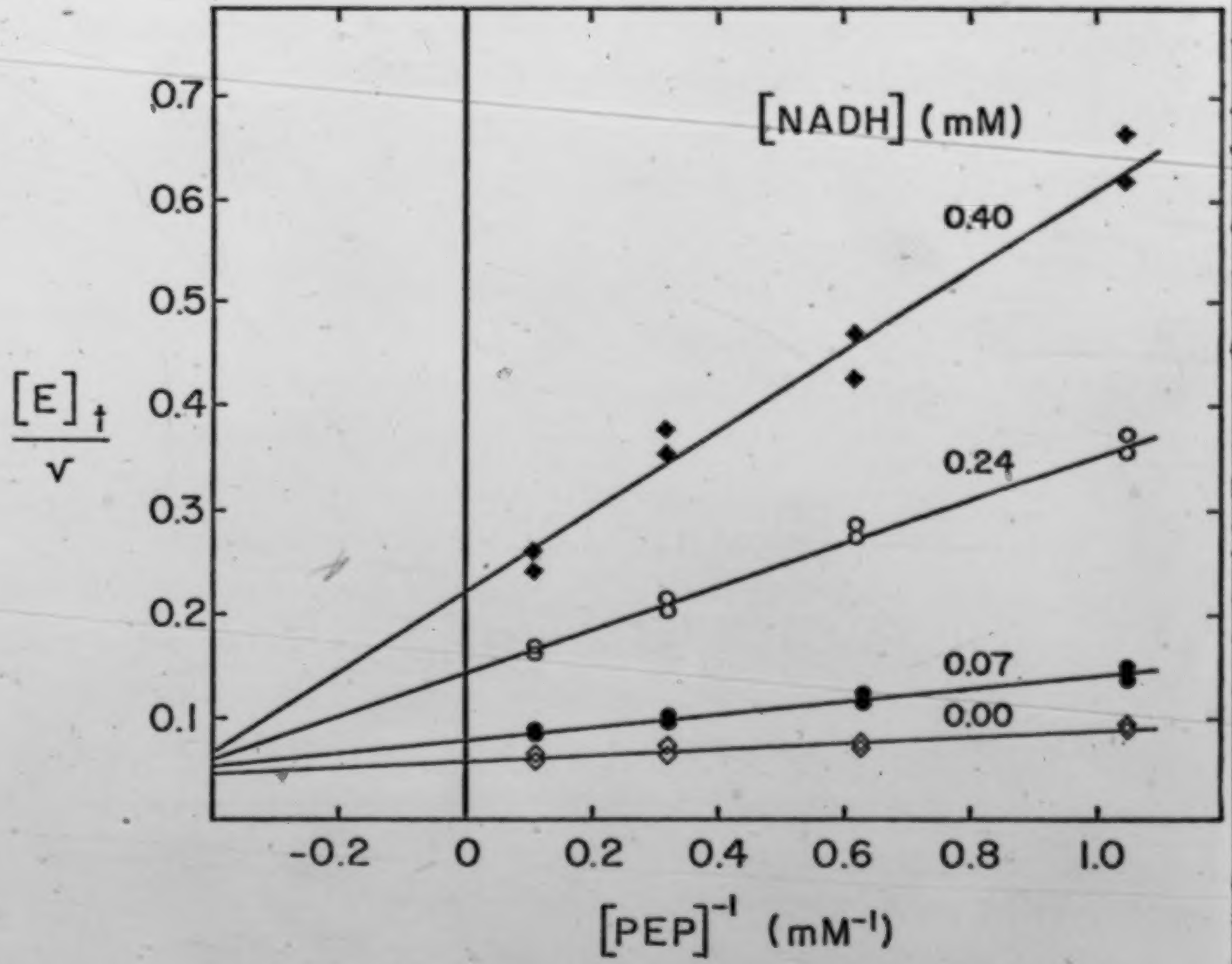
[NADH] (mM)
0.40
0.24
0.07
0.00
$\frac{[E]_t}{v}$
0.7
0.6
0.5
0.4
0.3
0.2
0.1
-0.2
0
0.2
0.4
0.6
0.8
1.0
$[PEP]^{-1}$ (mM^{-1})

be due to a secondary effect on malate dehydrogenase, which is known to be inhibited by NADH (55). From our study of 'Comparison of Relative Rates' we observed that the rate of OAA formation measured by the colorimetric reaction was 20.7 μmoles/min/mg while that measured by the coupled enzymatic reaction in the presence of 0.2 mM NADH was slightly higher 28 μmoles/min/mg. Since Figs. 7 and 8 would require that 0.2 mM NADH inhibit the catalytic activity by almost 80%, this apparent inhibition is confined to the colorimetric assay and is therefore likely an artifact.

2. Comparison of Relative Rates

The relative rates of the overall carboxylation and of the overall decarboxylation compared to the ATP-dependent $H^{14}CO_3^- \leftrightarrow$ OAA exchange reactions are given in Table V. We calculate a smaller (fourfold) disparity in rate than that reported for the mammalian enzyme (60).

Before consideration of the disparity in rates we must account for the ATP dependency of the $HCO_3^- \leftrightarrow$ OAA exchange reaction. It must be recognized that this exchange need not reflect a partial reaction because it shows an obligatory requirement for ATP. In the presence of ATP and OAA, the enzyme is provided with all the necessary substrates to catalyze the overall decarboxylation to form products (PEP, HCO_3^- and ADP). Therefore, the most obvious rationale for the ATP dependence would involve exchange via overall forward and reverse reactions once sufficient PEP had accumulated to allow the reverse to proceed. This explanation is unattractive, however, in view of the relative rapidity of the exchange, the apparent lack of time lag (76) and the fact that the exchange is

Table V

Comparison of Relative Rates of Phosphoenolpyruvate Carboxykinase

	Reaction Rates	
	E. coli	pig liver**
Carboxylation Reaction		
1) Coupling PEPCK to MDH		
(a) $^{14}C\text{-}HCO_3^-$ incorporated into malate	29.5	
(b) Oxidation of NADH measured spectrophotometrically	28.3	1.0
2) Colorimetric assay	20.7	
Decarboxylation Reaction		
1) Coupling PEPCK to PK and LDH		
(a) Oxidation of NADH at 340 nm	N.D.	8.3
Mn-ATP-dependent $^{14}C\text{-}HCO_3^- \leftrightarrow$ OAA	109.0	30.0
Isotope Exchange at Chemical Equilibrium		
1) $^{14}C\text{-}ATP \leftrightarrow ADP$	0.317	
2) $^{14}C\text{-}HCO_3^- \leftrightarrow OAA$	1.23	

---

* Rate is expressed as µmoles per min per mg PEPCK.

** Rate is expressed as µmoles per min per 5×10^{-3} unit of purified PEPCK (60).

N.D. We were not able to repeat enzymatic decarboxylation of OAA since non-enzymatic decarboxylation was equally fast or faster.

inhibited, rather than stimulated, by the addition of PEP (Fig. 9)[4].

An alternative model, which we consider to be consistent with all available data, would envision a 'substrate synergism' role for ATP in promoting the $HCO_3^- \rightleftarrows$ OAA exchange. This concept was first developed to account for anomalous exchange kinetics of succinyl-CoA synthetase (26). With that enzyme the ATP $\rightleftarrows$ ADP exchange reflecting phosphoenzyme formation was found to be relatively slow, but stimulated by other substrates, suggesting that the catalytic site is fully active when all substrate-binding sites are filled. This phenomenon has been designated substrate synergism (26). For PEPCK, the ATP-dependent isotope exchange between $HCO_3^- \rightleftarrows$ OAA would be viewed in a similar manner with ATP effecting substrate synergism. ATP exhibits an all or none effect for the $HCO_3^- \rightleftarrows$ OAA exchange reaction, rather than a stimulation of a slow exchange. In this role ATP would be bound to the enzyme before OAA could be hydrolyzed. This is shown in the following scheme:

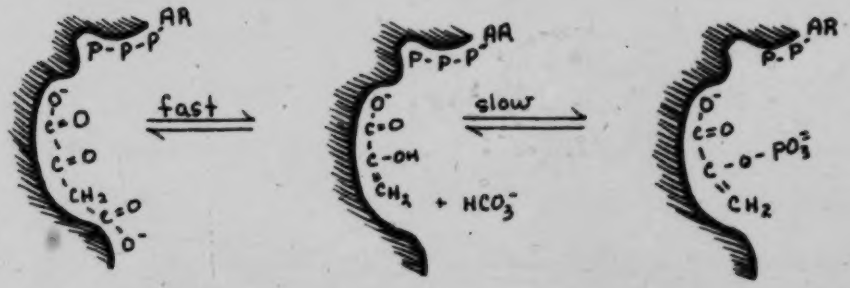

SCHEME C

---

[4] It is curious that PEP gives non-competitive inhibition with ATP for the ATP-dependent $HCO_3^- \rightleftarrows$ OAA exchange reaction (Fig. 9) whereas ATP gives competitive inhibition with PEP during the carboxylation reaction. (See Fig. 15 of Section 3 on Initial Rate Kinetics and Product Inhibition of this chapter.)

Figure 9 Double reciprocal plots of velocity *vs* [ATP] for the ATP-dependent isotope exchange reaction showing inhibitory effect of PEP. Other components of the assay solution were 3 mM $MnCl_2$, 2.2 mM DTT, 40 mM $KHCO_3$, 2 mM OAA and 0.1 M imidazole-HCl, pH 6.8. $^{14}C-KHCO_3$ (3×10^4 cpm/μmole) was the isotope added to the assay.

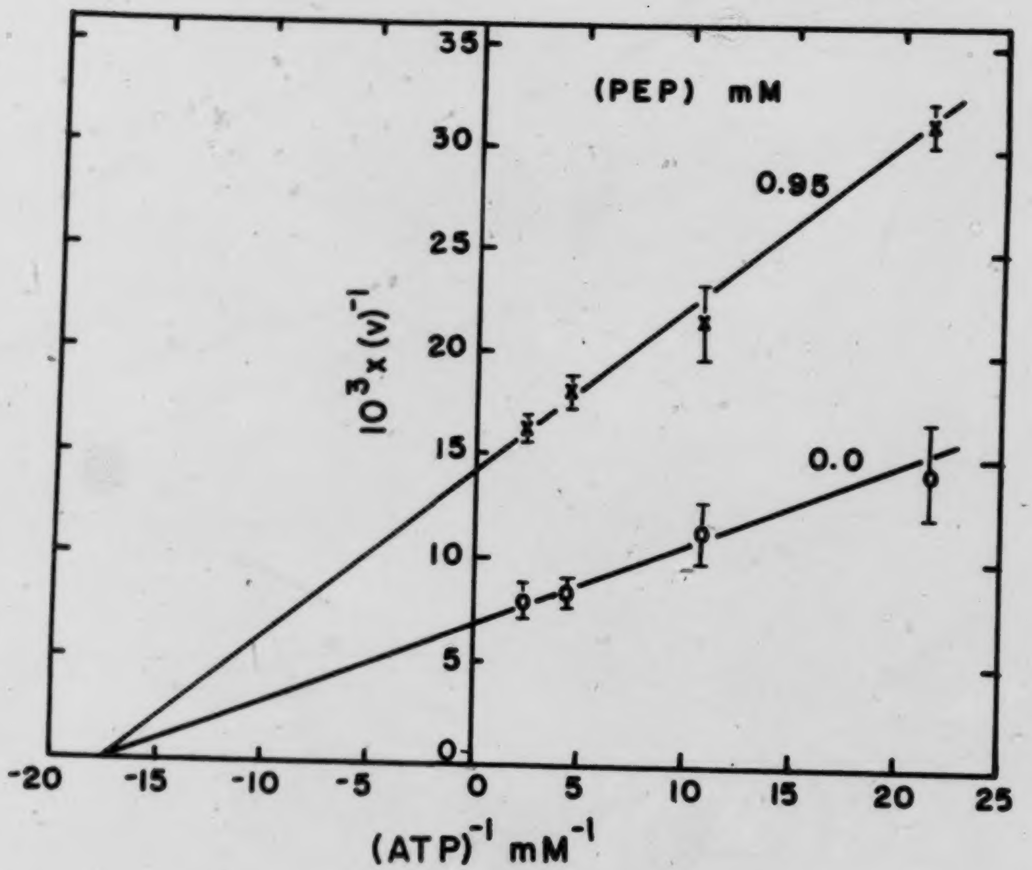
(PEP) mM
0.95
0.0
$10^3 x (v)^{-1}$
35
30
25
20
15
10
5
0
-20
-15
-10
-5
0
5
10
15
20
25
$(ATP)^{-1}$ mM^{-1}

Scheme C illustrates that the fast step is the hydrolysis of OAA to enolpyruvate and bicarbonate, accounting for the ^{14}C exchange in question. It seems to be essential that ATP is attached to its site before this reaction can occur, and to be particularly important that the γ-phosphoryl group of ATP is appropriately ligated, since ADP cannot replace ATP. The slow step following the hydrolysis of OAA is the transfer of the terminal phosphate of ATP to enolpyruvate to form PEP. Inhibition of the exchange by PEP must be the result of formation of Michaelis complexes containing that substrate which are thereby removed from the pool of enzyme catalyzing the rapid exchange.

A special case for the substrate synergism by ATP could involve transfer of its terminal phosphoryl group to the enzyme, forming a phosphoenzyme capable of catalyzing the exchange as shown in the following illustration:

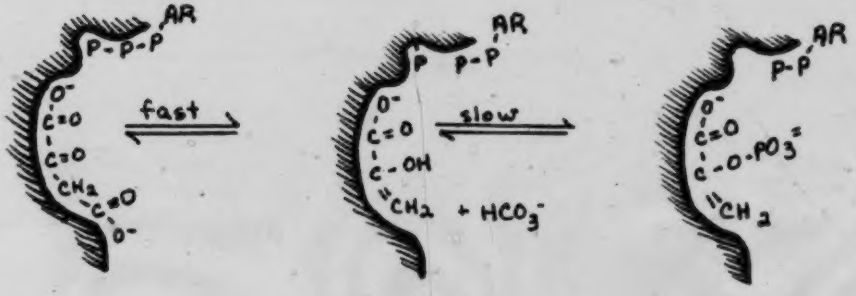

SCHEME D

Such a scheme is supported indirectly by our observation that ADP will not replace ATP, nor will the β,γ-methylene analogue of ATP (See Section 5 of this chapter). However, this model would be expected to exhibit an ATP ⟷ ADP exchange if ADP is released following phosphoenzyme formation. When ^{14}C-ATP and cold ADP were incubated, in the presence of PEPCK and absence of other reactants, no exchange was observed. (See Fig. 18 of Section 4 of this chapter, in which ATP ⟷ ADP exchange occurred only in the presence of other reactants.) Furthermore, incubating the enzyme with γ-^{32}P-ATP showed no incorporation of label into the protein peak following separation on a Sephadex G-150 column.[5] Therefore direct tests for phosphoenzyme formation and reversible ATP cleavage render Scheme D unlikely. The failure of β,γ-CH_2-ATP to support the exchange must then be interpreted in terms of strict structural requirements near the scissile bond. The carbon-bridged terminal phosphate on β,γ-CH_2-ATP probably has the wrong spatial orientation to fit the cavity on the enzyme. This latter argument is in agreement with Scheme C in which intact ATP effects substrate synergism and supports the lack of a phosphorylated enzyme intermediate.

Scheme C appears to offer the most feasible explanation that is in agreement with our experimental findings. It is surprising that the ATP-dependent exchange assay has been routinely used throughout the literature without an adequate model for its chemical mechanism. In the past, other workers have combined the data of the isotope exchanges with net reactions in their study of initial rates and product inhibition. We fear this to be imprudent, since comparisons between rates of net reactions and of isotope exchanges are not easily interpretable (26), and also because several detailed characteristics of the respective reactions differ in this particular case.

---

[5] No radioactivity appeared in the fractions where the protein eluted from the Sephadex G-150 column, only background counts (56 cpm) were received. If phosphorylation of PEPCK had occurred, a minimum of 10^5 cpm would be associated with the protein peak.

Increasing concentrations of HCO_3^- (up to 50 mM) and ATP (up to 4 mM) gave rise to normal Michaelis-Menten kinetics without inhibiting the ATP-dependent exchange reaction. This is at variance with Wright and Sanwal's report (Fig. 1, Ref. 51) whose plot of velocity *vs* [ATP] showed ATP to be inhibiting at concentrations > 1 mM. OAA, on the other hand, does not follow a normal substrate saturation curve. In agreement with Fig. 1 of Ref. 51, the reciprocal plot becomes hyperbolic concave-up at a concentration of > 1 mM OAA. This is shown on Fig. 10. Such substrate inhibition may be attributed to abortive or dead-end complex formation between the substrate and one or more enzyme forms at high concentrations of substrate (107). The Michaelis constant, K_m, for OAA determined from a primary plot as the x intercept is 0.67 mM. (Fig. 10).

We can now return our attention to the differences in rates of the net reactions compared to ATP-dependent $HCO_3^- \leftrightarrow$ OAA exchange. In order to assess the significance of the apparent differential in relative rates, we measured the relative isotope exchange rates of $H^{14}CO_3^- \leftrightarrow$ OAA and ^{14}C-ATP $\leftrightarrow$ ADP at chemical equilibrium. We found the $H^{14}CO_3^- \leftrightarrow$ OAA exchange to be fourfold greater than the ATP $\leftrightarrow$ ADP exchange at specific concentrations of substrates and products. Such data may be used to make a choice of kinetic mechanism from among various possibilities. The following sections on 'Initial Rate Kinetics and Product Inhibition' and a more detailed study of the 'Isotope Exchanges at Chemical Equilibrium' will focus more attention on these aspects of the reaction mechanism.

Figure 10. Double reciprocal plotsof velocity *vs.* [OAA] showing substrate inhibition at concentrations of OAA at concentrations >1 mM. Other components of the assay are 2 mM $MnCl_2$, 2.2 mM DTT, 0.4 mM ATP, 50 mM $KHCO_3$ and 0.1 M imidazole-HCl, pH 6.8. Isotope incorporation into OAA was measured by the ATP-dependent OAA $\leftrightarrow$ ^{14}C-HCO_3^- (5 x 10^3 cpm/μmole) exchange reaction.

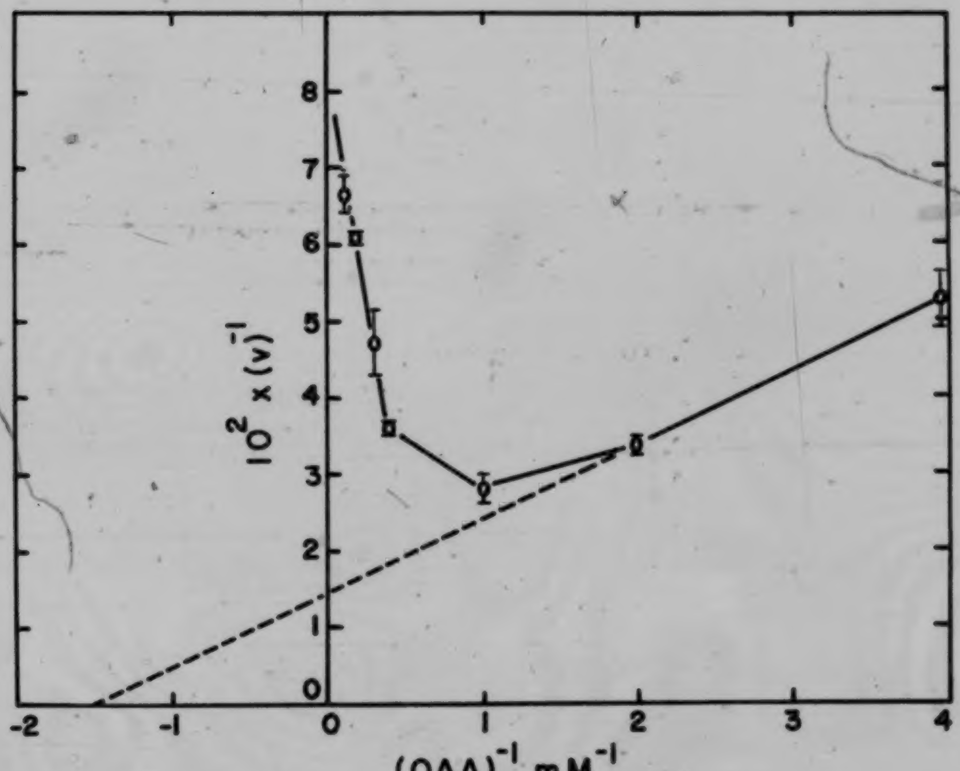
$10^2 \times (v)^{-1}$
8
7
6
5
4
3
2
1
0
-2
-1
0
1
2
3
4
$(OAA)^{-1}$ mM^{-1}

3. Initial Rate Kinetics and Product Inhibition

Three-substrate enzymatic mechanisms may be divided into two classes - sequential and ping-pong. A sequential mechanism requires that all three substrates be present on the enzyme prior to product formation, whereas the ping-pong type mechanism is one in which substrate addition and product release occur alternately, usually with covalent derivatives of the enzyme occurring as intermediates. Sequential mechanisms for PEPCK could be one of the four following types: 1) random ter (rapid equilibrium), 2) ordered-ter, 3) partially ordered - C where A and B add randomly and 4) partially ordered - A where B and C add randomly. A ping-pong mechanism that is chemically acceptable for PEPCK would be bi uni uni uni. Kinetic equations have been derived in the literature for the above-mentioned schemes by Cleland (36) and by Fromm (107). In addition to these algebraic approaches, the method of Cleland (108) allows predictions of initial rate patterns and product inhibition patterns by inspection of the various possible kinetic mechanisms for PEPCK. The conclusions drawn from such an analysis for PEPCK are given on Table VI for initial rate kinetics.

Initial rate kinetic patterns presented on Table VI for the few reaction schemes proposed predict a pattern of straight lines that intersect to the left of the ordinate for the random ter and the partially ordered - C reaction mechanisms. The fully ordered ter mechanism predicts one set of lines to be parallel and the others intersecting whereas the remaining two mechanisms, partially ordered - A and ping-pong lists two sets of lines to be parallel and one intersecting.

Table VI

Type of Line Patterns of Double Reciprocal Plots Predicted by Inspection for several Sequential and a Ping-Pong Terreactant Mechanisms

Mechanism		Substrates			Line Pattern
		A	B	C	
I	Random-ter (rapid equilibrium)	vary	vary	sat'g	I
		vary	sat'g	vary	I
		sat'g	vary	vary	I
II	Ordered ter	vary	vary	sat'g	I
		vary	sat'g	vary	P
		sat'g	vary	vary	I
III	Partially ordered -A (BC add randomly)	vary	vary	sat'g	P
		vary	sat'g	vary	P
		sat'g	vary	vary	I
IV	Partially ordered -C (AB add randomly)	vary	vary	sat'g	I
		vary	sat'g	vary	I
		sat'g	vary	vary	I
V	Ping-pong (bi uni uni uni)	vary	vary	sat'g	I
		vary	sat'g	vary	P
		sat'g	vary	vary	P

I: Intersecting

P: Parallel

Double reciprocal plots of our initial rate studies are shown of Figs. 11 to 13 for the carboxylation reaction for which one substrate was varied together with a second substrate while the third was at fixed saturating concentrations. These studies were done in the absence of products. For each individual line, the data were analyzed by a programme written for the Olivetti-Underwood Programme 101 which calculated weighted values and standard errors for Michaelis constants and maximum velocity (114). Fig. 11 shows a plot of 1/v *vs* 1/ADP as PEP was increased from 0.08 mM to 1.08 mM and HCO_3^- was 92% saturating. If we assume that the slope of each line has the same percent standard error as that calculated for its respective K_m value, the lines on Fig. 11 may be considered parallel within one standard error. By the same criterion, the family of lines plotted on Fig. 12 may also be parallel. This shows a plot of 1/v *vs* $1/HCO_3^-$ as PEP was increased from 0.08 mM to 0.22 mM and ADP was 88% saturating. Fig. 13 is a plot of 1/v *vs* 1/ADP as HCO_3^- was increased from 2.31 mM to 38.5 mM and PEP was 92% saturating. The family of lines show a converging pattern. The slope of each line differs by more than two standard errors when the concentration of the varied substrate (HCO_3^-) is less than its K_m value. As shown on Fig. 13, when HCO_3^- concentration was raised to 23.08 mM and 38.5 mM no change in slope and no difference in rate is observed; the lines are almost superimposable.

Assuming for the moment that the line patterns of Figs. 11 and 12 are parallel, the initial rate data are compatible with two of the five reaction schemes proposed on Table VI. The mechanism could either be partially ordered - A or sequential ping-pong (bi uni uni uni). However, the ping-pong mechanism is unattractive since no covalent enzyme intermediate has been detected for PEPCK. We would therefore be left with the

Figure 11. Double reciprocal initial velocity plots showing effects of varying [ADP] and [PEP] at a fixed saturating concentration of HCO_3^-. The reaction mixture contained in a final volume of 1.3 ml 0.1 M imidazole-HCL, pH 6.8, 10 mM $MnCl_2$ 1.5 mM DTT, 150 mM HCO_3^- and PEPCK (0.11 units). The PEPCK assay was coupled to MDH (2.5 units) in the presence of 0.3 mM NADH.

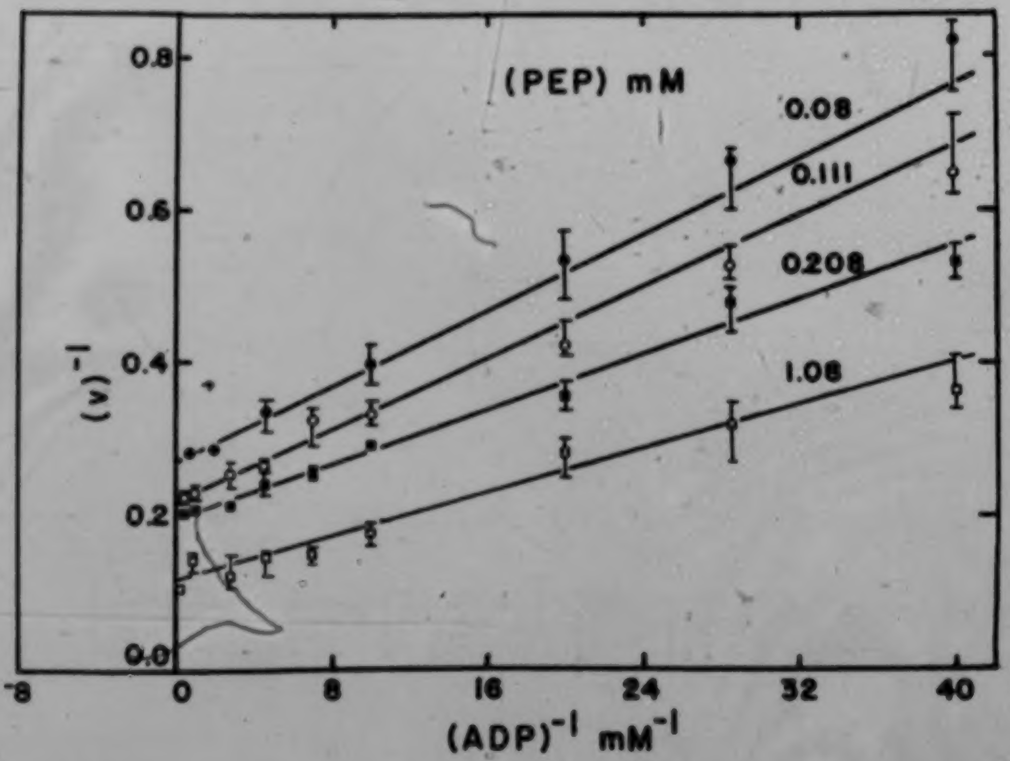
(PEP) mM
0.08
0.111
0.208
1.08
(v)$^{-1}$
0.0
0.2
0.4
0.6
0.8
-8
0
8
16
24
32
40
(ADP)$^{-1}$ mM^{-1}

Such a scheme is supported indirectly by our observation that ADP will not replace ATP, nor will the β,γ-methylene analogue of ATP (See Section 5 of this chapter). However, this model would be expected to exhibit an ATP $\leftrightarrow$ ADP exchange if ADP is released following phosphoenzyme formation. When ^{14}C-ATP and cold ADP were incubated, in the presence of PEPCK and absence of other reactants, no exchange was observed. (See Fig. 18 of Section 4 of this chapter, in which ATP $\leftrightarrow$ ADP exchange occurred only in the presence of other reactants.) Furthermore, incubating the enzyme with γ-^{32}P-ATP showed no incorporation of label into the protein peak following separation on a Sephadex G-150 column.[5] Therefore direct tests for phosphoenzyme formation and reversible ATP cleavage render Scheme D unlikely. The failure of β,γ-CH_2-ATP to support the exchange must then be interpreted in terms of strict structural requirements near the scissile bond. The carbon-bridged terminal phosphate on β,γ-CH_2-ATP probably has the wrong spatial orientation to fit the cavity on the enzyme. This latter argument is in agreement with Scheme C in which intact ATP effects substrate synergism and supports the lack of a phosphorylated enzyme intermediate.

Scheme C appears to offer the most feasible explanation that is in agreement with our experimental findings. It is surprising that the ATP-dependent exchange assay has been routinely used throughout the literature without an adequate model for its chemical mechanism. In the past, other workers have combined the data of the isotope exchanges with net reactions in their study of initial rates and product inhibition. We fear this to be imprudent, since comparisons between rates of net reactions and of isotope exchanges are not easily interpretable (26), and also because several detailed characteristics of the respective reactions differ in this particular case.

---

[5] No radioactivity appeared in the fractions where the protein eluted from the Sephadex G-150 column, only background counts (56 cpm) were received. If phosphorylation of PEPCK had occurred, a minimum of 10^5 cpm would be associated with the protein peak.

Increasing concentrations of HCO_3^- (up to 50 mM) and ATP (up to 4 mM) gave rise to normal Michaelis-Menten kinetics without inhibiting the ATP-dependent exchange reaction. This is at variance with Wright and Sanwal's report (Fig. 1, Ref. 51) whose plot of velocity *vs* [ATP] showed ATP to be inhibiting at concentrations > 1 mM. OAA, on the other hand, does not follow a normal substrate saturation curve. In agreement with Fig. 1 of Ref. 51, the reciprocal plot becomes hyperbolic concave-up at a concentration of > 1 mM OAA. This is shown on Fig. 10. Such substrate inhibition may be attributed to abortive or dead-end complex formation between the substrate and one or more enzyme forms at high concentrations of substrate (107). The Michaelis constant, K_m, for OAA determined from a primary plot as the x intercept is 0.67 mM. (Fig. 10).

We can now return our attention to the differences in rates of the net reactions compared to ATP-dependent $HCO_3^- \leftrightarrow$ OAA exchange. In order to assess the significance of the apparent differential in relative rates, we measured the relative isotope exchange rates of $H^{14}CO_3^- \leftrightarrow$ OAA and ^{14}C-ATP $\leftrightarrow$ ADP at chemical equilibrium. We found the $H^{14}CO_3^- \leftrightarrow$ OAA exchange to be fourfold greater than the ATP $\leftrightarrow$ ADP exchange at specific concentrations of substrates and products. Such data may be used to make a choice of kinetic mechanism from among various possibilities. The following sections on 'Initial Rate Kinetics and Product Inhibition' and a more detailed study of the 'Isotope Exchanges at Chemical Equilibrium' will focus more attention on these aspects of the reaction mechanism.

Figure 10. Double reciprocal plots of velocity *vs.* [OAA] showing substrate inhibition at concentrations of OAA at concentrations >1 mM. Other components of the assay are 2 mM $MnCl_2$, 2.2 mM DTT, 0.4 mM ATP, 50 mM $KHCO_3$ and 0.1 M imidazole-HCl, pH 6.8. Isotope incorporation into OAA was measured by the ATP-dependent OAA $\leftrightarrow$ ^{14}C-HCO_3^- (5 x 10^3 cpm/μmole) exchange reaction.

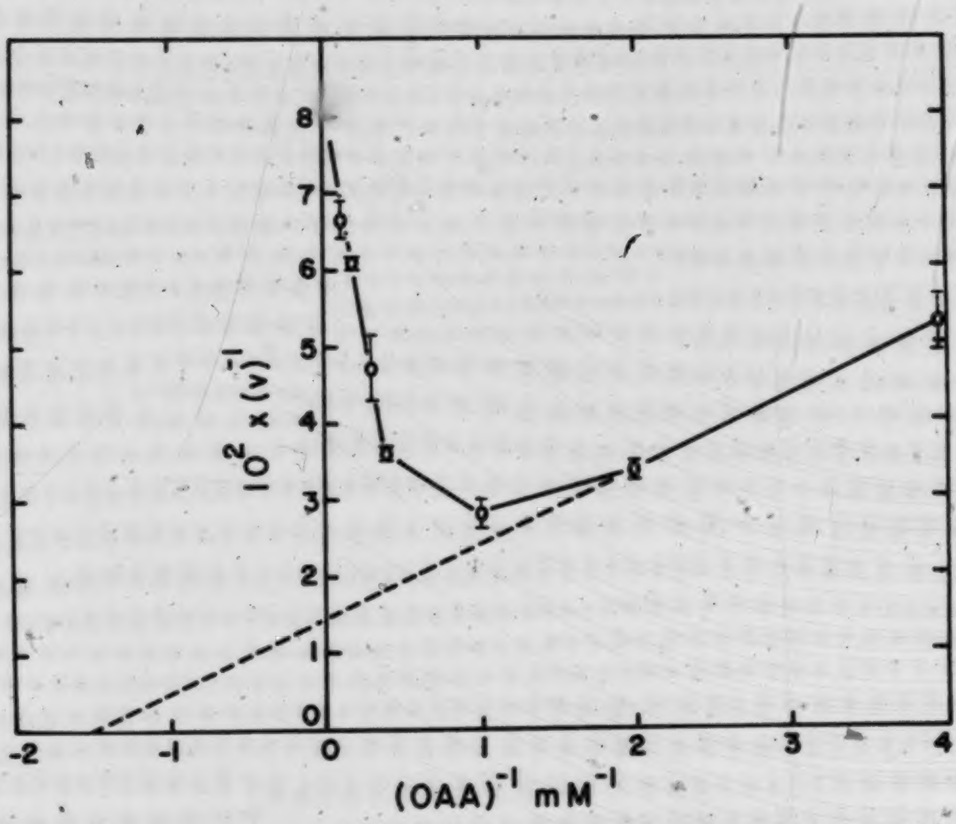
$10^2 \times (v)^{-1}$
0
1
2
3
4
5
6
7
8
-2
-1
0
1
2
3
4
$(OAA)^{-1}$ mM^{-1}

3. Initial Rate Kinetics and Product Inhibition

Three-substrate enzymatic mechanisms may be divided into two classes - sequential and ping-pong. A sequential mechanism requires that all three substrates be present on the enzyme prior to product formation, whereas the ping-pong type mechanism is one in which substrate addition and product release occur alternately, usually with covalent derivatives of the enzyme occurring as intermediates. Sequential mechanisms for PEPCK could be one of the four following types: 1) random ter (rapid equilibrium), 2) ordered-ter, 3) partially ordered - C where A and B add randomly and 4) partially ordered - A where B and C add randomly. A ping-pong mechanism that is chemically acceptable for PEPCK would be bi uni uni uni. Kinetic equations have been derived in the literature for the above-mentioned schemes by Cleland (36) and by Fromm (107). In addition to these algebraic approaches, the method of Cleland (108) allows predictions of initial rate patterns and product inhibition patterns by inspection of the various possible kinetic mechanisms for PEPCK. The conclusions drawn from such an analysis for PEPCK are given on Table VI for initial rate kinetics.

Initial rate kinetic patterns presented on Table VI for the few reaction schemes proposed predict a pattern of straight lines that intersect to the left of the ordinate for the random ter and the partially ordered - C reaction mechanisms. The fully ordered ter mechanism predicts one set of lines to be parallel and the others intersecting whereas the remaining two mechanisms, partially ordered - A and ping-pong lists two sets of lines to be parallel and one intersecting.

Table VI

Type of Line Patterns of Double Reciprocal Plots Predicted by Inspection for several Sequential and a Ping-Pong Terreactant Mechanisms

Mechanism	Substrates			Line Pattern
	A	B	C	
I Random-ter (rapid equilibrium)	vary	vary	sat'g	I
	vary	sat'g	vary	I
	sat'g	vary	vary	I
II Ordered ter	vary	vary	sat'g	I
	vary	sat'g	vary	P
	sat'g	vary	vary	I
III Partially ordered -A (BC add randomly)	vary	vary	sat'g	P
	vary	sat'g	vary	P
	sat'g	vary	vary	I
IV Partially ordered -C (AB add randomly)	vary	vary	sat'g	I
	vary	sat'g	vary	I
	sat'g	vary	vary	I
V Ping-pong (bi uni uni uni)	vary	vary	sat'g	I
	vary	sat'g	vary	P
	sat'g	vary	vary	P

I: Intersecting

P: Parallel

Double reciprocal plots of our initial rate studies are shown of Figs. 11 to 13 for the carboxylation reaction for which one substrate was varied together with a second substrate while the third was at fixed saturating concentrations. These studies were done in the absence of products. For each individual line, the data were analyzed by a programme written for the Olivetti-Underwood Programme 101 which calculated weighted values and standard errors for Michaelis constants and maximum velocity (114). Fig. 11 shows a plot of 1/v *vs* 1/ADP as PEP was increased from 0.08 mM to 1.08 mM and HCO_3^- was 92% saturating. If we assume that the slope of each line has the same percent standard error as that calculated for its respective K_m value, the lines on Fig. 11 may be considered parallel within one standard error. By the same criterion, the family of lines plotted on Fig. 12 may also be parallel. This shows a plot of 1/v *vs* $1/HCO_3^-$ as PEP was increased from 0.08 mM to 0.22 mM and ADP was 88% saturating. Fig. 13 is a plot of 1/v *vs* 1/ADP as HCO_3^- was increased from 2.31 mM to 38.5 mM and PEP was 92% saturating. The family of lines show a converging pattern. The slope of each line differs by more than two standard errors when the concentration of the varied substrate (HCO_3^-) is less than its K_m value. As shown on Fig. 13, when HCO_3^- concentration was raised to 23.08 mM and 38.5 mM no change in slope and no difference in rate is observed; the lines are almost superimposable.

Assuming for the moment that the line patterns of Figs. 11 and 12 are parallel, the initial rate data are compatible with two of the five reaction schemes proposed on Table VI. The mechanism could either be partially ordered - A or sequential ping-pong (bi uni uni uni). However, the ping-pong mechanism is unattractive since no covalent enzyme intermediate has been detected for PEPCK. We would therefore be left with the

Figure 11. Double reciprocal initial velocity plots showing effects of varying [ADP] and [PEP] at a fixed saturating concentration of HCO_3^-. The reaction mixture contained in a final volume of 1.3 ml 0.1 M imidazole-HCL, pH 6.8, 10 mM $MnCl_2$ 1.5 mM DTT, 150 mM HCO_3^- and PEPCK (0.11 units). The PEPCK assay was coupled to MDH (2.5 units) in the presence of 0.3 mM NADH.

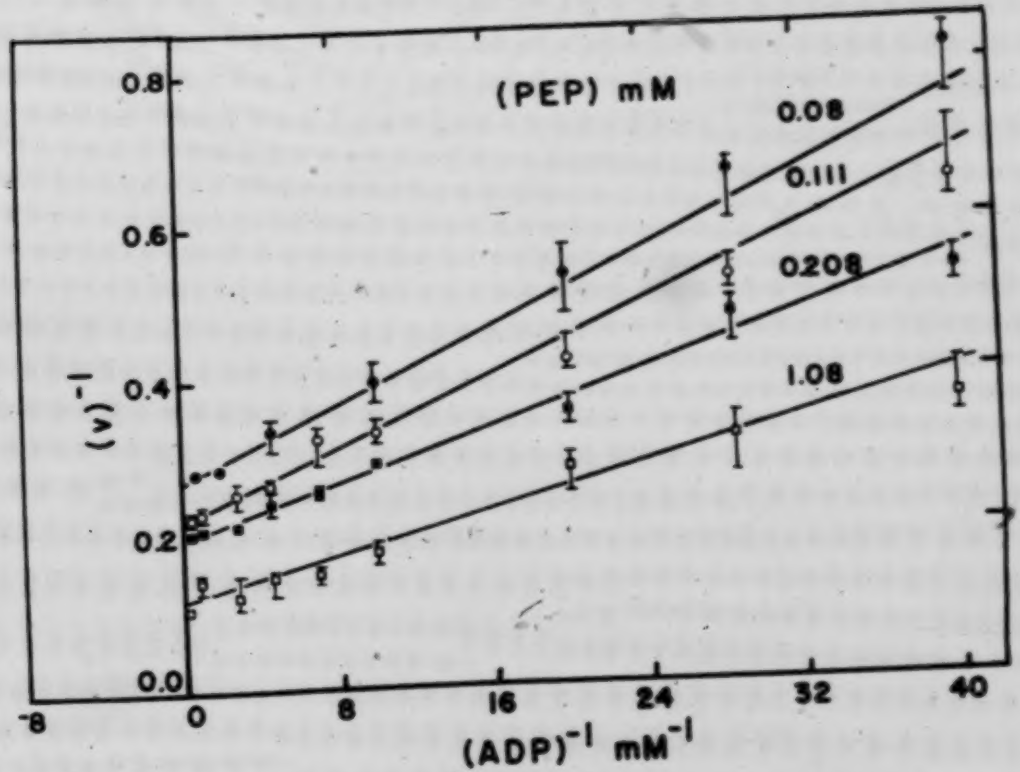
(PEP) mM
0.08
0.111
0.208
1.08
$(v)^{-1}$
0.0
0.2
0.4
0.6
0.8
-8
0
8
16
24
32
40
$(ADP)^{-1}$ mM^{-1}

Figure 12. Double reciprocal initial velocity plots showing effects of varying [HCO_3^-] and [PEP] at saturating ADP concentration. The reaction mixture contained in a final volume of 1.3 ml 0.1 M imidazole - HCl, pH 6.8, 10 mM $MnCl_2$, 1.5 mM DTT, 0.38 mM ADP and PEPCK (0.11 units). The assay was coupled to MDH (2.5 units) in the presence of 0.3 mM NADH.

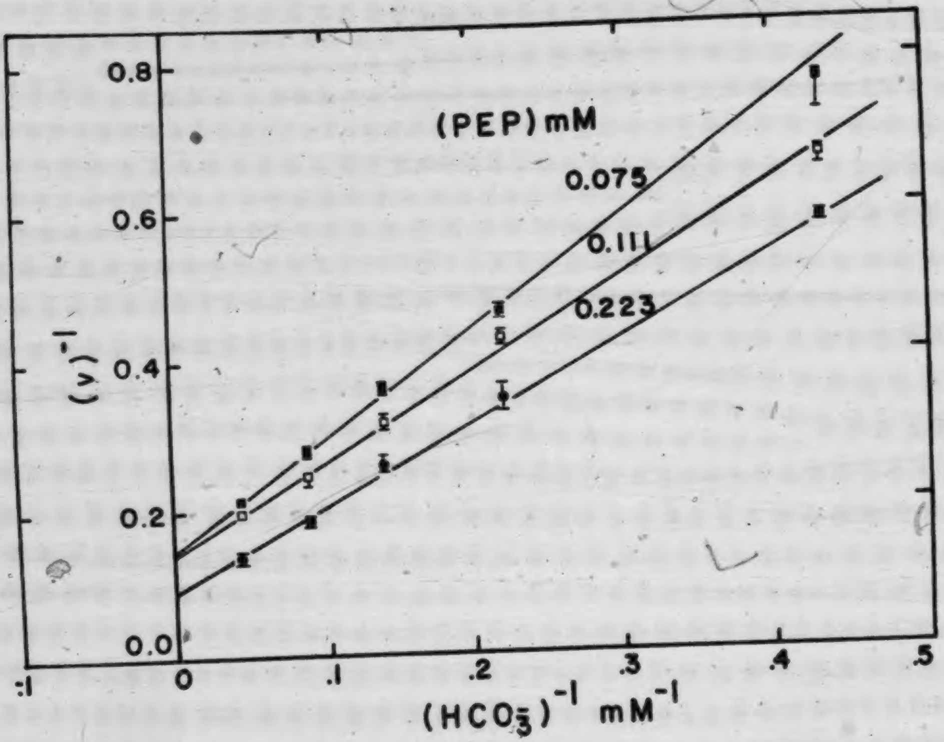
0.8
0.6
0.4
0.2
0.0
$(v)^{-1}$
(PEP) mM
0.075
0.111
0.223
-.1
0
.1
.2
.3
.4
.5
$(HCO_3^-)^{-1}$ mM^{-1}

Figure 13. Double reciprocal initial velocity plots showing effects of varying [ADP] and [HCO_3^-] at a fixed saturating concentration of PEP. The reaction mixture contained in a final volume of 1.3 ml 0.1 M imidazole - HCl, pH 6.8, 10 mM $MnCl_2$, 1.5 mM DTT, 0.82 mM PEP and PEPCK (0.11 units). The PEPCK assay was coupled to MDH (2.5 units) in the presence of 0.3 mM NADH.

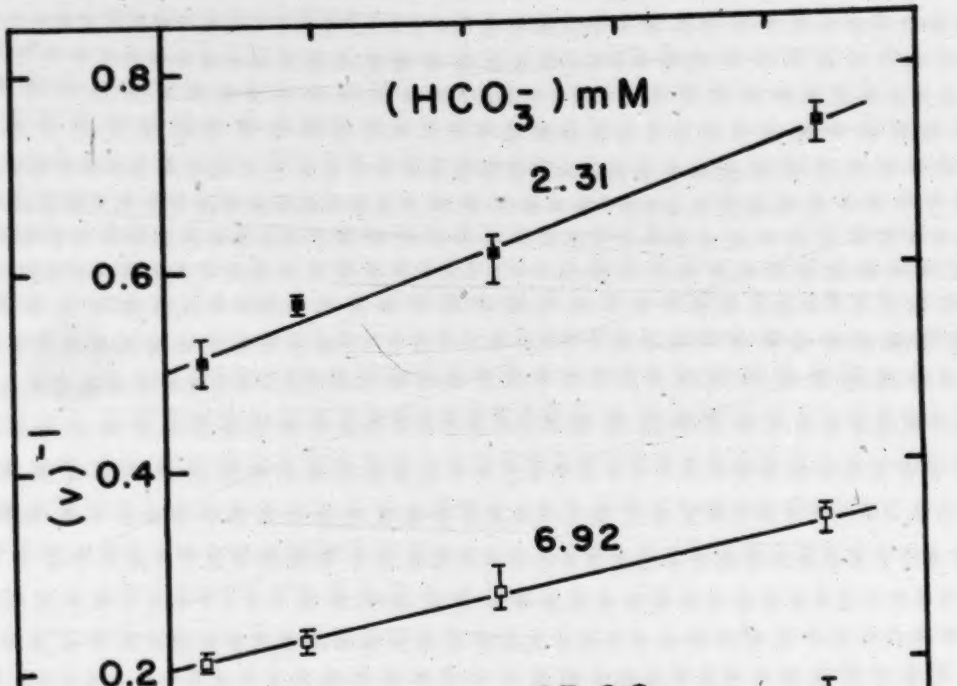
(HCO$_3^-$) mM
2.31
6.92
23.08
38.50
(v)$^{-1}$
0.0
0.2
0.4
0.6
0.8
-3
0
3
6
9
12
15
(ADP)$^{-1}$ mM^{-1}

partially ordered - A sequential mechanism. The patterns of lines on Figs. 11-13 are compatible with PEP adding first in an obligatory binding order and then HCO_3^- and ADP binding randomly before any products are released. This sequential mechanism is shown in the following scheme.

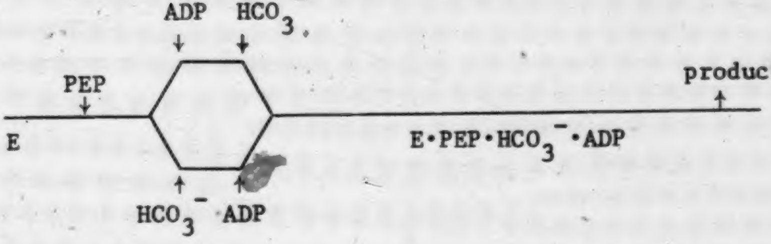

SCHEME: E

However, if we consider the pattern of lines for all three plots to be truly converging rather than parallel, Scheme E is not the correct mechanism. Two other mechanisms of the five listed on Table VI would be consistent with such a converging pattern, random ter and partially ordered - C. From initial rate studies alone, as shown on Figs. 11 to 13 for the reaction in one direction only, it is impossible to differentiate between the random ter and the partially ordered - C mechanism. Product inhibition was undertaken to answer some of the questions that were posed by the initial rate study.

Patterns of product inhibition by ATP are shown on double reciprocal plots in Figs. 14 and 15. Fig. 14 is a plot of 1/v versus 1/ ADP when

Figure 14. Double reciprocal plots of velocity versus [ADP] at increasing concentrations of ATP and near-saturating concentrations of HCO_3^- and PEP. The reaction mixture contained to a final volume of 1.3 ml 0.1 M imidazole -HCl, pH 6.8, 10 mM $MnCl_2$, 1.5 mM DTT, 38.5 mM HCO_3^-, 0.82 mM PEP and PEPCK (0.11 units). The assay was coupled to MDH (2.5 units) in the presence of 0.3 mM NADH.

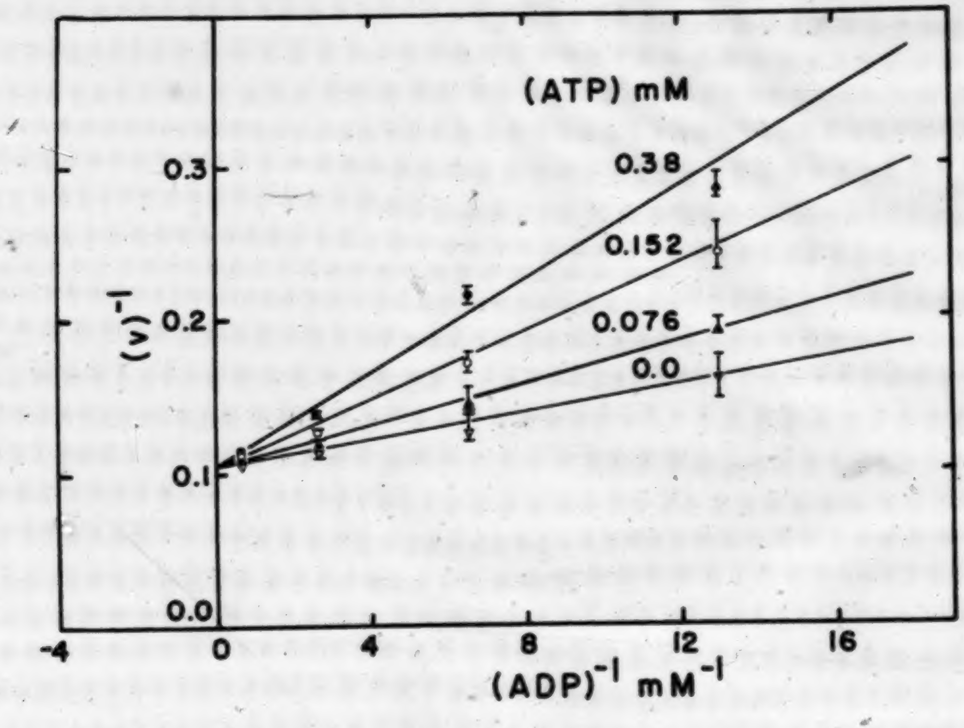
(ATP) mM
0.38
0.152
0.076
0.0
$(v)^{-1}$
0.3
0.2
0.1
0.0
-4
0
4
8
12
16
$(ADP)^{-1}$ mM^{-1}

Figure 15. Double reciprocal plots of velocity versus [PEP] at increasing concentrations of ATP and near-saturating concentrations of HCO_3^- and ADP. The reaction mixture contained to a final volume of 1.3 ml 0.1M imidazole -HCl, pH 6.8, 10 mM $MnCl_2$, 1.5 mM DTT, 38.5 mM HCO_3^-, 1.54 mM ADP and PEPCK (0.11 units). The assay was coupled to MDH (2.5 units) in the presence of 0.3 mM NADH.

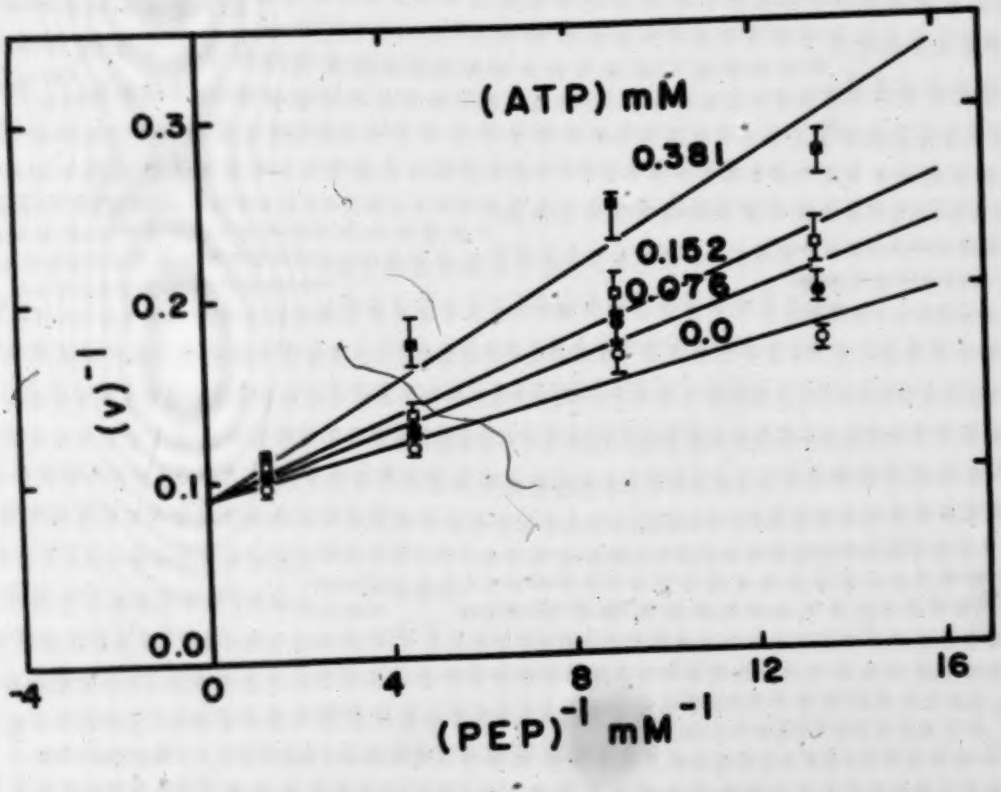
(ATP) mM
0.381
0.152
0.076
0.0
$(v)^{-1}$
0.0
0.1
0.2
0.3
-4
0
4
8
12
16
$(PEP)^{-1}$ mM^{-1}

ATP was increased from zero to 0.38 mM and HCO_3^- and PEP were at fixed levels of 3 and 12 times their K_m values, respectively. The family of lines which were drawn by computer analyses intersect on the 1/v axis. A similar plot is presented in Fig. 15 in which PEP was the varied substrate and HCO_3^- and ADP are at fixed levels of 3 and 30 times their K_m values. In both cases competitive inhibition is observed. The common point of intersection of the 1/v axis corresponds to the approximate V_{max} (11 μmoles/min/ml) for this reaction.

Figs. 16 and 17 are similar inhibition studies, but for these experiments the two substrates that were maintained at fixed concentrations were not near saturating concentrations but kept at their approximate K_m values. Under such conditions we also observe competitive inhibition with either ADP or PEP as the variable substrate. Since the two fixed substrates are at low concentration, the point of intersection of the 1/v axis is well below the maximum velocity expected when all substrate sites on the enzyme are saturated. However the K_m values for ADP and PEP calculated from Figs. 16 and 17 are quite independent of the degree of saturation of the remaining substrate binding sites. Fig. 16 exhibits the same K_m value for ADP in the presence of non-saturating concentrations of PEP and HCO_3^- as it does when these substrates were saturated (Fig. 14). The same observation is made on Fig. 17 which shows the same K_m value for PEP under non-saturating concentrations of ADP and HCO_3^- as it does when these two substrates were saturated (Fig. 15).

Inhibition by ATP as shown on Figs. 14 to 17 is suggestive of either a totally rapid equilibrium random mechanism or a partially ordered - C

Figure 16. Double reciprocal plots of velocity versus [ADP] at increasing concentrations of ATP and fixed concentrations of PEP and HCO_3^- at their approximate K_m values. The reaction mixture contained to a final volume of 1.3 ml 0.1 M imidazole -HCl, pH 6.8, 10 mM $MnCl_2$, 1.5 mM DTT, 9.2 mM HCO_3^-, 0.069 mM PEP and PEPCK (0.11 units). The assay was coupled to MDH (2.5 units) in the presence of 0.3 mM NADH.

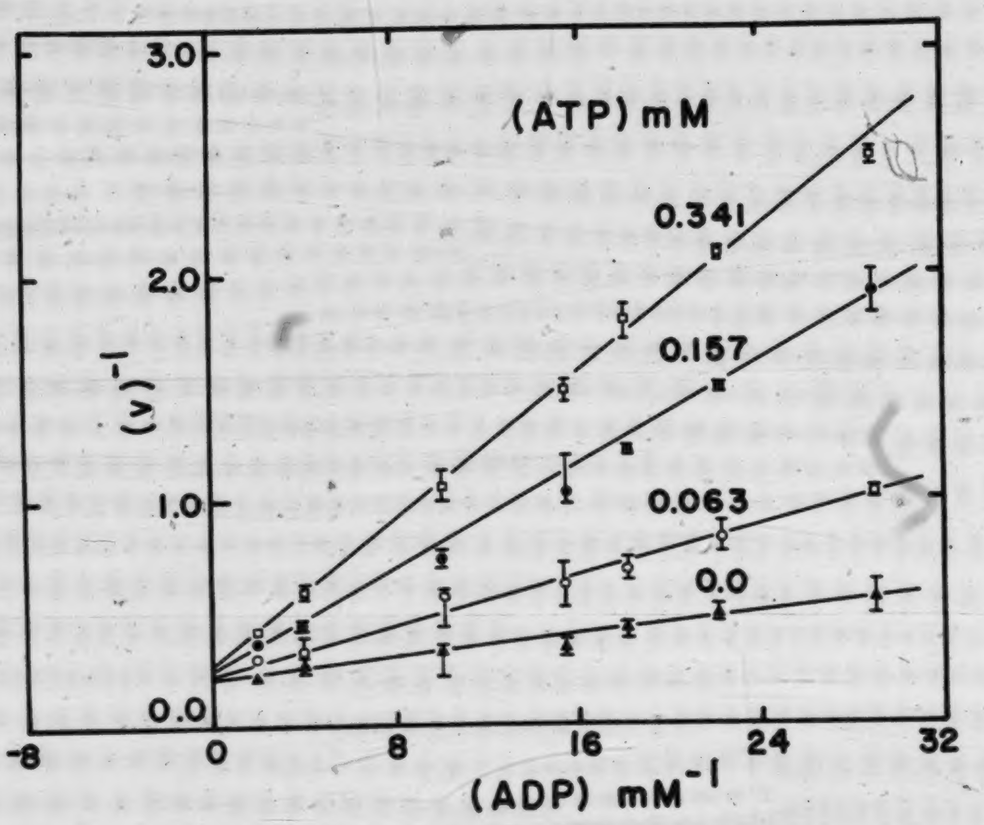
(ATP) mM
0.341
0.157
0.063
0.0
3.0
2.0
1.0
0.0
(v)⁻¹
-8
0
8
16
24
32
(ADP) mM⁻¹

Figure 17. Double reciprocal plots of velocity versus[PEP] at increasing concentrations of ATP and fixed levels of ADP and HCO_3^- at their approximate K_m values. The reaction mixture contained to a final volume of 1.3 ml 0.1 M imidazole - HCl, pH 6.8, 10mM $MnCl_2$, 1.5 mM DTT, 19.2 mM HCO_3^-, 0.023 mM ADP and PEPCK (0.11 units). The assay was coupled to MDH (2.5 units) in the presence of 0.3 mM NADH.

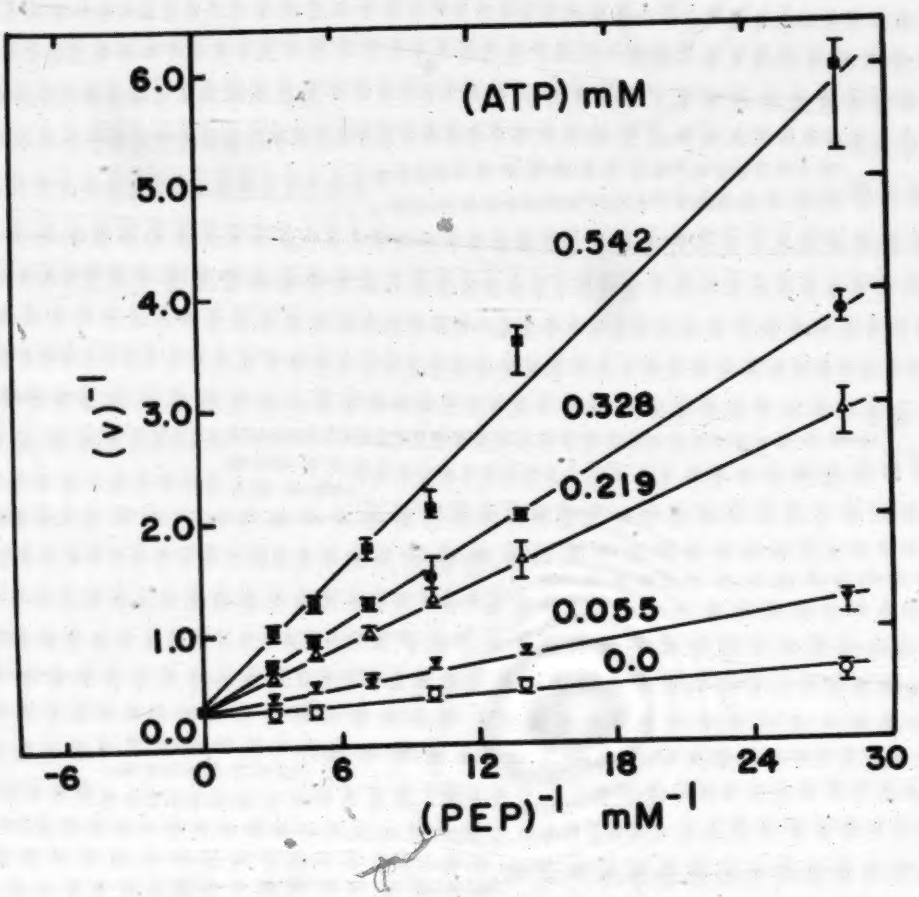
(ATP) mM
0.542
0.328
0.219
0.055
0.0
$(v)^{-1}$
6.0
5.0
4.0
3.0
2.0
1.0
0.0
-6
0
6
12
18
24
30
$(PEP)^{-1}$ mM^{-1}

mechanism. These two mechanisms were also selected from initial rate kinetics when we considered Figs. 11 to 13 to be patterns of intersecting lines. Therefore, from product inhibition patterns we can discount Scheme E which depicted the partially ordered - A mechanism. The following section deals with the kinetic studies of isotope exchange at chemical equilibrium, providing further information to allow selection of one of the models proposed above.

The K_m values for all the substrates of PEPCK are given in Table VII. All values were determined in the presence of Mn^{2+} as the added divalent cation rather than Mg^{2+} which was used in previous studies (51). The Michaelis constants for the substrates of the carboxylation reaction (PEP, ADP and HCO_3^-) were calculated from the primary double reciprocal plots from our initial rate studies (Figs. 11 to 13). The constants for ATP and OAA, on the other hand, were calculated from the ATP-dependent $HCO_3^- \leftrightarrow$ OAA exchange reaction (see Figs. 9 and 10 of the previous section). The K_m value for HCO_3^- could be determined by either the overall carboxylation or the ATP-dependent exchange reaction; from both assays the value was approximately 13 mM.

The K_m values reported in Table VII are decidedly lower than previously reported by Wright and Sanwal (51) and those given by our own work discussed under Section 1 of this chapter. For both reports such determinations for the carboxylation reaction of PEPCK were done by the colorimetric assay. This assay indicated inhibition by NADH which later proved to be an artifact (106) and it also seems to produce inaccurate K_m values. For example, with this assay Wright and Sanwal (57) reported a K_m value for PEP of 8 mM in the presence of $MgCl_2$ while our own work shows the

Table VII

K_m and K_i values for Substrates of PEPCK

Substrates	K_m (mM)	K_i (mM)
PEP	0.07	0.06[a]
ADP	0.05	--
HCO_3^-	13.0	--
ATP	0.06	0.04[b]
OAA	0.67	--
$MnCl_2$	0.09	--

[a] Calculated from Fig. 9

[b] Calculated from Figs. 16 and 17.

K_m to be reduced to 0.5 mM in the presence of $MnCl_2$. However, with the coupled enzymatic assay the latter value is calculated to be almost 10 fold lower at 0.07 mM. Previously determined K_m values of OAA and ATP by the ATP-dependent $HCO_3^- \leftrightarrow$ OAA exchange reaction (51) in the presence of $MgCl_2$ were 1.5 and 2.0 mM respectively. However in the presence of $MnCl_2$ the K_m values established for OAA and ATP were 0.67 and 0.06 mM, respectively.

The decrease in Michaelis constants when $MnCl_2$ replaced $MgCl_2$ has previously been observed by Ballard (53) for PEPCK from sheep and chicken liver. A threefold decrease of the K_m value of OAA was reported for the mitochondrial enzyme when Mn^{2+} replaced Mg^{2+}. He also noted a fourfold increase in maximum velocity in the presence of $MnCl_2$ relative to that observed with $MgCl_2$. The latter difference was not as pronounced in our results which showed a 1.5 fold increase in velocity, but a more pronounced decrease in Michaelis constants. The K_m for $MgCl_2$ for the bacterial enzyme was reported (51) to be 4 mM, and that of $MnCl_2$ was found in the present study to be 0.09 mM. Both of these values are within the range of their physiological concentrations (109). Ballard (53) stressed the physiological importance of lowering the K_m for OAA since the effect would place the value in the range of the mitochondrial OAA concentration. $MnCl_2$ may also play a significant role since it forms more stable Mn^{2+} - ITP and Mn^{2+} - GTP than the respective Mg^{2+} complexes (110). Holton and Nordlie (111) found synergistic velocity effects when both Mg^{2+} and Mn^{2+} were present together in the reaction mixture for pig liver mitochondrial PEPCK. They observed the effects of the two ions to be almost additive and postulated a role of a Mg-ITP complex in phosphoryl transfer, plus a separate role of Mn^{2+} in facilitating the decarboxylation of OAA.

The above-described effects of Mn^{2+} on K_m indicate that such an explanation is too simple.

4. Isotope Exchange Rates at Chemical Equilibrium

With three substrates and two products PEPCK offers many possibilities for study of isotope exchange rates. The relative rates of such exchanges can provide information about possible binding orders of substrates to the enzyme. For our experiments we chose the first two of four possible exchanges: 1) ATP ↔ ADP, 2) HCO_3^- ↔ OAA, 3) PEP ↔ OAA and 4) ATP ↔ PEP. These pairs were chosen, as will become clear, in order to include a 'similar' and 'dissimilar' combination, thus enabling us to recognize certain competitive effects on the exchange kinetics.

Fig. 18 shows the rates for both ADP ↔ ATP and HCO_3^- ↔ OAA exchanges. These are smooth hyperbolic curves that level off at R[6] = 2.5 and 2.0 mM/min/mg, respectively. At the plateau PEPCK is saturated with ADP and ATP, the substrate-product pair varied at constant ratio. At the highest concentrations tested, ADP was raised to 20 times its K_m and ATP was raised to 8 times its K_m. The increase of ADP and ATP to near saturating levels produced no detectable reduction in the exchange rates of either pair. Since ATP is known to be competitive with ADP from our product inhibition study, this pair was raised in constant concentration ratio to circumvent inhibitory effects. Neither ADP nor ATP showed competition for either the HCO_3^- or OAA site. To maintain chemical equilibrium (K_{eq} is high, 3.1 M at pH 7.5 (80)) the PEP concentration was raised to 0.3 M for the HCO_3^- ↔ OAA exchange and to 0.05 M for the ADP ↔ ATP exchange.

---

[6] In all cases the units for R are given in mM/min/mg for a total volume of 0.5 ml.

Figure 18. Effects of varying [ADP] in constant ratio with [ATP] on the rate of HCO_3^- ⇌ OAA exchange and on the rate of ATP ⇌ ADP exchange. For the $H^{14}CO_3^-$ ⇌ OAA exchange the ADP/ATP ratio was 5. Other components for this exchange were 0.1 M tris-HCl, pH 7.5, 3 mM DTT, 2 mM $MnCl_2$, 10 mM HCO_3^-, 5.0 mM OAA, 320 mM PEP and PEPCK (0.7 units). For the ^{14}C-ATP ⇌ ADP exchange the ADP/ATP ratio was 4.0. Other components for this exchange were 0.1 M tris-HCl, pH 7.5, 3 mM DTT, 2 mM $MnCl_2$, 150 mM HCO_3^-, 10 mM OAA, 53.5 mM PEP and PEPCK (8×10^{-3} units). Total volume was 0.5 ml.

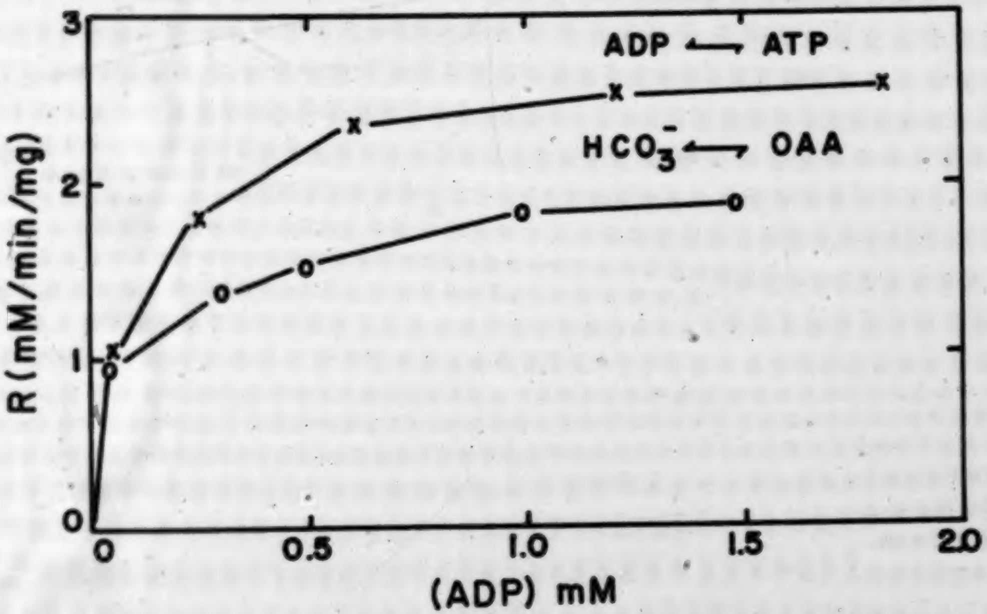
ADP ⟶ ATP
HCO_3^- ⟶ OAA
R (mM/min/mg)
0
1
2
3
0
0.5
1.0
1.5
2.0
(ADP) mM

Fig. 19 shows the same exchange rates as a function of the concentrations of HCO_3^- and OAA. The $HCO_3^- \leftrightarrow$ OAA exchange rate was faster than the ADP $\leftrightarrow$ ATP exchange rate, these being 2.6 and 1.5 mM/min/mg, respectively. The PEP concentration for these exchanges was somewhat lower, 0.17 M for $HCO_3^- \leftrightarrow$ OAA and 0.09 M for ADP $\leftrightarrow$ ATP. Lowering the concentration of PEP increased the rate for $HCO_3^- \leftrightarrow$ OAA (see Figs. 18 and 19) and conversely increasing PEP concentration decreased the ADP $\leftrightarrow$ ATP exchange.

In multisubstrate enzyme systems, compulsory binding of substrates has important predictable effects on exchange rates at equilibrium (112). In the PEPCK system, for example, if HCO_3^- or OAA were the last reactants to add in a compulsory sequence, a continued increase in the concentration of HCO_3^- and OAA while other reactants remained constant and in equilibrium would be expected to give a continued increase in $HCO_3^- \leftrightarrow$ OAA exchange rate, but lead to a decrease in the ADP $\leftrightarrow$ ATP interchange rate. On the other hand, if the reactants add randomly to the enzyme, a continued increase in both isotope exchange rates to a maximum would be observed when the enzyme was saturated. Both Figs. 18 and 19 exclude a mechanism of fully ordered binding sequence, since no decrease to zero in the interchange was observed. To this point our data are consistent with a random sequence of substrate binding and product release. Random substrate binding was one of the models proposed in the previous section of this chapter from initial rate and product inhibition studies.

Fig. 20 illustrates the rates of exchange reactions when PEP and ATP were the substrate-product pair to be increased. The ADP $\leftrightarrow$ ATP interchange shown on the bottom curve of Fig. 20 is similar to the curves

Figure 19. Effects of varying [OAA] in constant ratio with [HCO_3^-] on the rate of HCO_3^- ⇄ OAA exchange and on the rate of ATP ⇄ ADP exchange. For the $H^{14}CO_3^-$ ⇄ OAA exchange the ratio of OAA/HCO_3^- was 1.25. Other components for this exchange were 0.1 M tris-HCl, pH 7.5, 3 mM DTT, 2 mM $MnCl_2$, 0.3 mM ADP, 0.013 mM ATP, 171 mM PEP and PEPCK (0.7 units). For the ^{14}C-ATP ⇄ ADP exchange the ratio of OAA/HCO_3^- was 0.13. Other components for this exchange were 0.1 M tris-HCl, pH 7.5, 3 mM DTT, 2 mM $MnCl_2$, 0.12 mM ATP, 0.55 mM ADP, 92 mM PEP and PEPCK (0.014 units). Total volume was 0.5 ml.

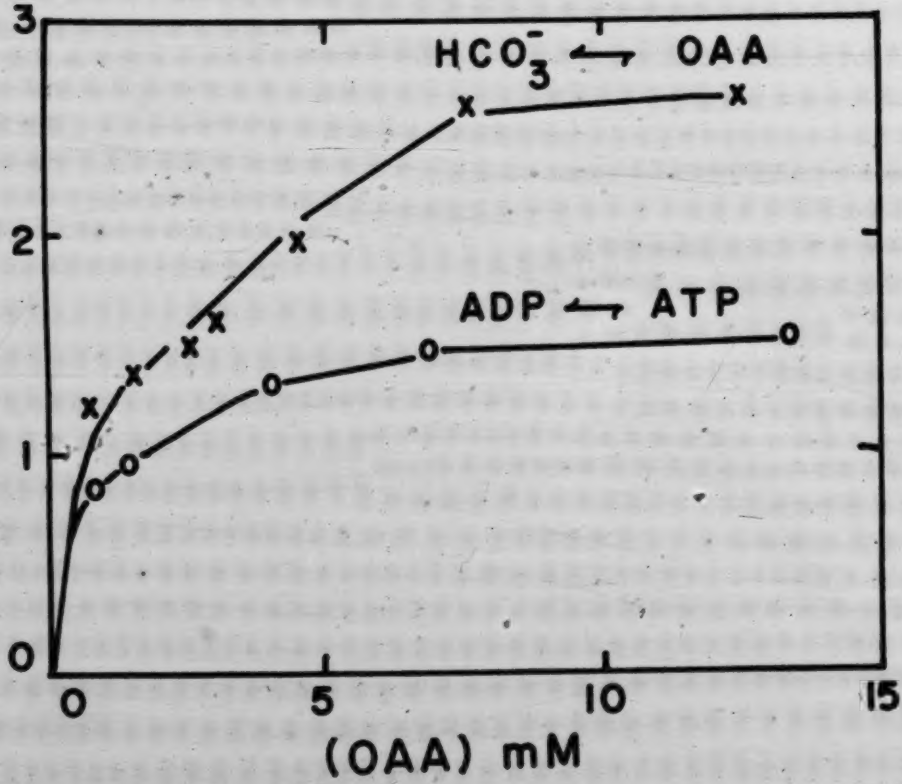
$HCO_3^- \rightleftharpoons OAA$
ADP ⇌ ATP
R (mM/min/mg)
0
1
2
3
(OAA) mM
0
5
10
15

Figure 20. Effects of varying [ATP] in constant ratio with [PEP] on the rate of exchange of HCO_3^- ⇌ OAA and ATP ⇌ ADP. For the $H^{14}CO_3^-$ ⇌ OAA exchange the ratio of ATP/PEP was 0.024. Other components for this exchange were 0.1 M tris-HCl, pH 7.5, 3 mM DTT, 40 mM $MnCl_2$ 38.6 mM ADP, 20 mM HCO_3^-, 10 mM OAA and PEPCK (0.7 units). For the ^{14}C-ATP ⇌ ADP exchange the ratio of ATP/PEP was 0.1. Other components of the assay were 0.1 M tris-HCl, pH 7.5, 3 mM DTT, 10 mM $MnCl_2$, 8.44 mM ADP, 150 mM HCO_3^- 4 mM OAA and PEPCK (8×10^{-3} units). Total volume was 0.5 ml.

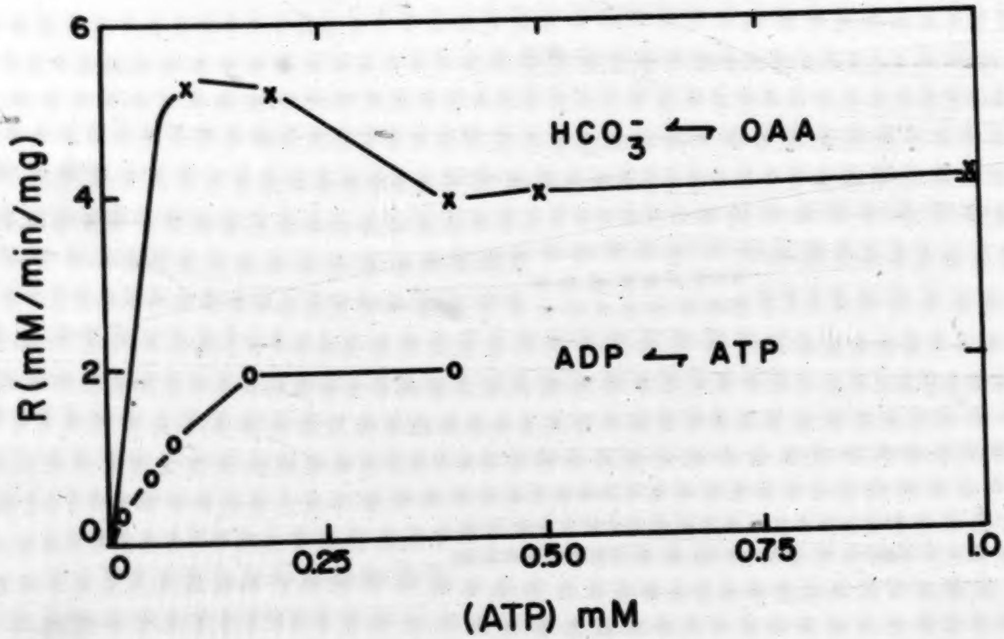
6
4
2
0
R(mM/min/mg)
0
0.25
0.50
0.75
1.0
(ATP) mM
HCO_3^- ⇌ OAA
ADP ⇌ ATP

on Figs. 18 and 19. It shows a saturation curve that levelled off at R = 2 mM/min/mg. The smooth curve indicates that neither ATP nor PEP (PEP is varied from 0 to 4 mM) compete for the ADP or ATP binding sites, respectively. In marked contrast, the HCO_3^- ⇌ OAA interchange plot produces a maximum rate of R = 5.4 mM/min/mg followed by a decrease to a rate of 4 mM/min/mg. At this level the rate is constant and does not decrease with further elevation of [PEP] and [ADP]. PEP concentration in this experiment varied from 0 to 41 mM. Maximum interchange occurred at 4 mM PEP and levelled off at approximately 16 mM PEP. This effect could be the result of several possible causes. 1) PEP could be in direct competition for the OAA binding site, although complete inhibition of the exchange would be expected at sufficiently high [PEP]. 2) The decrease in rate is suggestive of a partially compulsory binding pathway of PEP binding after HCO_3^- and/or ATP after OAA in the reverse direction. 3) Since the rate decreased to a lower level, but not to zero, this observation is consistent with the presence of ATP or PEP decreasing but not preventing the dissociation of HCO_3^- or OAA. The above inhibition could not be observed for the ADP ⇌ ATP exchange because it is below the range of PEP concentration that produced the stimulatory and inhibitory effects in the HCO_3^- ⇌ OAA interchange.

Fig. 21 is a similar experiment to that of Fig. 20 except [PEP] and [OAA] are increased at constant ratio.[7] The rate of ADP ⇌ ATP exchange rises in a smooth saturation curve with a maximum rate of 2

---

[7] Note that in this experiment the curves are plotted to different concentration scales on the abscissa.

Figure 21. Effects of varying [PEP] in constant ratio with [OAA] on the exchange rates of HCO_3^- ↔ OAA and ATP ↔ ADP. For the $H^{14}CO_3^-$ ↔ OAA exchange the ratio of PEP/OAA was 4.1. Other components of this assay were 0.1 M tris-HCl, pH 7.5, 3 mM DTT, 40 mM $MnCl_2$, 38 mM ADP, 1 mM ATP, 20 mM HCO_3^- and PEPCK (0.21 units). For the ^{14}C-ATP ↔ ADP exchange the ratio of PEP/OAA was 5.0. Other components of this assay were 0.1 M tris-HCl pH 7.5, 3 mM DTT, 2 mM $MnCl_2$, 0.54 mM ADP, 0.09 mM ATP, 105 mM HCO_3^- and PEPCK (0.014 units). Total volume was 0.5 ml.

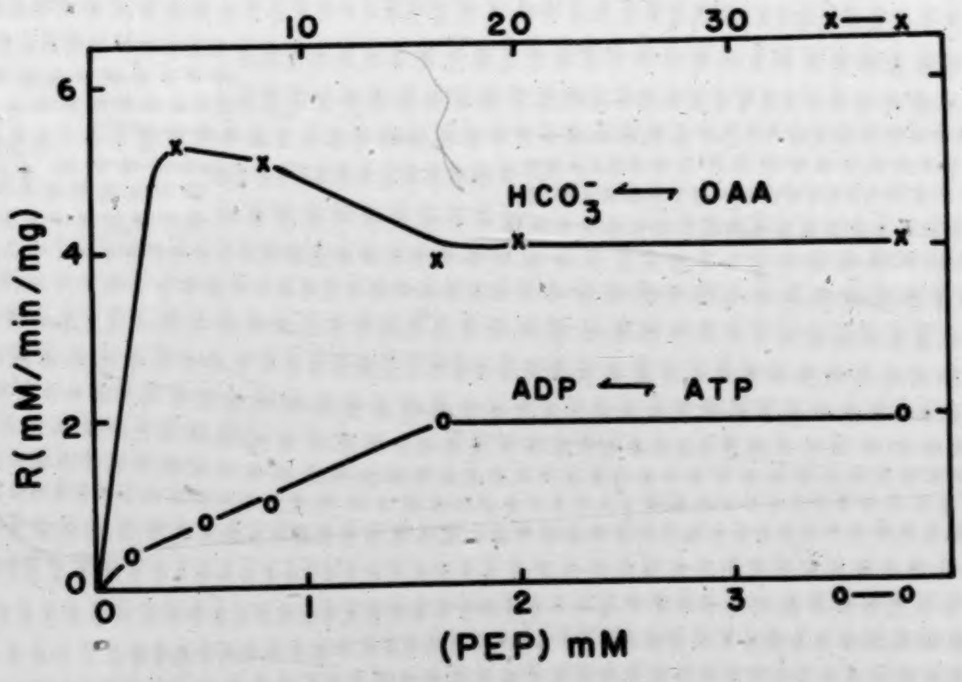
10
20
30
x—x
6
4
2
0
R (mM/min/mg)
$HCO_3^- \leftrightarrow OAA$
ADP ↔ ATP
0
1
2
3
o—o
(PEP) mM

mM/min/mg. The rate is not inhibited by the increase in PEP concentration, presumably because this is only raised to 4 mM which is below its inhibitory concentration. The $HCO_3^- \leftrightarrow$ OAA exchange rate is stimulated to 5.4 mM/min/mg at 4 mM PEP and levels off at 16 mM PEP to a rate of 4 mM/min/mg. The same explanations for the inhibitory effect for Fig. 20 can be applied to Fig. 21, except for competitive inhibition by PEP at the OAA binding locus, since increasing [PEP] and [OAA] in constant ratio eliminates competition between them for the same binding site. Inhibition of the exchange due to PEP binding in a partially compulsory order after HCO_3^- is still a possibility, whereas inhibition due to a compulsory binding order of OAA and ATP can be ruled out since ATP was not varied during this experiment. The third argument given for Fig. 20 could also be applied to Fig. 21. The dissociation of HCO_3^- or OAA may be decreased due to the increase of the PEP and ATP. However, only PEP is common to both experiments, and it is likely responsible for the apparent partial inhibition. Such inhibition suggests that PEP binds in a partially compulsory order after HCO_3^-, decreasing the dissociation of OAA from the enzyme complex.

Bumpy saturation curves may not have been observed for the interchange of $HCO_3^- \leftrightarrow$ OAA in Figs. 18 and 19 because in both cases the initial PEP concentration was beyond the range where stimulation and inhibition is apparent. However the effect of PEP can be detected by the disparity in rates, summarized in Table VIII. Whenever PEP concentration was over 0.05 M the rate of $HCO_3^- \leftrightarrow$ OAA was affected. Such a dramatic effect is not associated with the ADP $\leftrightarrow$ ATP interchange which is less sensitive to PEP concentration.

Table VIII

Effect of PEP Concentration on the Rates of Exchange of HCO_3^- ⟷ OAA and ATP ⟷ ADP

PEP (M)	Rate of HCO_3^- ⟷ OAA	Rate of ADP ⟷ ATP
0.300	2.0	-
0.170	2.7	-
0.090	-	1.5
0.050	-	2.5
0.041	4.0	-
0.004	5.4	2.0

Rates are given in mM/min/mg

Total volume of assay was 0.5 ml.

Results given above eliminate the partially ordered - C mechanism which was consistent with the results from initial rates and product inhibition studies. While we cannot rule out complex inhibiting relationships as the cause of the depressed rate of exchange,[8] the data may be easily interpreted in terms of a sequential mechanism with a preferred binding sequence. The partially ordered - C mechanism can be eliminated since no exchange was completely inhibited when another reactant pair was increased. However if the mechanism is rapid equilibrium random, we should expect all exchange rates to be identical. This was not the case. For example, Figs. 18 - 21 show disparity in rate of interchange between HCO_3^- ↔ OAA and ADP ↔ ATP. This could be the result of the concentrations of reactant in each experiment which could not be kept at the same level for both exchanges. In a previous section on 'Comparison of Relative Rates', however, several experiments were reported in which the concentrations of reactants were identical for both the HCO_3^- ↔ OAA and ADP ↔ ATP exchange; the rate of HCO_3^- ↔ OAA was four times greater than the ADP ↔ ATP exchange. The small disparity suggests that the central complex interconversion may be relatively slow. The observations that all substrate interchanges have rates within one order of magnitude of each other under the conditions tested may reflect a contribution of the rate of interconversion of the quaternary reactant-product complexes as well as substrate dissociation steps (77).

---

[8] In other similar studies (12, 77) competitive interactions have been avoided by experiments in which all reactants are elevated together in constant ratio. This is obviously not feasable here, since the asymmetric stoichiometry would result in displacement from equilibrium.

5. Nucleotide Specificity

Table IX lists the nucleotides and their effectiveness in participating in the nucleotide triphosphate-dependent $H^{14}CO_3^- \leftrightarrow$ OAA exchange reaction of PEPCK. The structures of the less common ATP analogues are shown on Fig. 22. Compared to ATP, all other nucleotides tested exhibit activity that ranges from 0 to 54%. Of the analogues tested, α,β-CH_2-ATP displayed the most activity. This analogue is not altered in its base and sugar moieties but has a methylene bridge between the α and β phosphate groups. β,γ-CH_2-ATP, in which the methylene is inserted between the terminal phosphate groups shows no activity as a substrate. As previously discussed the γ phosphate pocket on the enzyme must be occupied for ATP to fulfill its role in the ATP-dependent $HCO_3^- \leftrightarrow$ OAA exchange reaction; β,γ-CH_2-ATP must have the wrong orientation to substitute for ATP.

Other analogues of ATP are recognized as substrates. AraATP in which the ribose residue is replaced by arabinose displays 35% substrate activity. Alterations in the base moiety are more important. Tubercidin, in which 7-N is replaced by 7-C shows 30% residual activity, N-6-CH_3-ATP 21% activity and formycin only 17% activity. 1,N^6-etheno-ATP exhibits no substrate properties. The extra 5-membered ring is perhaps too bulky to be accommodated at the active site.

ADP and AMP are inert as substrates in the exchange reaction. However, deoxy-ATP gave 40% activity. GTP, dGTP, ITP and dITP were all poorer substrates than ATP.

E. coli PEPCK does not exhibit as stringent a requirement for nucleotide triphosphates as was previously thought (51). The nucleotide triphosphate site on the enzyme shows a wide tolerance for alterations in the base, sugar or

Table IX

Nucleotide Specificity for PEPCK

	% activity
ATP	100
ADP	0
AMP	0
dATP	40
GTP	30
dGTP	15
ITP	15
dITP	15
TuTb	30
araATP	35
N-6-CH_3ATP	21
FTP	17
εATP	0
β,γ-CH_2-ATP	0
α,β-CH_2-ATP	54

The ^{14}C-$KHCO_3^-$ ⇄ OAA exchange assay contained in a total volume of 0.5 ml the following: 0.1 M imidazole-HCl pH 6.8, 100 mM $KHCO_3$, 3.0 mM DTT, 10 mM $MnCl_2$, 2 mM OAA and 0.4 mM trinucleotides. 250,000 cpm of ^{14}C-$KHCO_3$ was added per assay.

Figure 22. Structures of tubercidin 5'-triphosphate, arabinose-ATP, N-6-CH_3 ATP, formycin 5'-triphosphate and ε ATP.

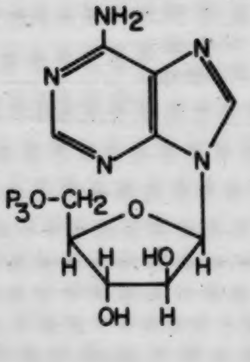

araATP

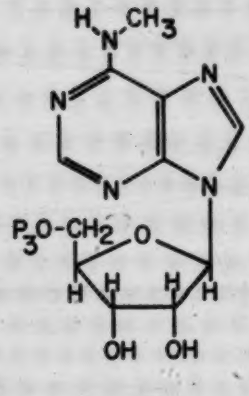

N-6-CH$_3$ATP

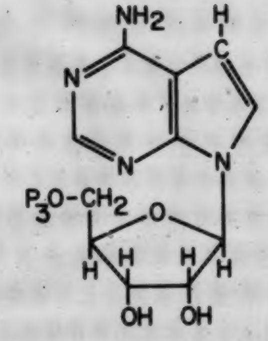

TuTb

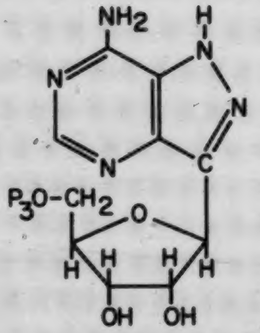

FTP

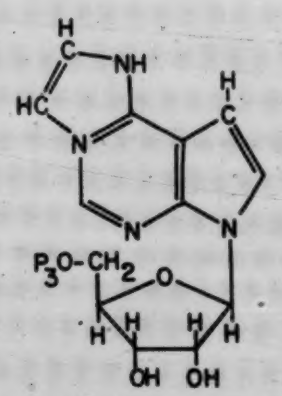

ε ATP

phosphate moieties. When the 6-N amino group was changed to a keto group as in GTP or ITP, or modified by methylating at the 6-N position recognition was not lost.

This study shows quite a broad specificity for nucleotide triphosphates for *E. coli* PEPCK. The degeneracy of its specificity with respect to purine nucleotides parallels that of SCS (113). For both enzymes, while ATP is clearly the preferred and physiologically important substrate, GTP and ITP can be used as substrates; the order of effectiveness is ATP>GTP>ITP.

CHAPTER VI

CONCLUSION

PEPCK shows very little resemblance to SCS, either in structure or reaction mechanism. PEPCK is a monomer under all circumstances and carries out its ter-bi reaction on a single polypeptide chain of molecular weight of 65,000. SCS, on the other hand, is a more complex tetrameric structure consisting of two unlike subunits $(\alpha\beta)_2$. The α subunit contains the potential phosphohistidine reaction intermediate and is capable of catalyzing its own phosphorylation in the absence of β (87). The phosphorylation of α subunit confers stability to the enzyme structure (31) and directs the correct refolding of the polypeptide (86), whereas no such reaction intermediate has been identified in PEPCK. PEPCK and SCS would appear to have no common origin in that they do not share the α subunit. The molecular weight trend of SCS (a tetramer of 140,000 in *E. coli* and a dimer of 70,000 in pig heart) is not upheld in PEPCK in which both the mammalian and *E. coli* enzyme have a similar monomeric structure of molecular weights of 73,000 (60) and 65,000 (our work), respectively.

Our molecular weight study with SCS by sedimentation equilibrium confirmed the tetrameric structure to have a molecular weight of 140,000. This result agreed well with previous determination of 146,000 by Leitzmann *et al.* (35). SCS is known to exist mostly in the tetrameric form which when phosphorylated is more stable than the apoenzyme which is described as possessing a 'loose' structure (31). It was therefore surprising to observe a tendency for this stable polymeric enzyme to dissociate to dimers and monomers during sedimentation equilibrium runs at low protein concentrations. Dissociation could perhaps be due to the fraction of SCS molecules that are not phosphorylated and are susceptible to falling apart, or it could be due to enzyme that has been damaged during isolation. It would be interesting to compare the dissociating tendency of the native enzyme with that of the reassociated tetramer. The recombined enzyme is fully phosphorylated (bearing one phosphoryl group per tetramer) yet exhibits only one half the reactivity of the native enzyme (86). By such a sedimentation equilibrium experiment a correlation could be made of the activity and the extent of dissociation, since no definite comparison can yet be made between the degree of phosphorylation and the extent of dissociation of the native enzyme.

It is surprising that SCS undergoes dramatic stabilization upon phosphorylation without a large structural change. By circular dichroism measurements no shift in the contributions of the three structural components could be detected following phosphorylation. The circular dichroism absorption spectra of the two enzyme forms were almost superimposable. Perhaps a more sensitive probe for measuring such changes would reveal that more subtle structural changes do take place.

The sequence of events in our work with PEPCK was exciting. Wright and Sanwal (51) had reported that the *E. coli* enzyme exhibited homotropic cooperativity in the presence of the inhibitor NADH. They assumed that the enzyme was an aggregate or associated in the presence of this effector. We then determined that PEPCK was monomeric under all conditions tested as was shown in Chapter IV. At this stage, we had a monomeric enzyme that gave sigmoidal saturation curves (Fig. 7 of Ref. 51). Reinvestigation of the NADH inhibition showed normal saturation curves with linear Lineweaver-Burk plots (Fig. 7 and 8) in agreement with our monomeric structure determination. However, very recently the inhibition of PEPCK by NADH has been attributed to an artifact (106) of the colorimetric assay used throughout this study.

The reaction mechanism of SCS determined by initial rate kinetics was not consistent with a ping-pong mechanism despite the participation of covalent-enzyme phosphate reaction intermediate. Using initial rate kinetic data as a sole test for a mechanism presents a possible danger of overlooking intermediates. Since enzymes involving covalent intermediates have generally shown ping-pong kinetics, a tendency may in turn arise to consider the lack of such kinetics as evidence against covalent reaction intermediates. Initial rate and isotope exchange studies supported a random sequential mechanism with a preferred pathway of ATP binding first and ADP dissociating last (38).

To elucidate the kinetic mechanism of PEPCK, similar studies of initial rate, product inhibition and isotope exchange at equilibrium were done. Initial rate kinetics did not allow us to choose between the ping-pong or several sequential mechanisms postulated on Table VI. Since no covalent intermediates could be isolated, a ping-pong mechanism was not an attractive model for this enzyme. From the listed sequential reaction mechanisms only the ordered - ter could be eliminated by initial rate studies. Further information was derived from the product inhibition study with ATP, showing competitive inhibition patterns with both ADP and PEP. These experiments narrowed our choice of reaction mechanism down to two schemes, random and partially ordered - C (where A and B add randomly). Isotope exchange studies at chemical equilibrium revealed the major reaction pathway to approximate fully rapid equilibrium random with a preferential order of substrate binding. This is apparent from the differential rates of interchange of the ATP ↔ ADP relative to the HCO_3^- ↔ OAA, and also from the bumpy exchange rate plots (Figs. 20 and 21). Such behaviour is due to PEP binding after HCO_3^-. However in none of the isotope exchange experiments did the rate tend towards zero as the concentration of a reactant pair is elevated, confirming that the preferred order of substrate attachment is not obligatory. By this study we have eliminated the partially ordered - C model proposed by the product inhibition experiments, leaving the fully random mechanism as the only one consistent with all kinetic data.

Although PEPCK is said to control the gluconeogenic flux (115) being the first committed enzyme of gluconeogenesis, no obvious controls have been discovered. OAA is at the centre of the branchpoint to many synthetic pathways besides gluconeogenesis. It combines with acetyl-CoA to form citrate which regulates the flux through the Krebs cycle, OAA is also a precurser in pyrimidine, sialic acid and aspartic acid synthesis. None of these products provide regulation by feed-back inhibition or by activation of PEPCK. It appears that the only control is on its synthesis, although the availability of substrate could serve as a control since OAA is present at very low concentrations in the cell. Since PEPCK seems to be an important control point, higher levels of control might exist which are either destroyed during the isolation procedure, such as interaction with other proteins.

The rat liver enzyme has been studied more extensively. Bentle and Lardy (47) showed that the rat enzyme is stimulated by divalent transition metal ions. Catalytic activity is increased by incubating cytosol PEPCK with Fe^{2+}, Mn^{2+}, Co^{2+} or Cd^{2+}. When pure enzyme was incubated with the above metal ions, all but Mn^{2+} failed to stimulate. A Mn^{2+} effect was also observed with the *E. coli* enzyme. It decreased considerably the K_m values of several substrates. The other metal ions were not tested with the bacterial enzyme. The activation of purified rat liver cytosol PEPCK by Fe^{2+} could be restored by the presence of a cytosol protein factor, ferroactivator (49). The stimulation of Mn^{2+} is quite different from the mode of action of Fe^{2+}, since Mn^{2+} activation is not protein-mediated but the metal ion alone is the activator. The activator protein is of comparable molecular weight to PEPCK and *in vitro* studies indicate that PEPCK combines with the activator in a ratio of 1:5. Physiologically PEPCK is thought to be activated mainly by Fe^{2+} rather than by Mn^{2+} or the other transition metals since iron is the most abundant transition metal ion in the cytosol (49). Mn^{2+} concentration is too low to be effective.

The ferroactivator and metal ions are the only reported effectors that alter the catalytic activity directly on the preexisting PEPCK protein. All other regulators exert their effect at the level of PEPCK synthesis. There is a large alteration in the rate of enzyme synthesis in response to the metabolic state of the animal. During starvation PEPCK is synthesized and during the refeeding cycle gluconeogeneses is shut down and PEPCK is repressed to a basal level (116). Similarly, in bacteria grown on glucose PEPCK synthesis is repressed but when the growth medium contains only 3- or 4-carbon compounds as the sole carbon source, gluconeogeneses is turned on and PEPCK synthesis increases up to 18-fold (46).

Although much is now understood about the basic features of bacterial PEPCK (its monomeric structure, physical parameters and reaction mechanism) the details of control must be brought into clearer focus. It would be interesting to see if the bacterial enzyme responds to the cytosol ferroactivator or if it responds to Fe^{2+} alone, since we did find a similarity in the Mn^{2+} response in both animal and bacterial enzymes. Further manipulation of PEPCK synthesis could be made with N^6, $0^{2'}$-dibutyryl cAMP to compare the response in *E. coli* with that of mammalian PEPCK. Regardless of whether the enzyme is from prokaryotic or eukaryotic cells the main control of its activity, namely induction and repression of synthesis, seems to be under the ultimate regulation of cAMP. As discussed above the liver enzyme is stimulated during conditions favouring elevated cAMP levels, while in *E. coli* conditions favouring cAMP-mediated catabolite repression correlate with reduced levels of PEPCK. Involvement of cAMP could be shown by growing *E. coli* cells in the presence of N^6, $0^{2'}$-dibutyryl cylic AMP.

REFERENCES

1. Taborsky, G. (1974) Advances in Protein Chemistry 28, 1.

2. Walsh, C.T. and Spector, L.B. (1971) Arch. Biochem. Biophys. 145, 1.

3. Solomon, F. and Rose, I.A. (1971) Arch. Biochem. Biophys. 147, 349.

4. Suzuki, F., Fukunishi, K. and Takeda, Y. (1969) J. Biochem. Tokyo 66, 767.

5. Cottam, G.L. and Srere, P.A. (1969) Biochem. Biophys. Res. Commun. 35, 895.

6. Mardh, S., Ljungström, O., Högstedt, S., and Zetterqvist, Ö. (1971) Biochim. Biophys. Acta 251, 419.

7. Das, N., Cottam, G.L. and Srere, P.A. (1971) Arch. Biochem. Biophys. 143, 602.

8. Kreil, G. and Boyer, P.D. (1964) Biochem. Biophys. Res. Commun. 16, 551.

9. Mitchell, R.A., Butler, L.G. and Boyer, P.D. (1964) Biochem. Biophys. Res. Commun. 16, 545.

10. Moffet, F.J., Wang, T. and Bridger, W.A. (1972) J. Biol. Chem. 247, 8139.

11. Gibson, J., Upper, C.D. and Gunsalues, I.C. (1967) J. Biol. Chem. 242, 2474.

12. Moffet, F.J. and Bridger, W.A. (1970) J. Biol. Chem. 245, 2758.

13. Chang, H.-C. and Lane, M.D. (1966) J. Biol. Chem. 241, 2413.

14. Brownie, E.R. and Bridger, W.A. (1972) Can. J. Biochem. 50, 719.

15. Ramaley, R.F., Bridger, W.A., Moyer, R.W. and Boyer, P.D. (1967) J. Biol. Chem. 242, 4287.

16. Utter, M.F. and Kolenbrander, H.M. (1972) in The Enzymes (ed., Boyer, P.D.), 3rd Edition, Vol. VI, p. 117, Academic Press, New York.

17. Bridger, W.A. (1971) Biochem. Biophys. Res. Commun. 42, 948.

18. Bridger, W.A. (1973) in The Enzymes (ed., Boyer, P.D.), 3rd Edition, Vol. 10, p. 581, Academic Press, New York.

19. Birktoft, J.J. and Blow, D.M. (1972) J. Mol. Biol. 68, 187.

20. Shotton, D.M. and Watson, H.C. (1970) Nature 225, 811.

21. Stroud, R.M., Kay, L.M. and Dickerson, R.F. (1974) J. Mol. Biol. 83, 185.

22. Harris, J.I. and Waters, M. (1976) in The Enzymes (ed., Boyer, P.D.) 3rd Edition, Vol. XIII, p. 1, Academic Press, New York.

23. Kretsinger, R.H. (1976) in Annual Review of Biochemistry (eds., Snell, E.E., Boyer, P.D., Meister, A. and Richardson, C.C.), Vol. 45, p. 239, Annual Reviews Inc., Palo Alto, California.

24. Kaufman, S. (1951) in Phosphorus Metabolism (eds., McElroy, W.D. and Glass, B.), Vol. I, p. 370, Johns Hopkins Press, Baltimore.

25. Hultquist, D.E., Moyer, R.W. and Boyer, P.D. (1966) Biochemistry 5, 322.

26. Bridger, W.A., Millen, W.A. and Boyer, P.D. (1968) Biochemistry 7, 3608.

27. Hager, L.P. (1957) J. Am. Chem. Soc. 79, 4864.

28. Cohn, M. (1959) J. Cell. Comp. Physiol. 54, 157.

29. Nishimura, J.S. and Meister, A. (1965) Biochemistry 4, 1457.

30. Nishimura, J.S. (1967) Biochemistry 6, 1094.

31. Wang, T. (1972) Ph.D. Thesis, University of Alberta.

32. Wang, T., Jurášek, L. and Bridger, W.A. (1972) Biochemistry 11, 2067.

33. Grinnell, F.L., Stollar, B.D. and Nishimura, J.S. (1969) Biochim. Biophys. Acta 185, 471.

34. Grinnell, F.L. and Nishimura, J.S. (1969) Biochemistry 8, 562.

35. Leitzmann, C., Wu, J.Y. and Boyer, P.D. (1970) Biochemistry 9, 2338.

36. Cleland, W.W. (1963) Biochim. Biophys. Acta 67, 104.

37. Wålinder, O., Zetterqvist, Ö. and Engström, L. (1969) J. Biol. Chem. 244, 1060.

38. Moffet, F.J. and Bridger, W.A. (1973) Can. J. Biochem. 51, 44.

39. Shrago, E. and Lardy, H.A. (1966) J. Biol. Chem. 241, 663.

40. Tilghman, S.F., Hanson, R.W. and Ballard, F.J. (1976) in Gluconeogenesis (eds., Hanson, R.W. and Mehlman, M.A.), p. 47, John Wiley & Sons, New York.

41. Böttger, I., Wieland, O., Brdiczka, D. and Pette, D. (1969) Eur. J. Biochem. 8, 113.

42. Krone, W., Huttner, W.B., Seitz, H.J. and Tarnowski, W. (1975) FEBS Lett. 52, 85.

43. Shrago, E., Lardy, H.A., Nordlie, R.C. and Foster, D.O. (1963) J. Biol. Chem. 238, 3188.

44. Gevers, W. (1967) Biochem. J. 103, 141.

45. Shrago, E. and Shug, A.L. (1969) Arch. Biochem. Biophys. 130, 393.

46. Hsie, A.W. and Rickenberg, H.V. (1967) Biochem. Biophys. Res. Commun. 29, 303.

47. Bentle, L.A. and Lardy, H.A. (1976) J. Biol. Chem. 251, 2916.

48. Bentle, L.A., Snoke, R.E. and Lardy, H.A. (1976) J. Biol. Chem. 251, 2922.

49. Bentle, L.A. and Lardy, H.A. (1977) J. Biol. Chem. 252, 1431.

50. Scrutton, M.C. and Young, M.R. (1972) in The Enzymes (ed., Boyer P.D.), 3rd Edition, Vol. IV, p. 1, Academic Press, New York.

51. Wright, J.A. and Sanwall, B.D. (1969) J. Biol. Chem. 244, 1838.

52. Garber, A.J. and Hansen, R.W. (1971) J. Biol. Chem. 246, 589.

53. Ballard, F.J. (1970) Biochem. J. 120, 809.

54. Kolenbrander, H.M., Chiao, Y.B. and Utter, M.F. (1970) unpublished observations.

55. Sanwal, B.D. (1970) Bacteriol. Rev. 34, 20.

56. Hryniuk, W.M., Brox, L.W., Henderson, J.F. and Tamaoki, T. (1975) Cancer Res. 35, 1427.

57. Blangy, D., Buc, H. and Monod, J. (1968) J. Mol. Biol. 31, 13.

58. Maeba, P. and Sanwal, B.D. (1968) J. Biol. Chem. 243, 448.

59. Schwartz, E.R., Old, L.O. and Reed, L.J. (1968) Biochem. Biophys. Res. Commun. 31, 495.

60. Chang, H-C., Maruyama, H., Miller, R.S. and Lane, M.D. (1966) J. Biol. Chem. 241, 2421.

61. Miller, R.S. and Lane, M.D. (1968) J. Biol. Chem. 243, 6041.

62. Felicioli, R.A., Barsacchi, R. and Ipata, P.L. (1970) Eur. J. Biochem. 13, 403.

63. Tsuboi, K.K. and Hudson, P.B. (1957) J. Biochem. 224, 879.

64. Johnson, D., MacCoss, M. and Narindrasorasak, S. (1976) Biochem. Biophys. Res. Commun. 71, 144.

65. Davis, B.J. (1964) Ann. N.Y. Acad. Sci. 121, 404.

66. Weber, K. and Osborn, M. (1969) J. Biol. Chem. 244, 4406.

67. Davies, G.E. and Stark, G.R. (1970) Proc. Nat. Acad. Sci. 66, 651.

68. Chervenka, C.H. (1970) A Manual of Methods for the Analytical Ultracentrifuge, Beckman Instruments, Palo Alto, California.

69. Wolodko, W.T. (1973) Ph.D. Thesis, University of Alberta.

70. Cohn, E.J. and Edsall, J.T. (1943) Proteins, Amino Acids and Peptides, p. 370, Reinhold, New York.

71. Babul, J. and Stellwagen, E. (1969) Anal. Biochem. 28, 216.

72. Layne, E. (1957) in Methods in Enzymology (eds., Colowick, S.P. and Kaplan, N.O.), Vol. III, p. 450, Academic Press, New York.

73. Bailey, J.L. (1967) Techniques in Protein Chemistry, Chapter II, p. 340, Elsevier Publishing Corp., Amsterdam.

74. Sober, H.A. (ed.) (1968) Handbook of Biochemistry, p. c-71, The Chemical Rubber Company, Cleveland, Ohio.

75. Siegelman, H.W., Wieczorek, G.A. and Turner, B.C. (1965) Anal. Biochem. 13, 402.

76. Utter, M.F. and Kurahashi, K. (1954) J. Biol. Chem. 207, 787.

77. Wedler, F.C. and Boyer, P.D. (1972) J. Biol. Chem. 247, 984.

78. Engers, H.D., Bridger, W.A. and Madsen, N.B. (1969) J. Biol. Chem. 244, 5936.

79. Engers, H.D., Bridger, W.A. and Madsen, N.B. (1970) Can. J. Biochem. 48, 755.

80. Jomain-Baum, M. (1976) Fed. Proc. Am. Soc. Biol. Chem. 35, 1758.

81. Boyer, P.D. (1959) Arch. Biochem. Biophys. 82, 387.

82. Boyer, P.D. and Silverstein, E. (1963) Acta Chem. Scand. 17, 5195.

83. Oikawa, K., Kay, C.M. and McCubbin, W.D. (1968) Biochim. Biophys. Acta 168, 164.

84. Teherani, J.A. and Nishimura, J.S. (1975) J. Biol. Chem. 250, 3883.

85. Harris, C.E., Kobes, R.D., Teller, D.C. and Rutter, W.J. (1969) Biochemistry 8, 2442.

86. Pearson, P.H. and Bridger, W.A. (1975) J. Biol. Chem. 250, 4451.

87. Pearson, P.H. and Bridger, W.A. (1975) J. Biol. Chem. 250, 8524.

88. Cha, C.-J., Cha, M. and Parks, Jr., R.E. (1967) J. Biol. Chem. 242, 2582.

89. Baccanari, D.P. and Cha, S. (1973) J. Biol. Chem. 248, 15.

90. Chen, Y.-H., Yang, J.T. and Martinez, H.M. (1972) Biochemistry 11, 4120.

91. Wolodko, W.T., personal communication (unpublished results).

92. Lowry, O.H., Rosebrough, N.J., Farr, A.L. and Randall, R. (1951) J. Biol. Chem. 193, 265.

93. Kohlhaw, G. and Boatman, G. (1971) Biochem. Biophys. Res. Commun. 43, 741.

94. Moore, S. and Stein, W.H. (1963) in Methods in Enzymology (eds., Colowick, S.P. and Kaplan, N.O.), Vol. VI, p. 819, Academic Press, New York.

95. Gray, W.R. (1967) in Methods in Enzymology (ed., Hirs, C.H.W.), Vol. XI, p. 469, Academic Press, New York.

96. Gray, W.R. (1967) in Methods in Enzymology (eds., Estabrook, R.W. and Pullman, M.E.), Vol. X, p. 139, Academic Press, New York.

97. Liu, T.-Y. and Chang, Y.H. (1971) J. Biol. Chem. 246, 2842.

98. Habeeb, A.F.S.A. (1972) in Methods in Enzymology (eds., Hirs, C.H.W. and Timasheff, S.N.), Vol. XXVIB, p. 457, Academic Press, New York.

99. Moore, S.,(1963) J. Biol. Chem. 238, 235.

100. Panagau, D., Orr, M.D., Dunston, J.R. and Blakley, R.L. (1972) Biochemistry 11, 2378.

101. Wyman, A. and Paulus, H. (1975) J. Biol. Chem. 250, 3897.

102. Shapiro, A.L., Vinuela, E. and Maizel, J.V. Jr. (1967) Biochem. Biophys. Res. Commun. 28, 815.

103. Cannata, J.J.B. (1970) J. Biol. Chem. 245, 792.

104. Cha, S. and Parks, R.E. Jr. (1964) J. Biol. Chem. 239, 1968.

105. Barzu, O., Abrudan, I., Proinov, I., Kiss, L., Ty, N.G., Jebeleanu, G., Goia, I., Kezdi, M. and Montsch, H.H. (1976) Biochim. Biophys. Acta 452, 406.

106. Goldie, A.H. and Sanwal, B.D. (1977) Proc. Can. Fed. Biol. Soc. 20, 105.

107. Fromm, H.J.,(1975) Initial Rate Enzyme Kinitics, p.145 Sprenger-Verlag, N.Y.

108. Cleland, W.W. (1963) Biochimica et Biophysica Acta, 67, 188.

109. Thiers, R.E. and Vallee, B.L. (1957), J. Biol. Chem. 226, 911.

110. Walaas, E. (1958) Acta Chem Scand. 12, 528.

111. Holten, D.D. and Nordlie, R.C. (1965) Bioch. 4 723.

112. Boyer, P.D. (1959) Arch. Biochem. Biophys. 82, 387.

113. Marakami, K., Mitchell, T., and Nishimura, J.S., (1972) J. Biol. Chem. 247, 6247.

114. Wilkinson, G.N. (1961) Biochem. J. 80, 324.

115. Williamson, J.R. (1967) Adv. Enzyme Regulation 5, 229.

116. Young, J.W., Shrago, E., Lardy, H.A. (1964) Bioch. 3, 1687.

APPENDIX I

PUBLISHED PAPERS ARISING FROM THIS WORK

P.H. Pearson, A. Krebs and W.A. Bridger, "The Subunits of Succinyl Coenzyme A. Synthetase", Proc. Canad. Fed. of Biological Soc. 17, 261 (1973).

Anita Krebs and William A. Bridger, "Some Physical Parameters of Succinyl Coenzyme A Synthetase of *Escherichia coli*", Can. J. Biochem. 52, 594-598 (1974).

Anita Krebs and William A. Bridger, "On the Monomeric Structure and Proposed Regulatory Properties of Phosphoenolpyruvate Carboxykinase of *Escherichia coli*", Can. J. Biochem. 54, 22-26 (1976).